Study on the Non-linear Metrics Contribution to Estimate Atrial Fibrillation Organization from the Surface Electrocardiogram

Matilde Julián Seguí

SUPERVISOR: José Joaquín Rieta Ibáñez

CO-SUPERVISOR: Raúl Alcaraz Martínez

Valencia, July 2015
Doctoral Thesis

ELECTRONIC ENGINEERING DEPARTMENT
UNIVERSIDAD POLITÉCNICA DE VALENCIA

Study on the Non-linear Metrics Contribution to Estimate Atrial Fibrillation Organization from the Surface Electrocardiogram

Editor: LiberLIBRO.com, July 2015

I.S.B.N.: 978-84-16393-14-5

Legal Dep.: AB-295-2015

Abstract

Atrial fibrillation (AF) is the most frequently diagnosed arrhythmia, characterized by an uncoordinated atrial electrical activation, thus causing the atria to be unable to pump blood effectively. Blood clots can be formed in the atria and, hence, AF patients have an increased risk of thromboembolic events. The prevalence of AF is expected to increase significantly in the next decades as the population ages. However, in spite of the intensive research performed in recent years, both the knowledge and the treatment of this arrhythmia still have to experiment a significant progress. Different hypotheses have been proposed to explain AF, however, the physiological mechanisms causing its initiation and maintenance are still not fully understood. Within this context, previous studies have reported that AF organization, which can be defined as the repetitiveness degree of the atrial activity pattern, correlates with the arrhythmia status as well as with the therapy outcome. Thus, the estimation of organization from the atrial activity pattern has been permanently targeted by signal analysis methods in recent years. In addition, estimating AF organization from surface electrocardiographic (ECG) recordings constitutes a very interesting approach because ECG recordings are easy and cheap to obtain. In fact, noninvasive AF organization indices have attained promising results in previous studies addressing the analysis of organization-related events. Nonetheless, the application of new nonlinear indices to the surface ECG still constitutes an open issue able to provide significant and clinically useful results through an improved estimation of AF organization.

Given that physiological time series often present a nonlinear and nonstationary behavior, their analysis through nonlinear methods could provide relevant clinical information. Hence, the objective of this doctoral thesis is to assess the use of a variety of nonlinear indices in the estimation of AF organization from single-lead noninvasive ECG recordings. Apart from the most common noninvasive AF organization estimators, such as Sample Entropy (SampEn) and the dominant atrial frequency (DAF), the following nonlinear indices have been studied: Fuzzy Entropy, Spectral Entropy, Lempel-Ziv Complexity and Hurst Exponents. Moreover, since the presence of noise and ventricular residuals affects the performance of nonlinear methods, the application of a strategy aimed at reducing these nuisances has been evaluated. Therefore, the application of these metrics over the atrial activity fundamental waveform, named the main atrial wave (MAW), has

been proposed in order to improve their performance in the estimation of AF organization. In this doctoral thesis, the following scenarios involving AF organization have been considered: the prediction of paroxysmal AF spontaneous termination, the study of the earlier signs anticipating AF termination and the classification between paroxysmal and persistent AF from short ECG recordings.

Firstly, the performance of the studied metrics discriminating events related to AF organization was tested making use of a reference database aimed at predicting AF spontaneous termination. In this study, most of the proposed indices provided higher accuracy than traditional AF organization estimators. Additionally, the MAW computation before estimating organization improved the performance in all the cases. Accuracy values higher than 90% were obtained with several indices, thus being able to be considered as promising tools for the estimation of AF organization from the surface ECG. In particular, the generalized Hurst exponents of order 1 and 2, $H(1)$ and $H(2)$, achieved outstanding results, thus being selected for later studies in this thesis. Furthermore, the computation of $H(2)$ depends on two critical parameters, namely, the analyzed interval length (L) and the maximum search window for self-similarities (τ_{max}). But given that no guidelines exist for its application to AF signals, a study with 660 combinations on these two parameters was performed, together with the sampling frequency (f_s) of the recording, in order to obtain their optimal combination in computing AF organization. On the other hand, previous works analyzing the spontaneous termination of AF have been only focused on the last 2 minutes preceding the termination. In contrast, a different scenario considering longer recordings to detect the earlier signs anticipating paroxysmal AF termination has been analyzed for the first time in this thesis. $H(2)$ was selected for the study because of its highest accuracy in AF termination prediction. Additionally, the DAF and SampEn were also computed as references. Through this study it has been corroborated that AF organization only varies significantly within the last 3 minutes before spontaneous termination. As a consequence, the early prediction of paroxysmal AF spontaneous termination does not seem feasible through the current signal analysis tools. Finally, $H(2)$ was applied in the classification between paroxysmal and persistent AF from short ECG recordings, achieving a higher diagnostic accuracy than DAF and SampEn. This result suggests that the analysis of ambulatory ECG recordings through $H(2)$ could be a future alternative to the use of Holter ECG recordings in the classification between paroxysmal and persistent AF.

An accurate quantification of AF organization in a straightforward way is crucial in determining the current progression of AF in every single patient. Given that the treatment of AF still is based on trial and error strategies, the present doctoral thesis aims at providing new insights in organization quantification, thus leading to useful clinical diagnostic techniques and aid tools with valuable contributions to tailored therapies of patients in AF. Future applications of the studied indices in different scenarios may also provide useful clinical information and contribute to the improvement of AF management, thus reducing costs for the healthcare providers and risks for the patients.

Resumen

La fibrilación auricular (FA) es la arritmia más frecuentemente diagnosticada y se caracteriza por una actividad auricular descoordinada, que impide que las aurículas bombeen la sangre de manera eficaz. Como consecuencia, se pueden formar coágulos en las aurículas, lo cual aumenta el riesgo de tromboembolismo. Se espera que la prevalencia de la FA aumente significativamente en las próximas décadas debido al envejecimiento de la población. Sin embargo, a pesar de la intensiva investigación desarrollada en estos últimos años, tanto el conocimiento relativo a esta arritmia como su tratamiento son todavía mejorables. Aunque se han propuesto distintas hipótesis para explicar la FA, los mecanismos que causan su inicio y mantenimiento no están completamente explicados. En este contexto, en estudios previos se ha relacionado la organización de la FA, que se puede definir como el grado de repetitividad de la actividad auricular, con el estado de la arritmia o su respuesta al tratamiento. Por ello, el análisis de las señales en FA se ha centrado en el estudio de la organización. Además, la estimación de la organización de la FA a partir de registros electrocardiográficos (ECG) de superficie resulta especialmente interesante porque la obtención del ECG es sencilla y barata. De hecho, los estimadores no invasivos de organización han logrado resultados prometedores en el análisis de eventos en FA. A pesar de todo, la aplicación de nuevos índices no lineales sobre el ECG de superficie es aún una cuestión abierta que puede proporcionar resultados útiles para la práctica clínica.

Puesto que el comportamiento de las bioseñales suele ser no lineal y no estacionario, su análisis mediante métodos no lineales puede proporcionar información clínica relevante. Así pues, el objetivo de esta tesis doctoral es evaluar el uso de distintos índices no lineales en la estimación de la organización de la FA a partir de una derivación del ECG de superficie. Además de los estimadores no invasivos de organización más comunes, como la entropía muestral (SampEn) y la frecuencia auricular dominante (DAF), se han estudiado los siguientes métodos no lineales: la entropía borrosa, la entropía espectral, la complejidad Lempel-Ziv y los exponentes de Hurst. Además, se ha estudiado el uso de una estrategia destinada a la reducción del ruido y los residuos de actividad ventricular porque éstos pueden afectar al desempeño de los métodos no lineales. Así pues, los índices estudiados también se han aplicado sobre la forma de onda fundamental de la actividad auricular, conocida como la onda auricular principal (MAW), para

mejorar su capacidad de estimar la organización de la FA. En esta tesis doctoral se han considerado los siguientes escenarios relacionados con la organización de la FA: la predicción de la terminación espontánea de la FA paroxística, el estudio de los primeros indicios de terminación espontánea de la FA y la clasificación entre FA paroxística y FA persistente a partir de registros ECG de corta duración.

En primer lugar, se estudió la capacidad de los índices estudiados para distinguir eventos relacionados con la organización de la FA mediante el análisis de una base de datos de referencia para la predicción de la terminación espontánea de la FA. La mayoría de los índices propuestos consiguieron una mayor precisión que los estimadores tradicionales de organización de la FA. Además, el uso de la MAW mejoró el desempeño de todos los métodos estudiados. Así, varios de los índices obtuvieron una precisión superior al 90% en la predicción de la terminación espontánea de la FA, por lo que se pueden considerar herramientas prometedoras para el estudio no invasivo de la organización. En particular, los exponentes de Hurst generalizados de orden 1 y 2, $H(1)$ y $H(2)$, lograron los mejores resultados de clasificación. Por otra parte, el cálculo de $H(2)$ depende de dos parámetros críticos: la longitud del intervalo analizado (L) y el tamaño máximo de la ventana donde buscar similitudes (τ_{max}). Puesto que no existen guías para la aplicación de $H(2)$ en señales de FA, se llevó a cabo un estudio con 660 combinaciones de esos dos parámetros junto con la frecuencia de muestreo (f_s) del registro para determinar la combinación óptima de valores para estimar la organización de la FA. Por otra parte, los trabajos previos que han estudiado la terminación espontánea de la FA se han centrado en los últimos 2 minutos antes de la terminación. Por contra, en esta tesis doctoral se han estudiado por primera vez registros de mayor duración con el objetivo de detectar los primeros indicios de la terminación de la FA. Se eligió el uso de $H(2)$ para este estudio por su alta precisión en la predicción de la terminación de la FA. Además, la DAF y SampEn se calcularon como referencias. En este estudio se ha comprobado que la organización de la FA solamente presenta variaciones significativas en los últimos 3 minutos antes de su terminación espontánea. Por ello, la predicción temprana de la terminación no parece posible con los medios actuales de análisis de la señal. Por último, se aplicó $H(2)$ para clasificar entre FA paroxística y FA persistente a partir de ECGs de corta duración, obteniendo una mayor precisión diagnóstica que la DAF y SampEn. Este resultado sugiere que el análisis de ECGs ambulatorios por medio de $H(2)$ puede ser en el futuro una alternativa al uso de registros Holter para la distinción entre FA paroxística y persistente.

La estimación sencilla y precisa de la organización de la FA es de gran importancia para determinar la progresión de la arritmia en cada paciente. Puesto que el tratamiento de la FA todavía se basa en estrategias de prueba y error, esta tesis doctoral pretende proporcionar nuevos puntos de vista para la estimación de la organización que podrían ser de utilidad en técnicas diagnósticas y herramientas de ayuda para el desarrollo de terapias a medida para los pacientes con FA. Las futuras aplicaciones de los índices estudiados en diferentes escenarios también pueden proporcionar información clínica útil y contribuir a mejorar la gestión de la FA, reduciendo sus costes asociados y los riesgos para los pacientes.

Resum

La fibril·lació auricular (FA) és l'arítmia més sovint diagnosticada i es caracteritza per una activitat auricular descoordinada, que impedix que les aurícules bomben la sang de manera eficaç. Com a conseqüència, es poden formar coàguls en les aurícules, la qual cosa augmenta el risc de tromboembolisme. S'espera que la prevalença de la FA augmente significativament en les pròximes dècades a causa de l'envelliment de la població. No obstant això, tant el coneixement relatiu a esta arítmia com el seu tractament són encara millorables, a pesar de la intensiva investigació efectuada en estos últims anys. Encara que s'han proposat distintes hipòtesis per a explicar la FA, els mecanismes que causen el seu inici i manteniment no estan completament explicats. En este context, en estudis previs s'ha relacionat l'organització de la FA, que es pot definir com el grau de repetitivitat de l'activitat auricular, amb l'estat de l'arítmia o la seua resposta al tractament. Per això, l'anàlisi dels senyals en FA s'ha centrat en l'estudi de l'organització. A més, l'estimació de l'organització de la FA a partir de registres electrocardiogràfics (ECG) de superfície resulta especialment interessant perquè l'obtenció de l'ECG és senzilla i barata. De fet, els estimadors no invasius d'organització han aconseguit resultats prometedors en l'anàlisi d'esdeveniments en FA. A pesar de tot, l'aplicació de nous índexs no lineals sobre l'ECG de superfície és encara una qüestió oberta que pot proporcionar resultats útils per a la pràctica clínica.

Ja que el comportament de les sèries temporals fisiològiques sol ser no lineal i no estacionari, la seua anàlisi per mitjà de mètodes no lineals pot proporcionar informació clínica rellevant. Així, doncs, l'objectiu d'esta tesi doctoral és avaluar l'ús de distints índexs no lineals en l'estimació de l'organització de la FA a partir d'una derivació de l'ECG de superfície. A més dels estimadors no invasius d'organització més comuns, com l'entropia mostral (SampEn) i la freqüència auricular dominant (DAF), s'han estudiat els següents mètodes no lineals: l'entropia borrosa, l'entropia espectral, la complexitat Lempel-Ziv i els exponents de Hurst. A més, s'ha estudiat l'ús d'una estratègia destinada a la reducció del soroll i els residus d'activitat ventricular perquè estos poden afectar l'exercici dels mètodes no lineals. Així, doncs, els índexs estudiats també s'han aplicat sobre la forma d'onda fonamental de l'activitat auricular, coneguda com l'onda auricular principal (MAW), per a millorar la seua capacitat d'estimar l'organització. En esta tesi doctoral s'han considerat els següents escenaris relacionats amb l'organització

de la FA: la predicció de la terminació espontània de la FA paroxística, l'estudi dels primers indicis de terminació espontània de la FA i la classificació entre FA paroxística i FA persistent a partir de registres ECG de curta duració.

En primer lloc, es va estudiar la capacitat dels índexs estudiats per a distingir esdeveniments relacionats amb l'organització de la FA per mitjà de l'anàlisi d'una base de dades de referència per a la predicció de la terminació espontània de la FA. La majoria dels índexs proposats van aconseguir una major precisió que els estimadors tradicionals d'organització de la FA. A més, l'ús de la MAW va millorar l'exercici de tots els mètodes estudiats. Així, alguns dels índexs van obtindre una precisió superior al 90% en la predicció de la terminació espontània de la FA, per la qual cosa es poden considerar ferramentes prometedores per a l'estudi no invasiu de l'organització. En particular, els exponents de Hurst generalitzats d'orde 1 i 2, $H(1)$ i $H(2)$, van aconseguir els millors resultats de classificació. D'altra banda, el càlcul de $H(2)$ depén de dos paràmetres crítics: la longitud de l'interval analitzat (L) i la grandària màxima de la finestra on buscar similituds (τ_{max}). Ja que no existixen guies per a l'aplicació de $H(2)$ en senyals de FA, es va dur a terme un estudi amb 660 combinacions d'eixos dos paràmetres junt amb la freqüència de mostratge (f_s) del registre per a determinar la combinació òptima de valors per a estimar l'organització de la FA. D'altra banda, els treballs previs que han estudiat la terminació espontània de la FA s'han centrat en els últims 2 minuts abans de la terminació. Per contra, en esta tesi doctoral s'han estudiat per primera vegada registres de major duració amb l'objectiu de detectar els primers indicis de la terminació de la FA. Es va triar l'ús de $H(2)$ per a este estudi per la seua alta precisió en la predicció de la terminació de la FA. A més, la DAF i SampEn es van calcular com a referències. En este estudi s'ha comprovat que l'organització de la FA només presenta variacions significatives en els últims 3 minuts abans de la seua terminació espontània. Per això, la predicció primerenca de la terminació no pareix possible amb els mitjans actuals d'anàlisi del senyal. Finalment, es va aplicar $H(2)$ per a classificar entre FA paroxística i FA persistent a partir d'ECGs de curta duració, obtenint una millor precisió diagnòstica que amb la DAF i SampEn. Este resultat suggerix que l'anàlisi d'ECGs ambulatoris per mitjà de $H(2)$ pot ser en el futur una alternativa a l'ús de registres Holter per a la distinció entre FA paroxística i persistent.

L'estimació senzilla i precisa de l'organització de la FA és de gran importància per a determinar la progressió de l'arítmia en cada pacient. Ja que el tractament de la FA encara es basa en estratègies de prova i error, esta tesi doctoral pretén proporcionar nous punts de vista per a l'estimació de l'organització que podrien ser d'utilitat en tècniques diagnòstiques i ferramentes d'ajuda per al desenrotllament de teràpies a mesura per als pacients amb FA. Les futures aplicacions dels índexs estudiats en diferents escenaris també poden proporcionar informació clínica útil i contribuir a millorar la gestió de la FA, reduint els seus costos associats i els riscos per als pacients.

Agradecimientos

Quiero expresar mi más sincero agradecimiento a todas las personas que me han apoyado durante el desarrollo de esta tesis.

En primer lugar, me gustaría dar las gracias a mis directores de tesis José Joaquín Rieta y Raúl Alcaraz por haberme iniciado en la carrera investigadora y por su esfuerzo y dedicación. Gracias por vuestros consejos y ayuda y por haber compartido vuestros conocimientos conmigo. Ha sido un privilegio poder trabajar con vosotros y espero que podamos seguir colaborando en el futuro.

También quiero dar las gracias a la gente de la Universidad Politécnica de Valencia y en especial a Antonio Hernández, con quien he tenido la oportunidad de trabajar, compartir y contrastar ideas.

Y por último tengo que dar las gracias a mi familia por su comprensión y apoyo constante.

Muchas gracias a todos. Esto no habría sido posible sin vosotros.

Contents

Chapter 1

Motivation, Hypothesis and Objectives

1.1 Motivation

Atrial fibrillation (AF) is the most common supraventricular arrhythmia found in clinical practice [1], being present in 1–2% of the general population [2]. AF is associated with a decreased quality of life and an increased mortality in older adults [2]. Moreover, AF is a major risk factor for stroke and congestive heart failure [3]. Consequently, it has a considerable impact on health care costs [3]. In Europe, AF management represents at least 15% of the healthcare budget in cardiac diseases [4]. Since AF prevalence increases with age [3], it is estimated that it will double in the next 50 years due to the aging of the population [5]. Moreover, the medical, social and economic aspects of AF are expected to worsen in the next decades [1]. Thus, AF is nowadays a major health challenge in Europe [2, 3].

AF is characterized by a disorganized electrical activity which produces an abnormal excitation of the atria and, as a result, the atria are unable to be contracted in a regular rhythm [2]. Hence, surface electrocardiographic (ECG) recordings show a notably disorganized atrial activity, called fibrillatory waves (f-waves), during AF instead of regular P-waves [6]. Moreover, AF is also associated with an irregular and often rapid ventricular rate [2, 6]. AF is subdivided into different stages. Its first stage is called paroxysmal AF and is characterized by self-

terminating episodes, which can last from seconds up to several days [2]. In contrast, when an external intervention is needed in order to restore sinus rhythm, it is called persistent AF [2]. Finally, when AF termination is not possible or not recommended, it is named permanent AF [2]. Besides, the presence of AF alters the atrial tissue electrophysiological properties in a way that facilitates the arrhythmia perpetuation [7, 8]. These changes are known as atrial remodeling. Due to remodeling, paroxysmal AF often progresses to longer and more frequent episodes [2] and many patients eventually develop persistent AF [9]. Furthermore, since the therapy outcome depends on the time lapse since AF onset [2], an early intervention would be interesting in paroxysmal AF patients in order to terminate the arrhythmia before it becomes persistent [10].

Despite the intensive investigation carried out in recent years, the physiological mechanisms that cause the onset and termination of this arrhythmia remain not fully explained [11]. As a consequence, present therapeutic approaches have significant limitations, including limited efficacy and a significant likelihood of adverse effects [2,12]. Within this context, intensive research has been performed in the recent years to apply signal processing strategies in the study of AF both from invasive and noninvasive recordings [13]. Regardless of the type of recording analyzed, previous studies have reported that the morphology of the fibrillatory waves changes constantly, as a consequence of the fibrillatory activity, showing different levels of organization [14]. AF organization can be defined as the degree of repetitiveness of the atrial activity (AA) signal pattern [15] and it is related to the arrhythmia maintenance as well as with the therapy outcome [16]. Given that the presence of different f-waves morphologies may reflect different activation patterns [17], the analysis of AF organization could play an important role in the exploration of the arrhythmia mechanisms as well as in the development of tailored therapies for patients in AF.

Several algorithms have been developed for the estimation of AF organization from atrial invasive recordings. The most typical invasive AF organization measurement technique is the fibrillatory rate or its inverse, named the dominant atrial cycle length (DACL) [18]. Other techniques applied in the study of AF organization from invasive recordings include the estimation of the atrial activations morphological similarity [19,20] and the use of several nonlinear analysis methods, such as correlation dimension [21], correlation entropy [21, 22], Shannon's entropy [23] and recurrence plots [24,25].

On the other hand, the study of AF from noninvasive recordings is particularly interesting because it avoids the risks associated with invasive methods [6]. Noninvasively, AF can be studied from the standard ECG [6] and body surface mapping (BSMP) [26]. With respect to the estimation of AF organization from ECG recordings, the most common noninvasive AF organization index is the dominant atrial frequency (DAF) [18], which is related to the DACL. This technique, however, is not appropriate for the study of the time-dependent properties of AF. Hence, time-frequency analysis techniques have been developed for the analysis of AF organization temporal variations [27]. Other works have been

focused on the analysis of the morphological similarities of the f-waves registered on the surface ECG [28–30]. Besides, previous studies have demonstrated that AF organization can also be estimated through the application of a nonlinear index, such as sample entropy (SampEn), to the atrial activity fundamental waveform, known as the Main Atrial Wave (MAW) [16]. Furthermore, the application of several other nonlinear indices to the atrial activity registered on the ECG has been tested in previous studies. Some of those methods are the spectral entropy [31], recurrence plots [32], correlation dimension, largest Lyapunov exponent and Lempel Ziv complexity [33]. Besides, other studies have defined organization indices based on the combination of the information provided by several ECG leads [34, 35]. Finally, AF spatiotemporal organization has been recently studied from the analysis of BSPM [26, 36].

The noninvasive estimation of AF organization has different applications, such as the study of AF spontaneous behavior, the prediction of the therapy outcome and the exploration of the autonomic functions [37]. Several previous works have focused on the prediction of the outcome of a variety of therapies, such as electrical cardioversion [38], pharmacological cardioversion [39, 40], ablation [35] and maze surgery [41] through noninvasive AF organization indices. Moreover, other studies reported promising results in the classification between paroxysmal and persistent AF [42–45]. Thereby, since ECG recordings are easy and cheap to obtain, the development of improved methods able to estimate AF organization from single lead ECGs would be very useful to easily provide additional information about AF mechanisms as well as in the development of tailored therapies.

1.2 Hypothesis

According to recent studies, highly disorganized AF produces f-waves with very dissimilar morphologies in the atrial activity extracted from the surface ECG, whereas more organized AF produces more repetitive waveforms [29]. To this respect, AF organization has been successfully estimated from the surface ECG through a nonlinear index [16]. In fact, the use of nonlinear methods in the analysis of biological signals has a particular interest because they can provide "hidden information" related to the underlying physiological mechanisms [46]. Moreover, the behavior of physiological processes is often described in the literature as nonlinear and non-stationary [47]. More concretely, atrial electrophysiological remodeling is a highly nonlinear process [48] and it is commonly accepted that the heart in AF presents a chaotic behavior at a cellular level [49]. Thus, the hypothesis of the present doctoral thesis can be formulated as: since nonlinear metrics estimate the regularity of a time series, the application of different nonlinear indices to the atrial activity pattern extracted from surface ECG recordings could improve the current state of the art in noninvasive AF organization estimation. As a result, these new methods might provide useful clinical information to improve our knowledge of the arrhythmia as well as to contribute in creating tailored therapies for patients in AF.

1.3 Objectives

The objective of this research is to define and optimize new non-invasive AF organization estimators based on the measurement of the atrial activity regularity, complexity and statistical self-similarity using nonlinear metrics. Therefore, a variety of nonlinear indices will be studied together with their ability in the discrimination among different AF organization degrees. More concretely, this research has the following specific objectives:

- Comparative between different regularity estimators applied to AF signals in order to determine which ones are the most promising tools for the study of AF organization.

- Prediction of spontaneous AF termination from the surface ECG by analyzing the regularity of the atrial activity using different nonlinear metrics. Since AF organization increases before the termination, this objective will allow to determine which indices classify between different organization degrees.

- Evaluation of the use of a previous band-pass filtering step in order to improve the diagnostic accuracy of the methods by reducing the effects of noise and ventricular residuals. More concretely, since previous studies have demonstrated that the use of the MAW improves significantly the performance of SampEn, the application of the studied metrics on the MAW will be evaluated.

- Determination of the optimal use of the most accurate index in the estimation of AF organization in order to maximize its diagnostic accuracy. Study of the effect of the parameters needed for the computation of the selected index, together with the computational data length and the sampling frequency of the recordings.

- Study of the AF organization time course prior to paroxysmal AF spontaneous termination through the application of nonlinear indices in order to detect the earliest changes taking place in the atria which lead to the restoration of the heart's normal rhythm. This objective will allow to determine how long can AF spontaneous termination be predicted with the present techniques before it happens.

- Discrimination between paroxysmal and persistent AF patients from short ECG recordings through nonlinear indices. This study is interesting because this application of the indices may become a faster alternative to the use of Holter ECG recordings, thus allowing an earlier intervention that could increase the likelihood of therapy success.

1.4 Structure of the thesis

The remaining of this document is divided into the following chapters.

- **Chapter 2.** In this chapter, the anatomy and physiology of the human heart are briefly explained. Next, the measurement of the heart's electrical activity via surface electrocardiographic recordings is introduced. Finally, the last part of this chapter is focused on AF and its organization estimation methods described in the literature.
- **Chapter 3.** This chapter describes the methodology applied in this study. Firstly, the analyzed databases are introduced. Next, signal preprocessing and extraction of the atrial activity from the ECG are explained. Next, the studied nonlinear metrics are presented. Finally, the different scenarios for the application of the nonlinear indices and the studied databases are described and the statistical analysis is explained.
- **Chapter 4.** In this chapter, the results of the studies introduced in Chapter 3 are systematically presented. These results include the performance of all the studied nonlinear indices in the prediction of AF spontaneous termination, the analysis of AF organization time course prior to its spontaneous termination and the classification between paroxysmal and persistent AF from short ECG recordings.
- **Chapter 5.** This chapter discusses analytically the results presented in Chapter 4, as well as their possible interpretations and clinical implications.
- **Chapter 6.** The conclusions of this work are presented in this chapter. Moreover, some possible future research lines are suggested. Finally, the contributions in scientific journals and conferences are enumerated.

Chapter 2

Heart Physiology, Electrocardiography and Atrial Fibrillation

The objective of this chapter is to provide a general view of atrial fibrillation and its study. Before that, basic concepts of electrocardiography, heart anatomy and heart physiology are introduced for a better understanding of the following sections.

This chapter is structured as follows. The anatomy and electrical activation of the human heart are briefly described in Section 2.1. Section 2.2 explains the basic electrocardiography concepts. Finally, atrial fibrillation is introduced in Section 2.3.

2.1 Heart anatomy and physiology

2.1.1 Heart anatomy

The heart is a muscular organ whose primary function is to pump blood throughout the body. This organ is located in the chest, behind the sternum, between the lungs and above the diaphragm. Located above the heart are the great vessels: the aorta, the pulmonary artery and vein, as well as the superior and inferior vena cava (see Figure 2.1). The heart is surrounded by the pericardium, which is a thin and fibrous bag-like structure. The weight of the human heart is about 250–300 g and its size is about that of a fist [50].

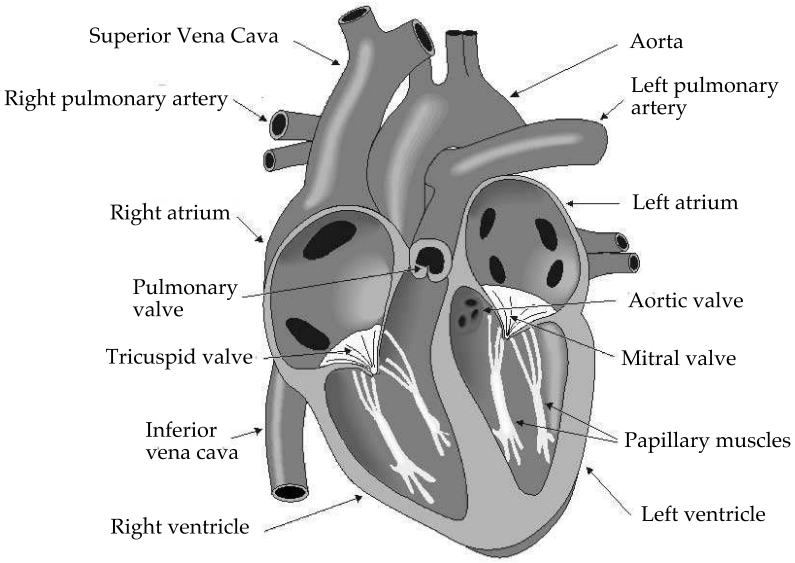

Figure 2.1. Anatomy of the human heart.

The walls of the heart are composed of cardiac muscle, called *myocardium*, which has striations like the skeletal muscle. This organ is divided into four chambers that drive blood into the two circuits that form the cardiovascular system. The upper chambers are the right and left atria and the lower ones are the right and left ventricles, as can be seen in Figure 2.1. The heart is oriented so that the anterior aspect is the right ventricle while the posterior aspect shows the left atrium. Although the cardiovascular system is divided into two separate circuits, both sides of the heart contract in a coordinated fashion. The inner walls of the heart are called the *endocardium*, while the outer wall is called the *epicardium*. Finally, the *septum* is the wall that separates both ventricles. To this respect, as is

shown in Figure 2.1, the septum and the left ventricular free wall are much thicker than the right ventricular free wall. In addition, there are four valves which, under normal conditions, let the blood flow in only one direction: the atrioventricular valves separate the atria from the ventricles, whilst the aortic and pulmonary valves separate the ventricles from the aorta and pulmonary artery, respectively (see Figure 2.1). Blood flow occurs only when there is a difference in pressure across the valves that causes them to open [51].

Regarding the blood flow, the blood from the systemic circulation returns to the heart through the right atrium after circulating through the body. Then, it goes to the right ventricle through the tricuspid valve. The right ventricle pumps blood into the pulmonary artery, through which it goes to the lungs for oxygenation. Oxygenated blood returns to the heart through the left atrium and from there it goes through the mitral valve to the left ventricle. Finally, the left ventricle pumps blood into the systemic circulation through the aorta. While passing through the body, oxygen in the blood is distributed to the tissues and then blood flows back to the heart through the veins [51, 52].

2.1.2 Electrical activation of the heart

Action potential

In the heart muscle cell (*myocyte*), the contraction is triggered by an electric activation. This electric impulse, called *action potential*, is generated by ion currents that flow through specific channels in the cell membrane once the cell's membrane potential has reached a critical value, called the *threshold potential* (see Figure 2.2). During non-activity periods, the cell's membrane potential has a constant value around -80 mV, called *resting potential* [50] and it is said that the cell is polarized. After an electrical stimulation, electric activation takes place from the inflow of sodium ions across the cell membrane, which modifies the intracellular potential (depolarization phase). The amplitude of the cardiac myocyte action potential is approximately 100 mV. Unlike nerve or skeletal muscle cells, a plateau phase follows the cardiac depolarization. Finally, repolarization phase, in which the cell's intracellular potential returns to its initial value, occurs as a consequence of the outflow of potassium ions. The duration of the cardiac myocyte action potential is around 300 ms [50].

After the depolarization, the cell cannot be stimulated again until its membrane potential reaches a certain value, which is approximately 60 mV. This time interval is called *refractory period* and in the cardiac muscle cells its duration is similar to that of the action potential. Another important difference between cardiac muscle and skeletal muscle is that in cardiac muscle the activations can propagate from one cell to another in any direction, generating rather complex activation wavefronts [50].

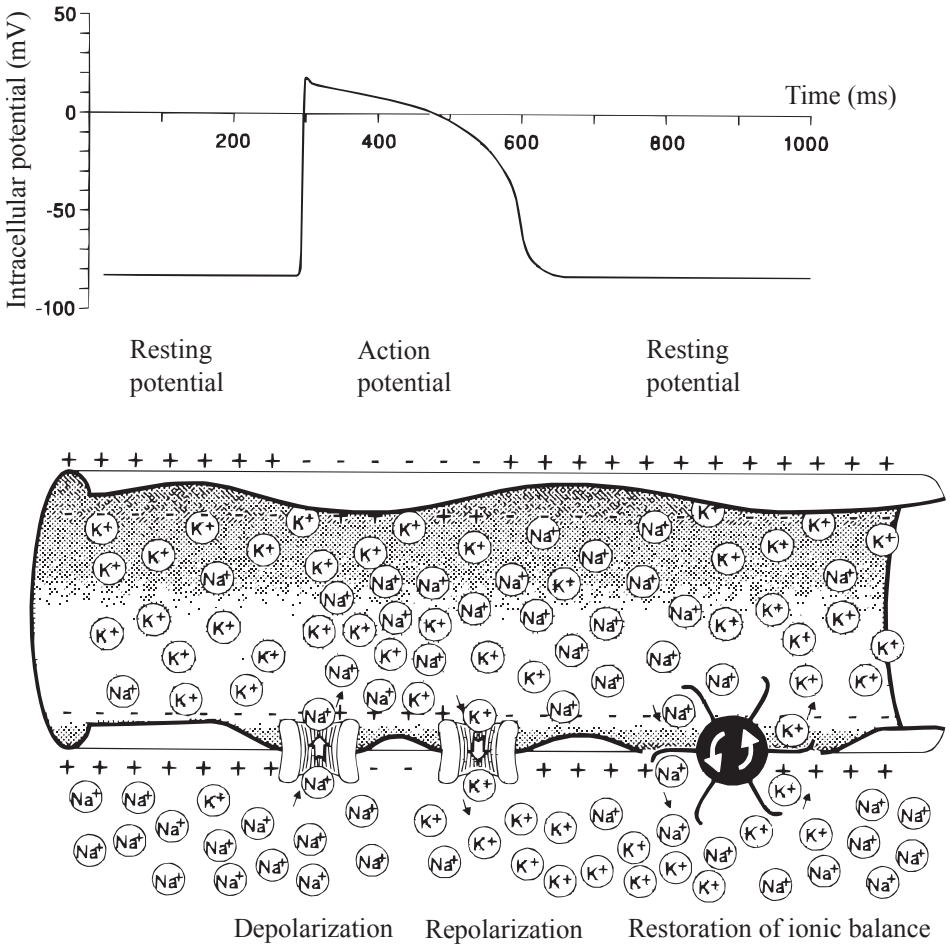

Figure 2.2. Generation of the action potential in the cardiac muscle cell.

Heart conduction system

These electrical impulses are generated and conducted by specialized cells in different regions of the heart, which are known as the heart conduction system (see Figure 2.3) [53]. In a normal heartbeat, the impulse is initiated in the *sinus node* (*sinoatrial or SA node*), which is located in the right atrium at the superior vena cava and consists of specialized muscle cells. The SA node in adult humans is about 10–20 mm long and 5 mm wide and it is located about 1 mm below the epicardium [53]. The SA node cells, which are also called *pacemaker cells*, are self-excitatory and generate an action potential at a rate of about 70 per minute. The activation propagates from the SA node through the atria by cell-to-cell conduction. The conduction velocity of action potentials in the atrial muscle is about

0.5 m/s [54]. The action potentials cause the atrial muscle cells contraction by a process named excitation-contraction coupling [53].

However, in the healthy heart, the activation cannot propagate directly to the ventricles because a nonconducting barrier of fibrous tissue is present [50, 51]. Hence, the action potentials propagate to the ventricles through a specialized region of cells located at the boundary between the atria and ventricles, called the *atrioventricular node* (*AV node*), which slows down the impulse conduction to about 0.05 m/s. This impulse conduction velocity allows sufficient time for a complete atrial depolarization and contraction (*atrial systole*) prior to the ventricular depolarization and contraction (*ventricular systole*) [50,51].

Next, the impulses propagate trough the *Bundle of His*, which separates into two branches along the septum. These specialized fibers conduct the impulses at a very rapid velocity (about 2 m/s). The bundle branches then divide into an extensive system of *Purkinje fibers* that diverge to the inner sides of the ventricular walls. The impulse propagation along these fibers occurs at a relatively high speed (about 4 m/s). Finally, a wavefront is formed in the ventricular wall, which propagates through the ventricular myocardium toward the outer wall by cell-to-cell conduction, causing the ventricular contraction [53, 54]. The waveforms generated by the cells in the different regions of the heart conduction system in a normal heartbeat and the resultant body surface potential (ECG) are displayed in Figure 2.4 [55]. Note that the action potential shape and duration vary depending on the region of the heart where it was generated.

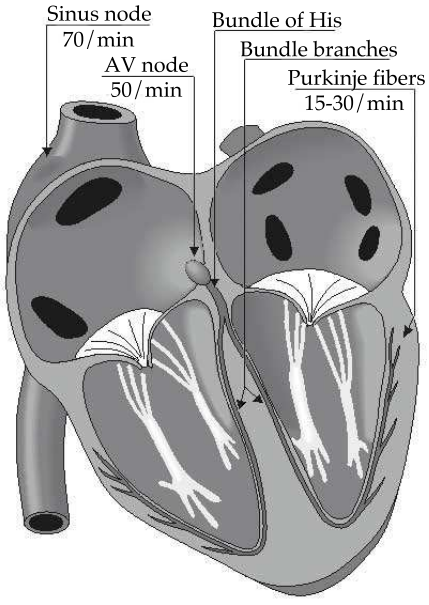

Figure 2.3. The heart conduction system. The intrinsic activation rates of each part are also displayed.

After each cardiac muscle region has been depolarized, repolarization occurs. Although repolarization is not a propagation phenomenon, it appears as if a wavefront propagated from epicardium to the endocardium due to the different durations of the action potential at the different regions of the myocardium [55].

Although all the cells of the heart conduction system are self-excitatory, the intrinsic activation rate of the SA node is higher than those of the other regions, which obliges the rest of cells to follow its rhythm. Hence, in case of SA node dysfunction, the impulse would be generated in a different region of the heart conduction system, thus resulting in a lower heart rate [53, 55]. For instance, the AV node cells present an intrinsic self-excitation frequency of about 50 pulses per minute [51]. In addition, abnormal self-excitation may also happen in the myocardium, which can result in either extra beats or the generation of a new cardiac rhythm for some period of time [53]. In this case, the site that generates the abnormal impulse is called an *ectopic focus*.

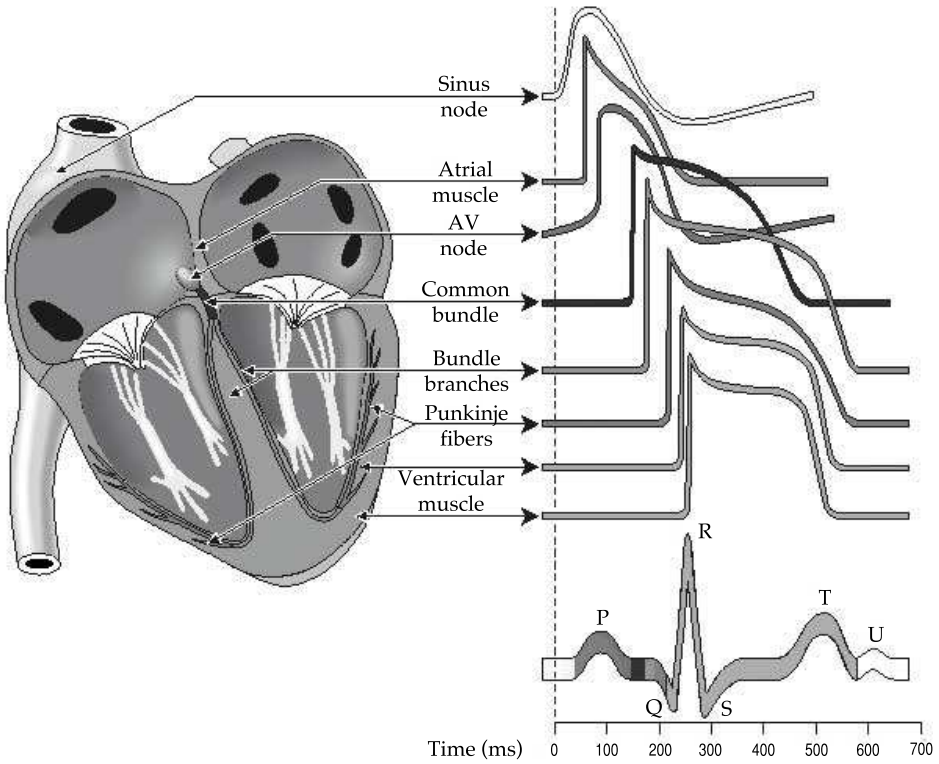

Figure 2.4. Action potential waveforms generated by the cells in each part of the heart conduction system during a normal heartbeat and the resulting surface potential (ECG).

2.2 Electrocardiography concepts

2.2.1 The electrocardiogram

The electrocardiogram (ECG) is a surface recording of the cardiac electrical activity. The body conducts the electrical currents generated by the heart. Hence, every pair of electrodes placed on the body surface may register the electrical activity of the heart, thus constituting an ECG lead [51]. These electrode leads are connected to a device that measures potential differences between selected electrodes, and the resulting signal is called an ECG [53].

2.2.2 Leads of the standard ECG

The standard ECG is composed by 12 beforehand fixed leads. There are two basic types of ECG leads: bipolar and unipolar. In bipolar leads the electrical potentials between a single positive electrode and a single negative electrode are measured. On the contrary, unipolar leads have a single positive electrode and a use combination of other electrodes as a composite negative electrode. In the standard ECG, unipolar leads are divided into two groups, named precordial and augmented leads [53, 56].

Bipolar leads

The three bipolar leads of the standard ECG were defined by Einthoven in 1908. Lead I measures the potential difference between the two arms. By convention, lead I configuration has the positive electrode on the left arm and the negative electrode on the right arm. Lead II has the positive electrode on the left leg and the negative electrode on the right hand. Finally, in lead III the positive electrode is on the left leg and the negative electrode is on the left arm [53]. That is:

$$\begin{aligned} \text{Lead I}: &\quad V_I = \Phi_L - \Phi_R \\ \text{Lead II}: &\quad V_{II} = \Phi_F - \Phi_R \\ \text{Lead III}: &\quad V_{III} = \Phi_F - \Phi_L \end{aligned} \tag{2.1}$$

where V_I, V_{II} and V_{III} are the voltage of leads I, II and III, respectively. Φ_L, Φ_R and Φ_L are the potential of the left arm, right arm, and left foot, respectively.

As can be seen in Figure 2.5, these three leads roughly form and equilateral triangle around the heart, which is called Einthoven's triangle [57]. Moreover, since the limbs can be viewed as long wire conductors, the electrodes can be placed either at the origin of the limb (shoulder or upper thigh) or at its end (wrists and ankles).

In lead I, maximum positive deflection will happen when a wave of depolarization travels parallel to the axis between the right and left arms. Similarly, a wave of depolarization traveling towards the left leg will give a positive deflection in both Leads II and III because their positive electrode is on the left leg. Therefore, Lead II will present a maximal positive reflection when the depolarization travels parallel to the axis between the right arm and the left leg, whilst a maximum positive deflection will be obtained in lead III when the depolarization wave travels parallel to the axis between the left arm and left leg [57].

The positive electrode for Lead I is said to be at zero degrees relative to the heart along the horizontal axis (see Figure 2.6). Similarly, the positive electrodes for Leads II and III are at 60 and 120 degrees relative to the heart, respectively. This construction of the electrical axis is called the Axial Reference System [57]. With this system, the greatest positive deflection in Lead II will occur when a wave of depolarization travels at +60º. Similarly, a wave of depolarization oriented +90º relative to the heart will produce equally positive deflections in both Lead II and III. In this latter case, no deflection will be shown in Lead I because the wave of depolarization is heading perpendicular to the 0º.

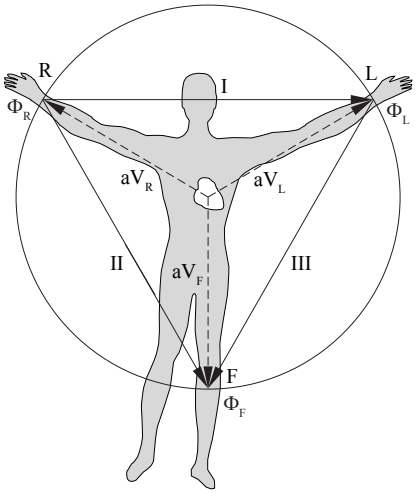

Figure 2.5. Limb leads: bipolar (I, II and III) and augmented (aV_L, aV_R and aV_F) leads. The bipolar leads roughly form an equilateral triangle (Einthoven's triangle), which has its center at the heart.

Augmented leads

Augmented leads have a limb positive electrode which is referenced against the average potential of the two remaining electrodes. Therefore, Lead aV_L has its positive electrode located on the left arm, whilst the positive electrode for Lead aV_R is located on the right arm and the positive electrode location for Lead aV_F is on the left leg (see Figure 2.5) [53]. Thus, the potentials of these leads are given by the following expressions:

$$\begin{aligned} aV_R &= \Phi_R - \tfrac{\Phi_L+\Phi_F}{2} \\ aV_L &= \Phi_L - \tfrac{\Phi_R+\Phi_F}{2} \\ aV_F &= \Phi_F - \tfrac{\Phi_R+\Phi_L}{2} \end{aligned} \tag{2.2}$$

These leads, coupled with the three bipolar leads, represent the activity in the frontal plane relative to the heart, as can be seen in Figure 2.6 [53]. Following the axial reference system, Lead aV_L is at -30 degrees relative to the Lead I axis, Lead aV_R is at -150 degrees and Lead aV_F is at 90 degrees. Hence, these six leads allow to define the direction of an electrical vector at any given instant in time [57]. For instance, Lead I will show the greatest positive amplitude if a wave of depolarization is spreading from right-to-left along the 0º axis. Likewise, if the direction of the electrical vector for depolarization is directed downwards (+90º), then aV_F will show the greatest positive deflection. If a wave of depolarization is moving from left-to-right at +150º, then the greatest negative deflection will be produced in Lead aV_R [57].

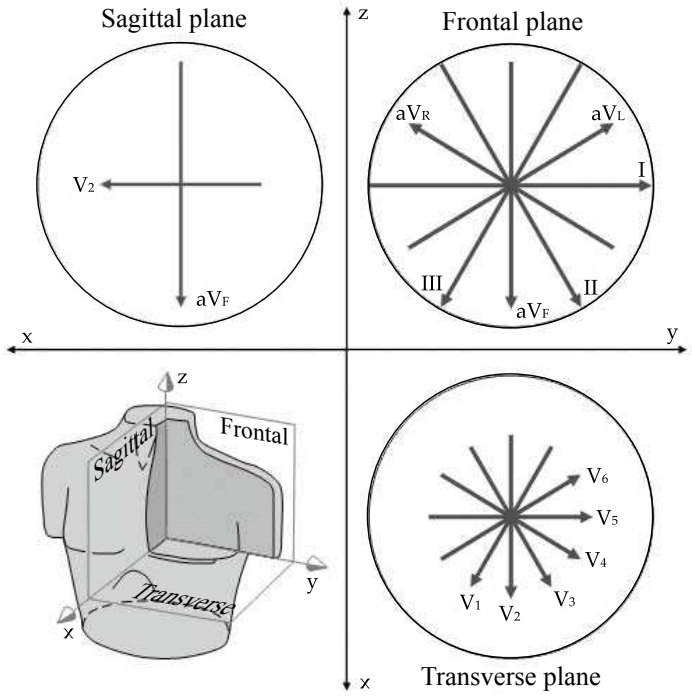

Figure 2.6. Projection of the 12-lead ECG system in three orthogonal planes.

Precordial leads

In order to record the heart electrical activity in a plane perpendicular to the frontal plane, the six precordial leads were defined by Wilson in 1944. The positive electrodes for these leads are located on the chest and their locations are displayed in Figure 2.7. The positive electrodes for Leads V_1 and V_2 are located at the fourth intercostal space, on the right and left border of the sternum, respectively. Lead V_4 has its positive electrode in the midclavicular line at the fifth intercostal space. The positive electrode for lead V_3 is located between those of leads V_2 and V_4. Finally, the positive electrodes for leads V_5 and V_6 are located at the same horizontal level as V_4, in the anterior axillary line and the midaxillary line, respectively [53].

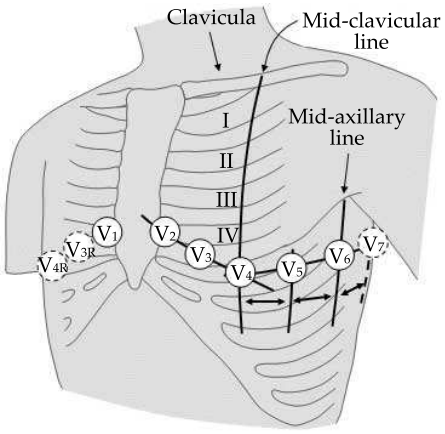

Figure 2.7. Locations of the positive electrodes for the precordial leads.

Regarding the reference for these leads, the ideal reference point would be located in the infinite. As a solution, Wilson proposed the use of the Wilson Central Terminal (WCT) as a reference for these unipolar leads. This reference was obtained by connecting a 5 kΩ resistor from each terminal of the limb leads to a common point (see Figure 2.8) [57]. Hence, the potential of the WCT is given by the following expression:

$$\Phi_{CT} = \frac{\Phi_R + \Phi_L + \Phi_F}{3} \tag{2.3}$$

Since the addition of the Einthoven triangle vertexes potentials is approximately zero, the potential of the WCT is approximately equal to that of a point located in the infinite. Therefore, the WCT can be considered as a satisfactory reference. Regarding the values of the resistors, the value of 5 kΩ is still widely used. However, modern ECG amplifiers present high input impedance values, which would allow the use of much higher resistances in order to increase the CMRR

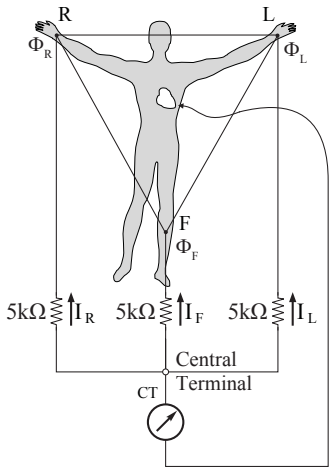

Figure 2.8. Wilson Central Terminal.

(common-mode rejection ratio) and decrease the size of the artifact introduced by the electrode/skin resistance [57].

Precordial leads are interpreted analogously to the limb leads. For example, a depolarization wave traveling towards a particular electrode on the chest will produce a positive deflection in that lead [57].

Content of the standard ECG

In principle, given that the cardiac source can be described as a dipole, the heart electrical activity could be completely described using a combination of only three leads: two of the limb leads for the frontal plane components plus one precordial lead for the anterior-posterior component. The lead V_2 would be a very good precordial lead choice since it is directed closest to the x axis. It is roughly orthogonal to the standard limb plane, which is close to the frontal plane (see Figure 2.6). Hence, the 12-lead ECG could be thought to have three independent leads and nine redundant leads [57]. However, the precordial leads are located close to the frontal part of the heart and thus they detect also non-dipolar components which have diagnostic significance. Therefore, the 12-lead ECG system has eight truly independent and four redundant leads [57].

Despite the existence of redundant information in the ECG leads, all 12 leads are usually recorded in order to enhance pattern recognition. As can be seen in Figure 2.6, this combination of leads gives the clinician an opportunity to compare the projections of the resultant activity in two orthogonal planes and at different angles.

2.2.3 Composing waves of the ECG

The normal ECG waves are illustrated in Figure 2.9. The various waves and complexes formed by the electrical activity of the heart have been labeled (in alphabetical order), P wave, QRS complex, T wave and U wave [56].

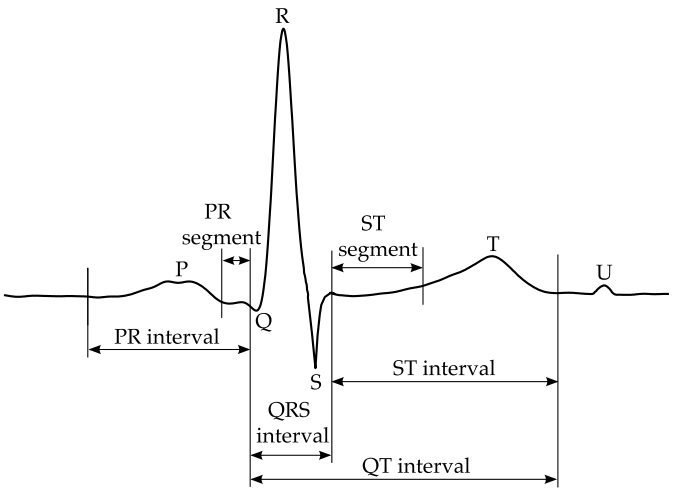

Figure 2.9. Waves of the normal ECG.

Since the impulse is generated in the SA node under normal conditions, the first wave of the ECG, called the P wave, is caused by the atrial depolarization. Normal P wave duration is usually < 100 ms [53]. After its propagation along the atrial wall, the electrical activation reaches the AV node. The propagation of the impulse through the AV node induces a delay in the propagation of the activation, which is reflected in the PR segment. Due to the small amount of cells involved in the conduction of the impulse along the AV node and the Bundle of His, the PR segment is an isoelectrical line. Next, the activation reaches the ventricles, producing the QRS complex, which reflects the ventricular depolarization. The first negative deflection after the P wave is called the Q wave, the R wave is defined as the first positive deflection after the P wave and the S wave is defined as the first negative deflection after the R wave. The typical QRS complex duration is about 70 ms. Finally, the repolarization of the ventricles produces the T wave. The QRS complex and T wave present higher amplitudes than the P wave because more cells are involved in their generation. Note that atrial repolarization cannot be seen in the normal ECG because it happens during the ventricular depolarization and, thus, it is concealed by the QRS complex, which has a much higher amplitude. The segment between the QRS complex and the T wave, named ST segment, is usually an isoelectric line. Sometimes, a small additional wave, called U wave, can be appreciated after the T wave. The significance of this wave is uncertain, but it may be due to the repolarization of the Purkinje System. Nevertheless, the interval between the end of the T wave and the P wave

is generally an isoelectrical line, named baseline. In addition, the RR interval, which is defined as the time interval between two consecutive R waves, defines the instantaneous heart rate [56].

2.2.4 Diagnosis

Since changes in the cardiac electrical activity or the volume conductor are reflected in the ECG, its analysis provides a useful tool for clinical diagnosis. In this sense, the interpretation of the ECG includes both the morphology of the waves and complexes and the timing of events and pattern repetitiveness over many beats. The ECG can be used in the diagnosis of a wide variety of abnormalities and diseases, such as [57]:

- Coronary artery disease. A disease in which blood flow to the heart and body is restricted due to hardening of the arteries (atherosclerosis).
- Heart attack, either previous or current. It alters the cellular action potentials and the propagation of the impulse and therefore it produces changes in the ECG. Thus, the ECG becomes essential for the diagnosis of heart attack.
- Arrhythmias. The term arrhythmia refers to a disturbance of the normal heart rhythm, which can be divided in to abnormally fast (tachycardias) or abnormally slow (bradycardias) heart rhythms. Although the standard ambulatory 12-lead ECG allows to diagnose some types of arrhythmias, other abnormalities are short lived and, thus, their diagnosis requires a prolonged Holter ECG monitoring. A particular case of arrhythmia is atrial fibrillation, which will be explained in Section 2.3.
- Cardiac hypertrophy. An enlarged cardiac cavity or thickened heart muscle.
- Cardiomyopathy. A disease in which the heart muscle functions improperly due to a variety of conditions.
- Pericarditis. Inflammation of the pericardium.
- Long QT syndrome. A disorder of the heart electrical system, which could lead to fainting (syncope) or sudden cardiac death.
- Myocarditis. Inflammation of the heart muscle due to viral or bacterial infection.
- Conduction defects. Alteration of the structures comprising the heart conduction system or presence of accessory pathways. For instance, in the Wolff-Parkinson-White syndrome, accessory atrioventricular pathways are present.
- Ionic effects. Abnormal extracellular ions concentrations may alter the cardiac electrical activity and produce changes in the ECG.

2.3 Atrial Fibrillation

2.3.1 Definition and epidemiology

Atrial fibrillation (AF) is the most common sustained arrhythmia found in clinical practice [1]. It is estimated that AF is present in 1–2% of the general population, affecting over 6 million Europeans [2] and 2.2 million North Americans [58]. AF prevalence is higher in men than in women [3] and increases progressively with age [1], rising to 5–15% in patients aged 80 years or over [3]. To this respect, the median age of AF patients is 75 years and the patients aged 80 years or older represent about 36% of all AF cases [59]. Thus, it is expected that AF prevalence will increase significantly in the next decades due to the aging of the population [5]. This increase in AF prevalence is expected to be more pronounced in the oldest age group [1]. Currently, AF accounts for more than one third of all hospitalizations due to cardiac arrhythmias [60]. As a consequence, AF has a significant impact on the economy. In fact, its management represents at least 15% of the healthcare budget in cardiac diseases in Europe and North America [4].

AF is a supraventricular tachyarrhythmia characterized by fast and uncoordinated atrial activations, causing the atria to be unable to be contracted effectively [2]. As a consequence, the atria are unable to pump blood, which causes a reduction of 5–15% in the cardiac output [2]. Besides, the lack of atrial effective contraction produces stagnant blood flow, especially in the atrial appendage, and predisposes to clotting. The dislodgement of a clot from the atrium results in an embolus. The most feared complication of AF is stroke, which occurs when an embolus is lodged in the brain. Moreover, an embolus can also affect other organs, such as the kidneys or the heart itself [61]. Hence, although AF itself does not represent a life-threatening condition, this arrhythmia is associated with an increased risk of stroke and all-cause mortality [1, 3]. In this sense, it is estimated that AF causes 15–25% of all strokes [62], and thus the increased mortality risk in AF patients is in part due to stroke. Moreover, death rates are doubled in AF patients independently of other death predictions [3].

On the other hand, during normal sinus rhythm heart rate is about 60 beats per minute at rest and 180 to 200 beats per minute at peak exercise. In contrast, during AF the atrial cells fire at rates of 400 to 600 times per minute [61]. However, due to the filtering function of the AV node, this disorganized atrial activity produces an irregular conduction of impulses to the ventricles and, as a result, the heartbeat becomes uneven [2], with a rate typically around 150 beats per minute in the absence of therapy [61]. Hence, the ventricular rate during AF is determined by the interaction between the AV node and the atrial activity [61]. As a consequence, AF is usually accompanied by symptoms related to the rapid and irregular heart rate, such as palpitations and exercise intolerance [63].

On the ECG, AF is characterized by the absence of P-waves, which are replaced by low-amplitude wavelets, known as fibrillatory waves (f-waves), that

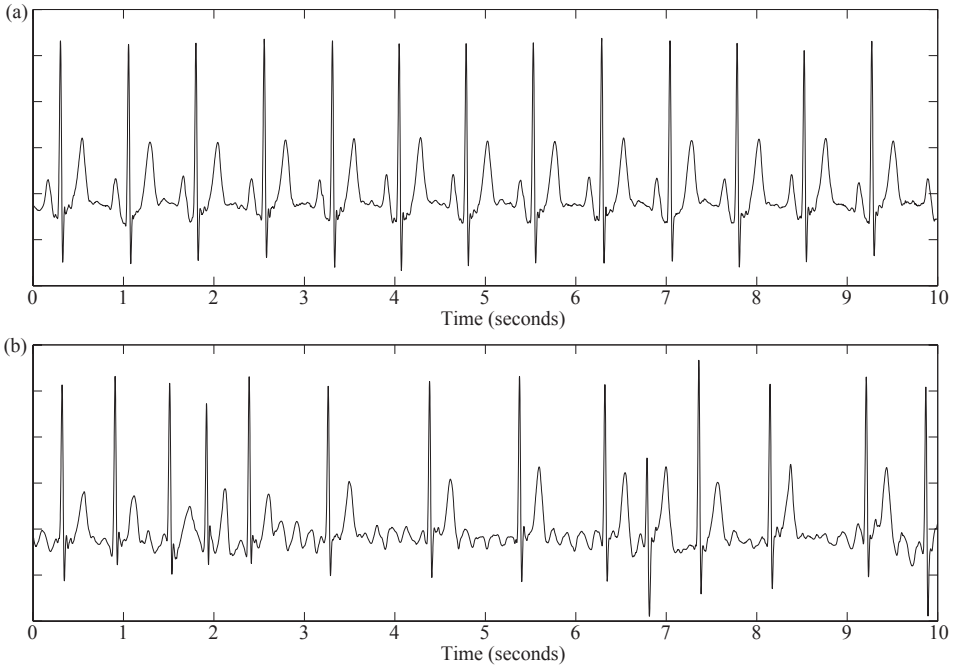

Figure 2.10. Surface ECG examples of (a) Normal Sinus Rhythm and (b) Atrial Fibrillation episode. Both ECG recordings are from the same patient. Note that in AF P-waves are replaced by lower amplitude f-waves and the ventricular rate becomes irregular.

are irregular in shape, amplitude and timing [6]. The differences between normal sinus rhythm and AF can be seen in Figure 2.10. Moreover, AF can be distinguished from atrial flutter because this latter arrhythmia shows a more regular atrial activity, with a rate of about 300 beats per minute, which produces characteristic saw-toothed atrial waves on the ECG. Since the ECG reflects the electrical activity of the heart, it provides a noninvasive tool for the study of AF. In this sense, leads V_1 and II present the highest atrial to ventricular amplitude ratio [6] and thus they are frequently selected for the study of the atrial activity.

2.3.2 Classification of AF

AF can appear in different stages, based on the presentation and duration of the arrhythmia episodes [2]:

- *Paroxysmal*: The arrythmia can terminate spontaneously and AF episodes last from seconds up to several days. Usually paroxysmal AF episodes last less than 48 hours. Although the probability of spontaneous termination after 48 hours in AF is low, paroxysmal AF episodes may last up to seven days.

- *Persistent*: Its termination requires an intervention, such as pharmacological or electrical cardioversion. AF episodes lasting more than seven days are considered persistent. In addition, the term *long-standing persistent AF* is applied when AF has lasted for more than a year.

- *Permanent*: The reversion to sinus rhythm is not possible or not recommended.

Moreover, paroxysmal AF episodes often become longer and more frequent as the arrhythmia progresses [2], and many patients eventually develop persistent AF [9]. In fact, it has been estimated that only 2–3% of AF patients remain in paroxysmal AF over several decades [9].

Besides, when no other atrial fibrillation episodes were observed before in the patient, the arrhythmia is referred to as *first detected*, regardless of its duration and its related symptoms. On the contrary, when two or more atrial fibrillation episodes are observed in the same patient, it is called *recurrent* AF [2].

On the other hand, the term *silent* AF is applied when the arrhythmia is asymptomatic and thus it may first manifest as an AF-related complication, such as a transient ischemic attack or a stroke [63]. To this respect, it is not uncommon to identify AF on a routine physical examination or ECG recording. In this case, the arrhythmia may be in any of its temporal stages and may remain undiagnosed for a long time [2]. According to the literature, approximately 15–30% of AF patients are asymptomatic [63].

Finally, the term *lone* atrial fibrillation applies to AF patients without clinical evidences of cardiopulmonary pathology. Lone AF patients who are under 65 years of age have the best prognosis [2].

2.3.3 Mechanisms of AF

The physiological mechanisms causing the onset and termination of AF are still not fully understood [11] and, thus, the outcome of the therapies is still unsatisfactory [2, 64]. With respect to AF onset, previous studies have reported that AF can be initiated by rapidly firing atrial ectopic foci, which are generally located in one or several of the pulmonary veins [65] (see Figure 2.11). Additionally, foci may also occur in the right atrium and infrequently in the superior vena cava or coronary sinus. Although the focal origin of AF is supported by experimental models, it is thought to be more important in paroxysmal AF than in persistent AF [2]. In this sense, previous studies have reported that pulmonary vein ablation is much more effective in paroxysmal AF than in persistent AF [2, 66].

Regarding the mechanisms involved in AF perpetuation, several hypotheses have been proposed in the literature. A well-known hypothesis to explain AF maintenance that has been widely accepted for many years was postulated by

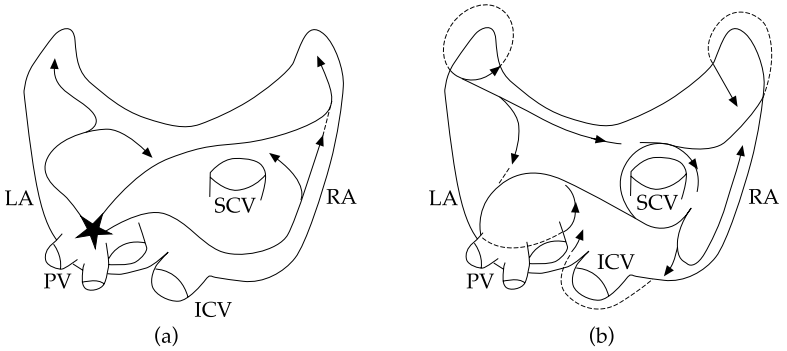

Figure 2.11. Electrophysiological mechanisms of AF. (a) Focal activation. The originating focus (represented by an asterisk) is often located in the region of the pulmonary veins. The arrows represent the propagation of the wavelets. (b) Multiple wavelets (reentries). The routes of the wavelets (indicated by arrows) vary along the time. LA: left atrium. RA: right atrium. PV's: pulmonary veins. SCV: superior cava vein. ICV: inferior cava vein.

Moe in 1962 [67]. This hypothesis is based on the fractionation of the wavefronts as they propagate through the atria, which results in a continuous propagation of multiple wavelets, called reentries [67]. To this respect, the number of simultaneous wavelets would depend on the atrial refractory period, mass, and conduction velocity [11]. Moreover, these parameters present severe inhomogeneities in AF [68]. For instance, large atria and short refractory periods would increase the number of simultaneous reentries. Furthermore, theoretical models as well as invasive studies both in humans and animals have reported results consistent with this hypothesis [69, 70]. In this sense, several studies have reported a decrease in the number of reentries before AF termination, thus generating simpler waveforms [69, 71, 72]. Consequently, during AF termination, f-waves evolve to P-waves [6]. Moreover, according to previous studies, the number of circulating wavelets in the atria is inversely related to the likelihood of spontaneous termination in paroxysmal AF [70]. Thus, sustained AF would likely have more simultaneous reentries than non-sustained AF.

On the other hand, different authors have suggested that AF is driven by a small amount of localized focal sources, named rotors in the literature [73]. According to this hypothesis, the activation wavefront rotates surrounding a pivot point, which remains unexcited, but not refractory, thus allowing the source to drift [73,74]. This pivot point is known as rotor or phase singularity. A stationary rotor would produce a spiral wavefront, whereas a meandering rotor would produce more complex excitation patterns, depending on its trajectory [74, 75]. Due to the curvature of the wavefront, the wavelength in a spiral wave is not constant and depends on the distance from the source [74]. A three-dimensional representation of a spiral wave is called scroll wave and its center of rotation is a filament whose shape may vary depending on the substrate [74]. Recent studies in animals [76] and humans [77, 78] support the presence of rotors in the atria during AF. Furthermore, some authors have suggested that rotors could produce multi-

ple wavelets if the spiral wavefront hits an anatomical obstacle [79]. However, the current evidences supporting rotors as the main mechanism of AF maintenance in humans are still insufficient [80]. In this sense, several high-density mapping studies did not detect stable rotors in the atria during AF [81, 82]. Thus, the possible contribution of rotors to AF perpetuation is still an open issue.

Finally, a different hypothesis based on the heterogeneity of the atrial substrate has been proposed recently to explain AF maintenance [81]. In the normal healthy atrium, there are no significant differences between epicardial and endocardial activations. However, in AF patients, the alteration of the atrial tissue properties produces a progressive dissociation between epicardial and endocardial activation patterns [83]. As a consequence, fibrillation waves would be able to propagate between epicardium and endocardium, thus increasing the overall complexity of the atrial activation patterns [83, 84]. Hence, this transmural conduction may contribute to AF perpetuation [83]. Mapping studies, both in animals and humans, have detected breakthrough waves in the epicardium whose appearance cannot be explained by propagation in the epicardium [81,85]. Moreover, breakthrough waves were more frequent in persistent AF than in paroxysmal AF [81, 85]. Furthermore, the simultaneous mapping of endocardial and epicardial activations in a goat model revealed an increase in the dissociation between the activations in both layers as AF progressed [85]. These observations are consistent with the double layer hypothesis.

Regardless of the mechanisms explaining AF, previous studies have reported that the presence of AF alters the atrial electrophysiological properties in a way that promotes the arrhythmia perpetuation [7, 8]. These changes are known as atrial remodeling and include electrical, structural and contractile alterations in the atrial tissue [68]. To this respect, a shortening in the atrial effective refractory period after AF onset has been documented both in animal models [7] and humans [86]. Moreover, the initiation and perpetuation of reentries may also be facilitated by enhanced connective tissue deposition and fibrosis, which forms patchy areas of fibrotic tissue, thus increasing the atrial tissue heterogeneity [68, 82,87]. Finally, AF is often related to an increased atrial size, which allows the existence of simultaneous reentries, thus favoring the arrhythmia perpetuation [68].

2.3.4 Treatment of AF

The main goals of AF treatment are to prevent severe complications associated with this arrhythmia, such as stroke, and to reduce the symptoms. Several approaches are used in the treatment of this arrythmia [2]:

- Anticoagulants are often administered to prevent thromboembolism, which is one of the main complications associated with AF. In particular, anticoagulants are used before cardioversion because most thromboembolic events occur shortly after cardioversion [68]. However, the use of anticoagulants increases the risk of bleeding complications.

- Rate control medications are used to slow down the rapid heart rate associated with AF and reduce the symptoms related to a high and irregular ventricular rate [88]. These treatments may include drugs such as digoxin, beta blockers (atenolol, metoprolol, propranolol), amiodarone, disopyramide, calcium antagonists (verapamil, diltiazam), sotalol, flecainide, procainamide, quinidine, etc [2].

- Electrical cardioversion (ECV) may be used to restore normal heart rhythm with an electric shock. A disadvantage of this therapy is that it requires the use of anesthesia [89].

- Pharmacological cardioversion has a lower conversion rate than ECV, but it does not require the use of anaesthesia. In this sense, several drugs, such as ibutilide and propafenone, can restore sinus rhythm [89].

- Catheter ablation may be effective in persistent AF patients when medications do not work. In this procedure, thin and flexible tubes are introduced through a blood vessel and directed to the heart muscle [2]. Then a burst of radiofrequency energy is delivered to destroy or isolate tissue that triggers abnormal electrical signals, such as the pulmonary veins, or to block abnormal electrical pathways [90].

- Surgery can be used to disrupt electrical pathways that maintain AF by dividing the atria into electrically isolated areas. This technique is known as maze surgery. Surgical ablation is an alternative to surgical incisions, which allows faster procedures [90]. There are different possible forms of surgical ablation depending on its energy source, such as high-density focused ultrasound ablation, radiofrequency ablation and cryoablation [90].

- Atrial pacemakers can be implanted under the skin to regulate the heart rhythm.

Chapter 3

Materials and Methodology

In this chapter, the importance of the estimation of AF organization from the surface ECG is explained. Next, the studied metrics, as well as their application in the analyzed scenarios, are introduced. A variety of nonlinear indices, such as Fuzzy Entropy, Spectral Entropy, Lempel-Ziv Complexity and Hurst Exponents, have been proposed as possible noninvasive AF organization estimators. In addition, the two most well-know noninvasive AF organization indices, namely, the Dominant Atrial Frequency and Sample Entropy, have been included in the study as references.

This chapter is structured as follows. The studied databases are presented in Section 3.1. Next, atrial fibrillation organization and its estimation methods are explained in Section 3.2.1. Regarding the methodology of the present study, Section 3.2.2 presents the signal preprocessing and the extraction of the atrial activity from the ECG recordings. Next, since nonlinear metrics are sensitive to the presence of noise [16,91], a strategy to improve their performance through band-pass filtering is presented in Section 3.2.3. Section 3.2.4 introduces the studied metrics. Next, Section 3.2.5 describes the evaluation of the different nonlinear indices

in the estimation of AF organization and two different applications of the index that provided the best results are presented. Finally, Section 3.2.6 contains the performed statistical analysis.

3.1 Materials

In this doctoral thesis, the studied nonlinear indices have been applied in the discrimination of events related with AF organization in different scenarios. Since the use of a single database for all the proposed scenarios was not possible, a different database was analyzed for each test. Firstly, the ability of the studied metrics in the prediction of AF spontaneous termination was tested in order to assess their performance in the discrimination between different AF organization degrees. Next, the most accurate predictor of AF spontaneous termination was applied in the estimation of AF organization in two different scenarios: the study of the early prediction of AF spontaneous termination and the discrimination between paroxysmal and persistent AF from short ECG recordings. The studied databases are described in the following subsections.

3.1.1 Database analyzed in the prediction of AF termination

The AF Termination Database (AFTDB) [92], which is available at Physionet [93], was analyzed in order to assess the performance of the metrics that will be presented in Section 3.2.4 in the discrimination between different AF organization degrees. This database was selected because it has been analyzed in many previous works (see Table 5.1 in Chapter 5) and, thus, it could be considered as a reference database for the assessment of the performance of new methods. Besides, the use of a public database ensures that the selection of the recordings is not biased in benefit of any particular method. The AFTDB database contains 80 two-lead (II and V_1), 1 minute long Holter recordings of paroxysmal AF, sampled at a frequency of 128 Hz and digitized with 16-bit and 5 μV resolution. These signals are divided into three groups with different organization degrees:

1. Non-terminating AF episodes (group N, 26 signals), in which the arrhythmia was maintained for at least 1 hour after the end of the recording. Thus, the signals in this group, compared with the other groups in this database, present the lowest organization degree.
2. Immediately-terminating AF episodes (group T, 34 signals), which reverted to sinus rhythm 1 second after the end of the recording. These signals, compared with the other two groups, present the highest organization level.
3. Soon-terminating AF episodes (group S, 20 signals), whose termination happened within 1 minute after the end of the recording. These signals were extracted from the same AF episodes as some of the signals in group T.

3.1.2 Database studied in the early prediction of AF termination

Since the AFTDB only allows to analyze the last two minutes before AF spontaneous termination, a different database was analyzed in order to study the time course of AF organization prior to the termination. Thereby, 24-h ECG Holter recordings from 42 different PAF patients (26 men, mean age of 65.3 ± 7 years) with AF episodes lasting more than 2 hours were selected for this study. All the patients were under antiarrhythmic drug therapy with Amiodarone, anticoagulant therapy according to the guidelines for AF management [2] and none of them suffered from heart disease, hyperthyroidism or pulmonary disease. AF episodes were defined by absence of P-waves and irregular heart rhythm. The time course of AF organization was estimated over the longest AF episode of each recording. In addition, ECG segments from the same patients were selected 1 hour after the onset of the arrhythmia in order to compare their indices values with those from a time interval prior to AF termination long enough to detect changes indicative of the termination. These signals were digitized at 125 Hz and 16-bit resolution.

3.1.3 Database analyzed in the discrimination between paroxysmal and persistent AF

The application of the studied nonlinear metrics in the classification between paroxysmal and persistent AF required a different database because in the previous studies only paroxysmal AF recordings were analyzed. Thus, 24-hours Holter ECG recordings from 61 different patients with AF were selected for this study. These signals were digitized at 125 Hz and 16-bit resolution. Since ambulatory ECG recordings usually present a duration of few seconds, 10 seconds segments were selected from the recordings.

Paroxysmal AF (PAF) recordings were identified as showing AF episodes, which were defined by an irregular ventricular rate and the absence of a visible P wave, interrupted by normal sinus rhythm. In this sense, 32 of the Holter recordings corresponded to PAF and a total number of 100 PAF episodes, with durations ranging from 1 minute to 1170 minutes (mean duration 90.50 ± 187.11 minutes) were identified. The central 10 seconds of each PAF episode were selected for the analysis because previous works have shown that PAF presents higher organization near its onset and termination [94, 95]. Therefore, by selecting the central part of each episode the worst case is considered.

In the remaining 29 recordings AF was present during the whole 24 hours and no other supraventricular rhythm was found. These patients were classified as having persistent AF and their 10 seconds segments were selected randomly from the whole Holter recording. A total number of 100 ECG segments of persistent AF were selected for this study.

3.2 Methodology

3.2.1 Atrial Fibrillation organization estimation

Despite the incomplete understanding of AF mechanisms, previous studies have reported that AF organization, defined as the degree of repetitiveness of the atrial activity (AA) signal pattern [15], correlates with the likelihood of AF termination [16]. In the literature, AF organization has been related to the number of wavelets wandering the atrial tissue [15, 69, 96]. In this sense, the presence of fewer wavelets would produce a more repetitive pattern and, therefore, a higher degree of organization. Moreover, the different f-waves morphologies would reflect different activation patterns related to different amounts of reentries in the atrial tissue [17]. Thus, the study of AF organization plays an important role in the exploration of the mechanisms causing the onset, maintenance and termination of the arrhythmia. In addition, the estimation of AF organization could provide relevant clinical information on AF and, thus, it could contribute to improve AF treatment and help to make the appropriate decisions on its management [97]. Hence, various methods to estimate AF organization both from invasive and non-invasive recordings have been presented in the literature.

Invasive methods

In general, invasive cardiac recordings are known as electrograms (EGMs). There is a variety of atrial EGM modalities, including endocardial and epicardial mapping [98]. Invasive organization estimation methods were primarily introduced because the atrial signal presents a notably higher amplitude in invasive recordings than in the surface ECG. Over the years, several techniques have been described in the literature. AF temporal organization can be studied through the analysis of the signal's dynamic complexity in single-lead EGMs. Another approach is to analyze the coordination between electrical activations in multi-site measurements in order to study AF spatiotemporal organization. This latter approach allows to investigate the propagation of wavefronts through the atria and the dispersion of different electrophysiological parameters, such as the refractory period or the conduction velocity, along the atrial tissue [99].

The first invasive techniques to study AF organization were based on the direct observation of the signal [8]. To this respect, Wells et al. [100], classified atrial fibrillation EGMs into different categories based on the discreteness of the electrogram and the stability of the baseline. According to the classification proposed by Wells, *Type I AF* is characterized by discrete activity complexes separated by a clear isoelectric baseline, while *Type II AF* presents discrete atrial activity complexes. In this case, the baseline shows continuous perturbations. Finally, *Type III AF* is characterized by highly fragmented atrial EGMs, with no discrete complexes or isoelectric intervals.

However, the use of automatic methods could be more reliable than observation. In this sense, Barbaro et al. [101] tested several time and frequency domain metrics to classify among AF organization levels using Well's criteria. Moreover, Sih et al. [15] estimated AF organization using the mean-squared error in the linear prediction between two linear electrograms and classified between non-fibrillatory and fibrillatory rhythms. Additionally, Botteron et al. estimated AF spatial organization from the cross-correlation function of atrial EGMs [102]. Furthermore, AF organization has been estimated from the atrial activations morphological similarity [14, 19, 20, 103]. For instance, Faes et al. [14] applied minimum distance analysis to classify between AF organization degrees using Well's criteria. Moreover, Nollo et al. [19] classified among Well's AF categories using correlation waveform analysis. In addition, the coupling between two atrial EGMs has also been studied analyzing the waveforms similarity [103]. Finally, Ravelli et al. [20] analyzed AF spatiotemporal organization through the use of wave similarity maps and found differences between paroxysmal and persistent AF patients.

On the other hand, several authors have applied linear analysis techniques in the study of atrial EGMs [18]. To this respect, the most typical application of linear analysis is to determine the fibrillatory rate or its inverse, named the dominant atrial cycle length (DACL) [18]. For instance, Jais et al. [104] studied the heterogeneity of the DACL among different atrial regions. Regarding the applications of spectral analysis in the study of atrial EGMs, frequency mapping has been used to identify the sources maintaining AF in order to improve the efficiency of ablation therapies [105] because rapid and periodic activity usually appears in sites that are closely linked to foci. In this sense, high frequency sites near the pulmonary veins are often present in paroxysmal AF patients. In addition, frequency gradients between the left and right atria have also been investigated and differences between paroxysmal and persistent AF were reported [106]. Moreover, Ropella et al. [107] studied the spectral coherence between pairs of EGMs and reported much higher synchronization levels between EGMs in the 1–59 Hz band in non-fibrillatory than in fibrillatory rhythms. Besides, other authors have studied the relationship between the amplitude of the harmonic peaks and the defibrillation outcome [108].

A different approach in the estimation of AF organization from invasive recordings is the use of nonlinear indices. To this respect, recent observations suggest that the cardiovascular regulation mechanisms present nonlinear interactions [109]. Moreover, a chaotic behavior can be observed at a cellular level in AF [49] and atrial electrophysiological remodeling is a highly nonlinear process [48]. Therefore, the nonlinear study of AF organization may provide useful information on the arrhythmia mechanisms. In this sense, Hoekstra et al. [21] classified among different AF organization degrees through the measurement of correlation dimension and correlation entropy of atrial electrograms. Additionally, this previous work reported the existence of scaling regions in the atria, thus suggesting the existence of coordinated atrial activation patterns during AF. Correlation dimension [110] and correlation entropy [22] have also been applied to

EGMs registered in different atrial sites in order to estimate AF spatial organization. On the other hand, AF spatiotemporal organization has been studied from the recurrence plot quantification of the atrial electrogram [24, 25] and a certain degree of local organization was reported. Moreover, different entropy measurements, such as Shannon's entropy [23], SampEn, multiscale SampEn and causal entropy [111] have been applied in the study of AF spatiotemporal organization. Additionally, Shannon's entropy has been applied to the atrial EGM to identify complex fractionated electrograms [112], which have been identified as targets for AF ablation. Finally, Mainardi et al. [113] defined a synchronization index from the corrected cross-conditional entropy between two atrial EGM signals. In this latter study, nonlinear methods were more accurate than the linear strategies in the discrimination between fibrillatory and non-fibrillatory rhythms.

Noninvasive methods

Since surface ECG recordings allow to record data for long periods of time and they are easy and cheap to obtain, the noninvasive estimation of AF organization would be very interesting from a clinical point of view. In addition, the use of noninvasive methods would avoid the risks associated with invasive recordings [6]. Moreover, previous studies have shown that the surface ECG reflects the intraatrial activity organization [114, 115]. Hence, in recent years various noninvasive AF organization estimation methods have been developed. To this respect, noninvasive techniques are usually applied to lead V_1 because this lead presents the highest amplitude of the atrial activity, compared to the ventricular activity, due to its proximity to the right atrium [6].

Linear techniques, such as spectral analysis, have been widely applied in the analysis of AF from the surface ECG [18]. To this respect, the atrial activity power spectrum typically presents a distinct peak within the 3–9 Hz frequency band and the frequency corresponding to its maximum amplitude reflects the average fibrillatory rate of the nearby atrial tissue [116]. Thereby, this frequency, known as the Dominant Atrial Frequency (DAF), is the most well-known noninvasive AF organization index [18]. Since during AF local excitation typically occurs without any latency beyond the refractory period, the DAF is considered as an index of the atrial refractoriness [37]. Moreover, the DAF has been related to the number of wavelets wandering the atrial tissue [37]. In this sense, lower DAF values would correspond to longer wavelengths and, therefore, a lower number of reentries. As a consequence, lower frequency AF is more likely to terminate than higher frequency AF [91, 117] and, moreover, a higher DAF is associated with a higher risk of recurrence after ECV [118, 119]. However, this technique cannot analyze the time-dependent properties of AF.

Time-frequency analysis methods are applied in order to quantify the temporal variation of the fibrillatory rate [120]. In this sense, the spectral profile is a time-frequency analysis in which the resulting spectral peaks are more prominent than in the conventional spectral analysis [27], thus making easier the determina-

tion of the signal harmonic structure. In this method, a time-frequency distribution of successive short signal segments is first obtained. Next, the distribution is decomposed into a spectral profile and several parameters describing variations in the f-waves frequency and morphology. However, the presence of noisy segments affects the spectral profiles performance [121]. In order to avoid this effect, a method based on the use of a model that represents the peaks of the AF spectrum was added in order to decide whether a new segment should be included in the estimation of the spectral profile [121]. Finally, another technique aimed to improve time-frequency analysis is based on the use of a hidden Markov model to enhance noise robustness when tracking the DAF [122].

On the other hand, correlation based techniques have also been applied to estimate AF organization. To this respect, Narayan et al. [28] applied the correlation of the atrial activity with a template as an estimation of the atrial activity organization during different atrial arrhythmias. Moreover, recent studies have analyzed the morphological similarity of the f-waves registered noninvasively [29, 30]. In this sense, a regularity estimator based on an adaptive signed correlation index has been applied to classify among AF organization levels following Well's criteria [29]. Furthermore, a distance based approach has been applied in a recent study to estimate the f-waves morphological similarity in order to evaluate AF organization [30]. According to there previous studies [29, 30], more organized AF produces more repetitive atrial waveforms in the ECG than highly disorganized AF.

Regarding nonlinear analysis, the most widely used metric in the study of AF organization from the surface ECG is Sample Entropy [13] applied to the atrial signal fundamental waveform, called the main atrial wave [16]. However, the direct application of Sample Entropy to the atrial signal has been unsuccessful [91] because this index is sensitive to the presence of noise and interferences in the signal [91, 123]. Moreover, SampEn has also been applied to the wavelet domain of the atrial signal [124] and in different frequency subbands defined from the DAF [45] in order to consider the information contained in the signal's harmonics. Furthermore, the application of SampEn to the wavelet transform coefficients predicted with high accuracy AF spontaneous termination and the outcome of ECV [125]. In another study, the variability of the atrial activity wavelet coefficients was analyzed through central tendency measurement in order to predict AF termination [126]. With respect to the use of other nonlinear indices, Taha et al. [31] classified between atrial flutter and AF using spectral entropy, which is defined as Shannon's entropy applied to the signal's power spectrum. Besides, Kao et al. [33] applied correlation dimension, largest Lyapunov exponent and Lempel Ziv complexity to the atrial activity in order to distinguish between atrial flutter and AF and reported higher values of these nonlinear indices for AF. Finally, Sun and Wang [32] studied the spontaneous termination of paroxysmal AF by analyzing the structure of the atrial activity signal recurrence plot.

Besides, other authors have considered the complementary information contained in the different ECG leads. For instance, Uldry et al. [34] obtained the spec-

tral envelope of all pairs of precordial leads and then made use of two spectral multidimensional indices to discern between two AF organization levels. On the other hand, Meo et al. [35] defined a spatiotemporal AF organization measure based on weighted principal component analysis (PCA). In addition, other authors have defined AF organization estimators based on the use of non-standard ECG recordings. To this respect, Guillem et al. [26] analyzed the atrial activation patterns from body surface potential maps. Finally, Bonizzi et al. [36] studied the complexity and stationarity of the atrial activity from the PCA of body surface potential maps.

Clinical applications

Invasive AF organization estimation methods have been applied in the study of the arrythmia mechanisms. In this sense, the progressive disorganization of the atrial activations following AF onset has been studied from invasive recordings [95]. Moreover, previous works have analyzed the changes taking place in the atrial activity prior to AF termination [127, 128]. Additionally, invasive studies have also investigated the differences between paroxysmal and persistent AF [20, 105, 111]. Other interesting clinical applications of invasive methods are related to ablation. To this respect, AF organization can be applied in the identification of targets for ablation [105,112] and to anticipate the extent of ablation [72]. Moreover, the effects of antiarrhythmic drugs have also been evaluated through invasive AF organization estimation [113,129].

Regarding noninvasive organization estimation, those methods can be applied to automatically distinguish AF from other rhythms, such as atrial flutter [28,31,33]. In addition, the study of the DAF variations along the time has been applied to estimate the atrial remodeling time course and to analyze AF circadian variability [18]. Moreover, previous works have shown that AF organization relates to the arrhythmia behavior and the therapy outcome [16,37]. In this sense, a progressive increase in AF organization within the last two minutes preceding its spontaneous termination has been reported in a previous work [94]. Therefore, AF organization estimation from the surface ECG may predict the termination. To this respect, AF spontaneous termination prediction could be interesting from a clinical point of view because it might avoid unnecessary therapy and thus reduce its associated clinical costs. On the other hand, noninvasive AF organization estimation could be applied in the selection of the most suitable therapeutical approach for a patient. In this sense, previous studies have related AF organization estimated from surface ECG recordings with the outcome of several therapies, such as ECV [38], pharmacological cardioversion [39, 40], ablation [35] and maze surgery [41]. Besides, noninvasive studies have reported organization differences between paroxysmal and persistent AF [42–45] and between persistent and longstanding persistent AF [34]. Thereby, noninvasive AF organization estimation form ambulatory ECG recordings can be applied as an alternative to the use of 24 hours Holter ECG recordings to distinguish between paroxysmal and persistent AF [44, 45].

3.2.2 Signal conditioning and atrial activity extraction

In order to study the atrial activity from the surface ECG, the ventricular activity has to be cancelled out because in the ECG the QRST complexes typically present a higher amplitude than the atrial activity [130]. Moreover, the atrial and ventricular activity overlap both in time and frequency during AF [37] and, therefore, nonlinear signal processing is needed in order to extract the atrial activity. Hence, after preprocessing the signals in order to improve the analysis, the atrial activity was extracted from each ECG. Lead V_1 was selected for the analysis because in this lead the atrial activity presents the highest amplitude, compared to the ventricular activity, due to this lead's proximity to the right atrium [6]. Next, QRS complexes were detected making use of the Pan and Tompkins technique [131]. Finally, a QRST cancellation method, which is described below, was applied to the signals.

Preprocessing

Firstly, all the studied signals were upsampled to 1 kHz using a cubic spline interpolation method in order to obtain a better alignment with the QRST template in ventricular activity subtraction, as is recommended in the literature [37]. This previous step is important because a low sampling frequency could lead to large residuals of ventricular activity remaining in the signal after QRST cancellation [37]. Since the ventricular activity presents a higher amplitude than the atrial activity, the presence of large ventricular residuals could affect the method selected for the estimation of AF organization.

Besides, since the ECG is recorded on the body surface, the signal is contaminated with noise and interferences, such as baseline wander, powerline interferences and high frequency noise. Thereby, noise and interferences were reduced through appropriate digital filtering strategies. Baseline wander is a low-frequency disturbance which is usually produced by the patient's breathing or movement. The removal of this nuisance has a particular importance because it can affect the performance of the ventricular activity cancellation methods [37]. Thus, a bidirectional high-pass filter with 0.5 Hz cut-off frequency was used to remove baseline wander [132]. On the other hand instrumentation noise, muscular interferences and powerline interference harmonics are usual sources of high frequency noise. An eight order bidirectional IIR Chebyshev low-pass filter with 70 Hz cut-off frequency was applied to reduce this noise [133]. It is worth noting that, in both cases, bidirectional filtering was selected to avoid phase distortion. As for powerline interference, the use of an adaptive filtering strategy would be suitable because it is a repetitive signal and overlaps in frequency with the ECG. Hence, powerline interference was removed through an adaptive notch filter in order to preserve the ECG spectral information [134]. An example of ECG signal conditioning is shown in Figure 3.1.

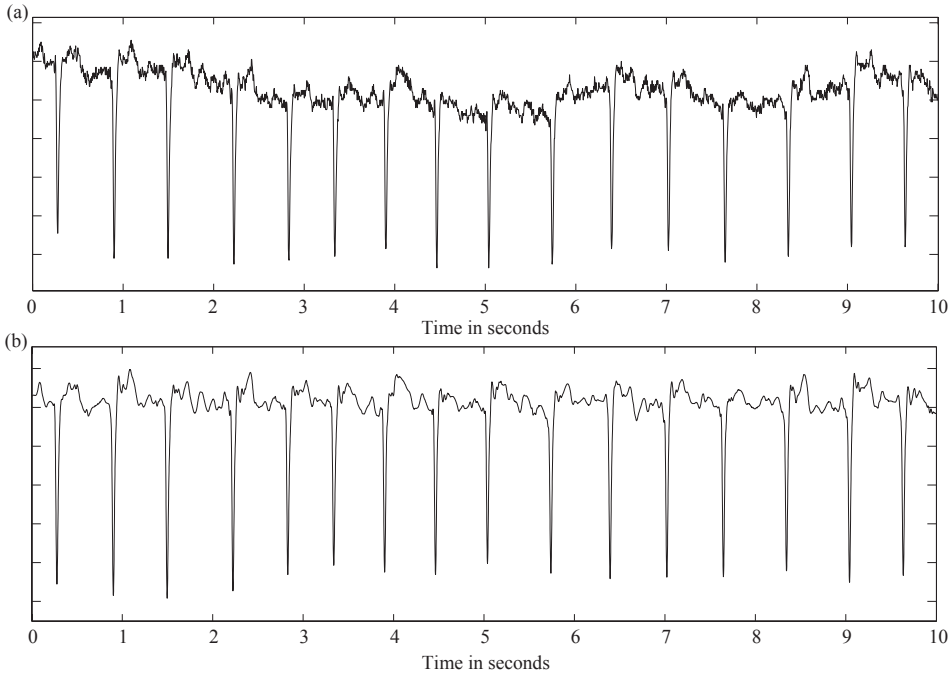

Figure 3.1. Examples of ECG signals (a) before preprocessing and (b) after preprocessing.

Ventricular activity cancellation

There are different QRST cancellation methods defined in the literature, such as the average beat subtraction (ABS) [135], the adaptive singular value cancellation method (ASVC) [136], the spatiotemporal cancellation [137] and the blind source separation method [138]. Multilead methods, such as the spatiotemporal cancellation [137] and the blind source separation method [138], were developed to provide an accurate estimation of the AA in standard 12-lead ECGs [139]. These methods can be also applied in Holter ECG recordings, where usually only 2 or 3 leads are available, or in single-lead ECG signals. However, in this latter case, their performance would be considerably reduced because these methods exploit the ECG spatial diversity to cancel out the ventricular activity [140]. Therefore, since Holter ECG recordings have been analyzed in this work and only lead V_1 has been studied, a single-lead cancellation method was selected. To this respect, single-lead cancellation methods, such as the ABS [135] and the ASVC [136], are based on the fact that atrial and ventricular activities are statistically uncoupled during AF [140].

Furthermore, the ventricular waveforms present a high temporal redundancy in the ECG [141], although different wave morphologies and minor variations in the QRST shape may exist [141]. The most common single-lead cancellation technique is the ABS method [135], which was developed for the detection of P

waves during ventricular tachycardia [135] and then was applied to the study of the f-waves in AF [130]. This method generates the ventricular template as the average of the detected beats. Thus, a precise alignment of the QRST complexes is needed [140]. However, the ABS method often presents ventricular residuals due to variations in the QRST morphology [6]. Hence, the ASVC method was selected because it is more robust against variations in the ventricular activity waveform [136].

In the ASVC technique the QRST template is generated from the singular value decomposition of the detected beats [136]. For this purpose, all beats are temporally aligned using its R peak timing and then each QRST complex can be represented by a column vector of the matrix $\mathbf{X} \in \Re^{L \times N}$ [136]:

$$\mathbf{X} = [\mathbf{x}_1, \mathbf{x}_2, \ldots, \mathbf{x}_N], \tag{3.1}$$

where $\mathbf{x}_i$ contains L samples of i-th complex, and N is the total number of QRST complexes in the analyzed ECG.

Next, the matrix $\mathbf{X}$ can be decomposed as

$$\mathbf{X} = \mathbf{U}\mathbf{S}\mathbf{V}^T, \tag{3.2}$$

where $\mathbf{U} \in \Re^{L \times N}$ is an unitary matrix so that $\mathbf{U}\mathbf{U}^T = \mathbf{I}$, $\mathbf{S} \in \Re^{N \times N}$ is an diagonal matrix, and $\mathbf{V} \in \Re^{N \times N}$ fulfills $\mathbf{V}\mathbf{V}^T = \mathbf{I}$. The N normalized principal components of $\mathbf{X}$ are contained in the matrix $\mathbf{U}$, so that the columns of $\mathbf{U} = [\mathbf{u}_1 \ldots, \mathbf{u}_N]$ are the eigenvectors of $\mathbf{X}$. Besides, the matrix $\mathbf{S}$ contains the eigenvalues or singular values, which are the amplitude coefficients corresponding to the N principal components of $\mathbf{X}$. Thus, the columns of the matrix $\mathbf{P} = \mathbf{U}\mathbf{S}$ contain the N non-normalized principal components of the ventricular activity. To this respect, the different components obtained from the matrix decomposition can be interpreted as follows [140]:

1. The eigenvector corresponding to the largest eigenvalue reflects the QRST morphology because the ventricular activity presents the highest variance in the ECG.

2. Subsequently, there are several components related to the atrial activity.

3. Finally, the remaining eigenvectors correspond to noise and interferences.

Hence, the ventricular template is constructed by adjusting the amplitude of the first principal component of $\mathbf{X}$, which is represented by $\mathbf{t}$, to the amplitude of the QRST complex under cancellation using the following expression:

$$\mathbf{t}_i = \frac{QR_i}{QR_{\mathbf{t}}} \cdot \mathbf{t}, \tag{3.3}$$

where QR_i and $QR_{\mathbf{t}}$ are the distances between the Q and R points of the i-th complex and template, respectively. Thus, the AA is estimated as

$$\widehat{\mathbf{X}}_{AA} = \mathbf{X} - \mathbf{T}, \tag{3.4}$$

where $\mathbf{T}$ is the matrix constituted by the column vectors $\mathbf{t}_i$:

$$\mathbf{T} = [\mathbf{t}_1, \mathbf{t}_2, \ldots, \mathbf{t}_N]. \tag{3.5}$$

Finally, a gaussian window with a length of $2M$ processed samples is applied to the AA over each transition in order to obtain an AA estimation without sudden transitions.

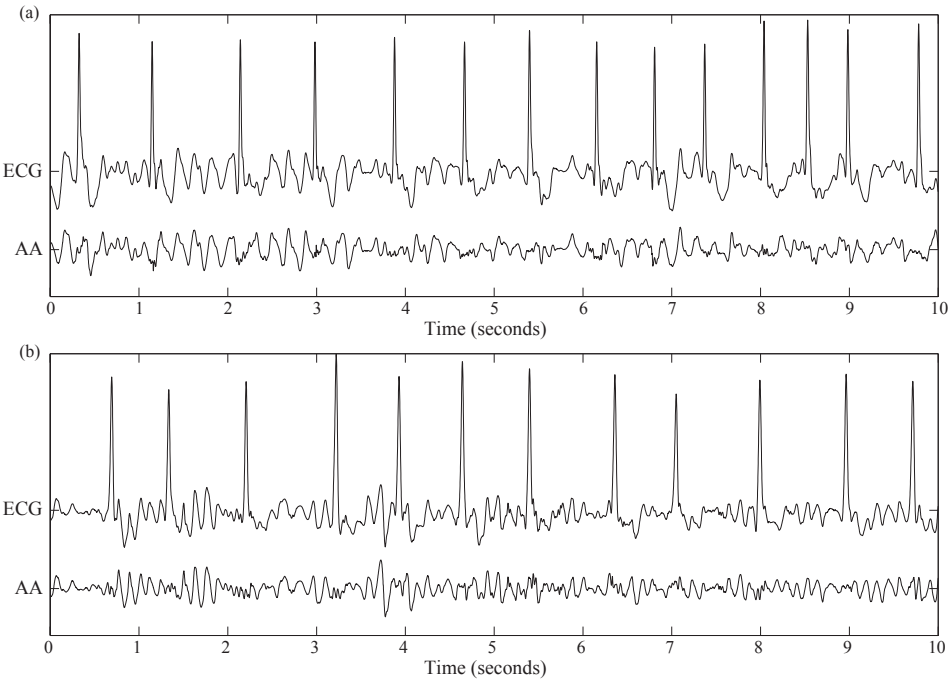

Figure 3.2. Examples of ventricular activity cancellation using the ASVC method for (a) paroxysmal AF and (b) persistent AF.

It is important to note that, in the ASVC method, the ventricular template is generated from the most similar QRST complexes to the one under cancellation [136]. Regarding the amount of QRST complexes needed to obtain the ventricular template, the ideal number is between 20 and 30 [136]. However, in short ECG recordings lasting only few seconds all beats should be used to generate the QRST template [136]. Figure 3.2 shows an example of the ventricular activity cancellation in two different AF signals using the ASVC technique.

3.2.3 Main Atrial Wave

Previous works have proved that the presence of QRST residuals and noise in the AA signal extracted from the ECG can degrade notably AF organization estimation using a nonlinear metric, such as SampEn [16, 91]. Hence, the extraction of the Main Atrial Wave (MAW) was proposed in previous studies [16, 142] in order to reduce the effect of these nuisances.

The MAW can be considered as the atrial activity main waveform and its wavelength is the inverse of the DAF [116]. In this sense, the estimation of the MAW regularity using SampEn has been validated as a measurement of AF organization in a previous work [115]. Regarding the use of the MAW, it has been applied in a variety of scenarios, including the prediction of paroxysmal AF spontaneous termination [123, 142], the discrimination between paroxysmal and persistent AF from short ECG recordings [44, 45] and the prediction of the therapy outcome [38, 41, 143]. Moreover, paroxysmal AF organization time course has been estimated from the MAW in the onset and termination of AF episodes [94, 144] and along onward AF episodes [145]. In addition, AF organization has also been estimated in a pilot study [146] through the application of LZC over the MAW.

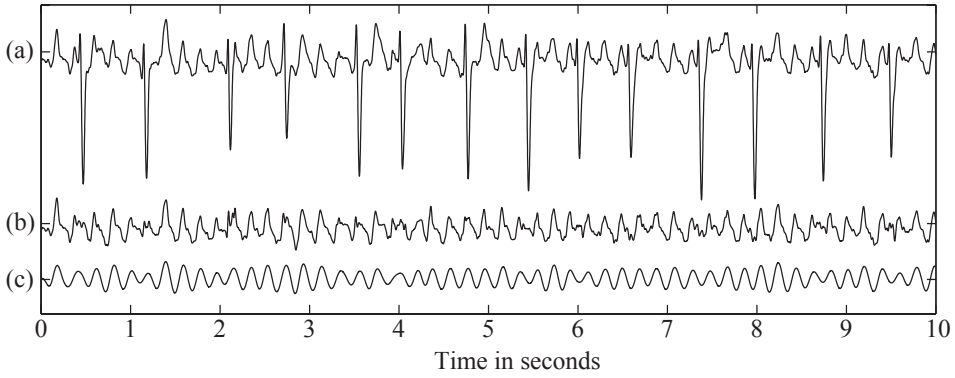

Figure 3.3. Example of MAW extraction. (a) Original ECG recording. (b) AA signal obtained after the ventricular activity cancellation. (c) Main Atrial Wave.

In order to obtain the MAW, a selective band-pass filtering centered on the DAF of each recording was applied to the AA. To this respect, the DAF was computed as will be described later in Section 3.2.4. Next, a bidirectional FIR filter was used in order to prevent phase distortion [147]. With respect to the filter design, a FIR filter was selected because this type of filters presents a high stability and can be designed with a linear phase impulse response. This filter was designed using the Chebyshev approximation, which allows to adjust all the filter parameters in order to obtain minimum ripple in the pass and stop bands. Therefore, the filter order, L, can be estimated by the Kaiser approximation [148]:

$$L = \frac{-20\log_{10}(\sqrt{\delta_1\delta_2}) - 13}{14.6\Delta f} + 1 \tag{3.6}$$

where δ_1 and δ_2 are the pass and stop bands ripple, respectively, and Δf is the transition bandwidth between bands. Since a selective filter must have δ_1 and δ_2 lower than 0.5% of the gain and Δf lower than 0.01 Hz, the filter order must be greater than 250. In this sense, in a previous work [123] the best results for SampEn were obtained with 768 filter coefficients and, thus, this filter order was used to extract the MAW.

Regarding the filter bandwith, its value should be lower than 6 Hz because most of the AF energy corresponds to the 3–9 Hz band [149]. Therefore, the filter was designed with a bandwith of 3 Hz because in previous works this value optimized the performance of SampEn [123]. Figure 3.3 shows an example of an AF signal and its corresponding MAW.

3.2.4 Studied metrics to compute AF organization

Dominant Atrial Frequency

The DAF is defined as the frequency corresponding to the highest Power Spectral Density (PSD) amplitude in the 3–9 Hz band [116] and it is inversely related to the atrial cycle length [116]. Therefore, the DAF can be considered as an indicator of the atrial refractoriness [116]. Previous studies have associated this parameter to AF maintenance and response to therapy [37]. For instance, the DAF acts as a predictor of the sinus rhythm maintenance after electrical cardioversion [118, 119]. Furthermore, the DAF correlates with the behavior of the arrythmia. Hence, low frequency AF is more likely to terminate spontaneously than high frequency AF [91,117]. Moreover, persistent AF shows higher DAF values than paroxysmal AF [42–44]. Several previous studies [114,116] have found that the DAF obtained from lead V_1 correlates with the fibrillatory rate measured from invasive recordings in the right atrium. Besides, it has been suggested that the DAF is related to the number of propagating wavelets in the atria [42]. Therefore, the DAF is considered as an established indirect estimator of AF organization [116].

Regarding the PSD estimation, the existing techniques can be divided into parametric and nonparametric methods, depending on the existing prior information about the signal origin. On one hand, parametric techniques assume a certain structure in the process that generated the signal, for instance an autoregressive model [150]. On the other hand, nonparametric methods estimate the PSD without such prior information. The most common nonparametric technique is the Welch periodogram [151]. In this method, the signal is divided into overlapping segments in order to maximize the number of segments that can be obtained from a finite length recording. Next, each segment is multiplied by a windowing function, which avoids a sharp truncation of the sequence, and the

Fast Fourier Transform (FFT) of each segment is then computed. Finally, the PSD is computed as the average of each segment's FFT [151]. It is important to note that the segment length determines the frequency resolution of the spectral estimation, and therefore a segment length of at least few seconds is recommended in order to obtain an accurate estimation of the DAF [18,37].

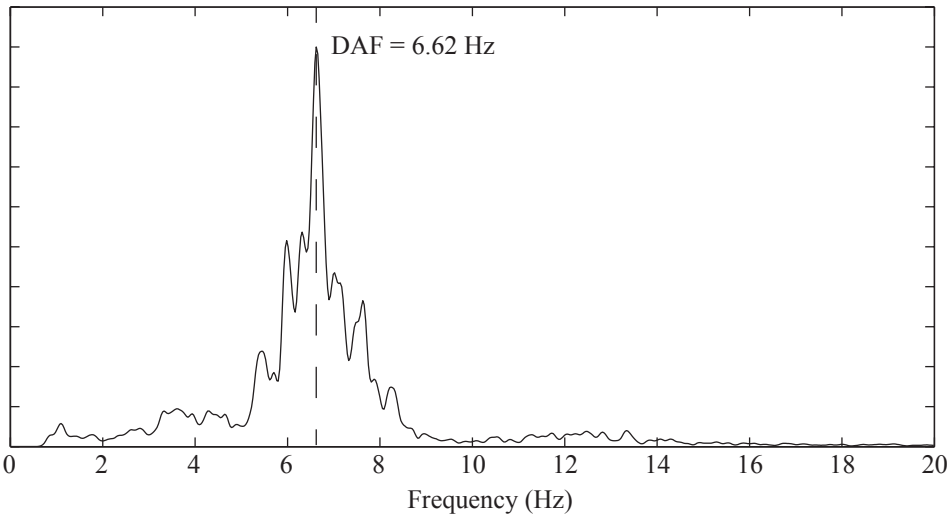

Figure 3.4. Example of DAF identification from the atrial signal PSD.

To obtain the DAF, the PSD of the signal was computed using the Welch periodogram because this method makes no a priori assumptions about the process that generated the signal. The peridogram was computed using a Hamming window of 4096 points in length, 50% overlapping between adjacent sections and 8192-points FFT as was suggested in previous works [138], thus obtaining a frequency resolution lower than 0.125 Hz. Then, the largest amplitude frequency within the 3–9 Hz band was selected as the DAF. Figure 3.4 shows an example of the PSD computed on an AA segment to obtain its corresponding DAF.

Sample Entropy

Sample Entropy (SampEn) has been applied as an estimator of AF organization in different scenarios [16], including the prediction of sinus rhythm maintenance after electrical cardioversion (ECV) [38,143], the prediction of maze surgery outcome [41], the classification between paroxysmal and persistent AF from ambulatory ECG recordings [44,45] and the prediction of paroxysmal AF spontaneous termination [123,142]. Moreover, the non-invasive AF organization estimation given by SampEn was validated by comparison with invasive recordings in a previous study [115]. In addition, SampEn has been applied in the study of paroxysmal AF organization time course within a single episode [94,144] and along consecutive episodes [145].

SampEn estimates the regularity of a time series, understood as the probability that two existing subsequences which are similar for m points remain similar for $m+1$ points [152]. It is important to note that self-matches are not included when calculating the probability and thus the value of SampEn is highly independent on the data length [152]. With respect to the interpretation of SampEn values, higher values correspond to more complex or irregular sequences. In order to compute SampEn, two input parameters must be specified, a run-length m and a tolerance window r.

Mathematically, given a time series $x[n] = x(1), x(2), ..., x(N)$ of length N, SampEn can be defined as follows [152]:

1. The first step is to form m vectors $X_m(1), \ldots, X_m(N-m+1)$, defined by

$$X_m(i) = [x(i), x(i+1), \ldots, x(i+m-1)], 1 \leq i \leq N-m+1. \tag{3.7}$$

   . These vectors represent m consecutive x values, starting with the ith point.

2. Then, the distance between vectors $X_m(i)$ and $X_m(j)$, $d[X_m(i), X_m(j)]$, is defined as the absolute maximum difference between their scalar components:

$$d[X_m(i), X_m(j)] = \max_{k=0,\ldots,m-1} \Big(|x(i+k) - x(j+k)| \Big) \tag{3.8}$$

3. Next, for a given $X_m(i)$, ϕ_i^m is defined as the number of j ($1 \leq j \leq N-m$, $j \neq i$), such that the distance between $X_m(i)$ and $X_m(j)$ is less than or equal to r. Then, for $1 \leq i \leq N-m$,

$$\phi_i^m(r) = \frac{1}{N-m-1} \phi_i^m \tag{3.9}$$

4. The probability that two sequences will match for m points is then denoted as $\phi^m(r)$

$$\phi^m(r) = \frac{1}{N-m} \sum_{i=1}^{N-m} \phi_i^m(r) \tag{3.10}$$

5. Next, the dimension is increased to $m+1$ and ϕ_i^{m+1} is calculated as the number of $X_{m+1}(i)$ within r of $X_{m+1}(j)$, where j ranges from 1 to $N-m$ ($j \neq i$). Then $\phi_i^{m+1}(r)$ is defined as

$$\phi_i^{m+1}(r) = \frac{1}{N-m-1} \phi_i^{m+1} \tag{3.11}$$

6. And the probability that two sequences will match for $m+1$ points is represented by ϕ^{m+1}

$$\phi^{m+1}(r) = \frac{1}{N-m} \sum_{i=1}^{N-m} \phi_i^{m+1}(r) \tag{3.12}$$

Finally, sample entropy can be defined as:

$$SampEn(m,r) = \lim_{N\to\infty} \Big\{ -\ln\Big[\frac{\phi^{m+1}(r)}{\phi^{m}(r)}\Big]\Big\} \tag{3.13}$$

which, for finite datasets, is estimated by the statistic

$$SampEn(m,r,N) = -\ln\Big[\frac{\phi^{m+1}(r)}{\phi^{m}(r)}\Big]. \tag{3.14}$$

Regarding the computational parameters values, SampEn is generally calculated using m equal to 1 or 2, and r between 0.1 and 0.25 times the standard deviation of the numeric sequence. The value of r is computed from the standard deviation of the time series in order to obtain a regularity metric independent from the scale and therefore not affected by uniform magnification or reduction processes [153]. However, in the case of AF organization estimation, a thorough study about optimal parameters selection [154] found that the optimal values are $m = 2$ and $r = 0.35$ times the standard deviation of the signal. Hence, these parameters values have been used in this work.

Fuzzy Entropy

Fuzzy Entropy (FuzzEn) has been proposed as a modification of SampEn in order to obtain a more accurate regularity estimation and a higher statistical stability in the study of biomedical signals [155]. This is because when computing SampEn the similarity between patterns is decided using an absolute two-state classifier represented by the Heaviside function [152]. Thereby, FuzzEn makes use of fuzzy sets theory [156] to measure the similarity degree among patterns. Thus, the two-state classifier used in SampEn computation is replaced by a continuous membership degree obtained from a fuzzy function which, in a general form, can be represented by the following expression:

$$D_{ij}^{m} = \mu(d_{ij}^{m}, r). \tag{3.15}$$

The resulting similarity degree, D_{ij}^{m}, is a real number and can vary from 0 to 1, with higher values corresponding to a higher similarity between patterns. Therefore, a third computational parameter, n, which acts as a weight of the vectors' similarity, is needed for calculating Fuzzen, aside from the parameters m and r defined for SampEn in the previous subsection.

Regarding the applications of FuzzEn, this index has been mainly applied in the characterization of surface electromyographic signals [155, 157]. On the other hand, FuzzEn has been applied recently in the study of heart rate variability [158, 159] and the detection of heart murmurs from the analysis of heart sounds [160]. Moreover, the use of Fuzzen in the study of AF organization was proposed in a

pilot study [161] because the use of this index could improve the results obtained using SampEn.

The mathematical definition of Fuzzen is very similar to SampEn [152]. Indeed, only two differences exist:

1. In order to obtain a similarity estimation based on the shape [155], baseline is removed when vectors $\mathbf{X}_i^m$ are defined (see equation 3.7)

$$\mathbf{X}_i^m = \{x(i), x(i+1), \ldots, x(i+m-1)\} - \frac{1}{m}\sum_{l=0}^{m-1} x(i+l). \tag{3.16}$$

2. The similarity degree D_{ij}^m between $\mathbf{X}_i^m$ and $\mathbf{X}_j^m$ is defined using a fuzzy function. This function should be continuous and convex in order to obtain a similarity degree which is maximum for identical patterns and does not present abrupt changes [155]. Thus, the following exponential function was selected [155]:

$$D_{ij}^m(n,r) = \exp\left(-\frac{(d_{ij}^m)^n}{r}\right). \tag{3.17}$$

Therefore the probability that two sequences will match for m points, denoted as ϕ^m, is computed as

$$\phi^m(n,r) = \frac{1}{N-m}\sum_{i=1}^{N-m}\left(\frac{1}{N-m-1}\sum_{j=1,j\neq i}^{N-m} D_{ij}^m\right). \tag{3.18}$$

Finally, FuzzEn is computed as the negative natural logarithm of the deviation of ϕ^m from ϕ^{m+1}, i.e.

$$\text{FuzzEn}(m,n,r) = -\lim_{N\to\infty}\left(\ln\frac{\phi^{m+1}(n,r)}{\phi^m(n,r)}\right), \tag{3.19}$$

which, for finite datasets, can be estimated by the statistic

$$\text{FuzzEn}(m,n,r,N) = -\ln\frac{\phi^{m+1}(n,r)}{\phi^m(n,r)}. \tag{3.20}$$

Hence, FuzzEn examines time series for similar epochs and assigns a non-negative number to the sequence, with larger values corresponding to more irregularity in the data [155]. Although m, n and r are critical in determining the outcome of FuzzEn, no guidelines exist for its application in the study of AF organization. In this sense, when n increases to infinity the fuzzy function becomes the Heaviside function [155] and this causes the loss of the detailed information. Therefore, a value of $n = 2$ was selected in order to obtain the maximum advantages of the use of a fuzzy function [155]. Regarding the parameters m, and r, the widely used values of $m = 2$ and $r = 0.25$ times the standard deviation of the original data for SampEn computation [16] were selected.

Spectral Entropy

Spectral Entropy (SpecEn) is computed by applying Shannon's entropy to the normalized power spectral density (PSD) of a signal $x(n)$ [162]. Thus, this metric quantifies the signal's spectral complexity and therefore SpecEn can be considered as an irregularity estimator [163]. In this sense, a high SpecEn value indicates a flat, uniform spectrum with a broad spectral content (e.g. white noise), whereas a predictable signal whose frequencies are mainly concentrated into few frequency bins (e.g., a sum of sinusoids) yields a low SpecEn value [164].

SpecEn has been used in the analysis of biosignals, such as electroencephalographic (EEG) recordings. To this respect, its applications include the monitoring of the anesthesia effect [165] and the detection of abnormalities, such as epilepsy [166]. With respect to the use of this index on ECG recordings, it has been applied in the identification of different cardiac rhythms [167]. Moreover, Taha et al. [31] applied SpecEn on the atrial activity extracted from the surface ECG to classify between atrial flutter and AF. This latter study reported that AF produced higher values of this index than atrial flutter. Hence, SpecEn could reflect the amount of wavelets existing in the atria and therefore it could estimate AF organization.

In order to compute SpecEn, the PSD in the selected band has to be normalized via its total power, i.e.

$$PSD_n = \frac{PSD}{\sum_{f=f_{min}}^{f_{max}} PSD(f)}, \tag{3.21}$$

such that $\sum_{f=f_{min}}^{f_{max}} PSD_n(f) = 1$, obtaining a probability distribution function in the frequency domain. Then, SpecEn can be computed as

$$\text{SpecEn} = -\frac{1}{\log(M)} \sum_{f=f_{min}}^{f_{max}} PSD_n(f) \log\Big(PSD_n(f)\Big), \tag{3.22}$$

where M is the number of frequency bins. The division by $\log(M)$ normalizes the metric to a scale from 0 to 1 [163].

In order to compute SpecEn the PSD of the analyzed signals was computed using the Welch Periodogram. As in the case of the DAF [115], a Hamming window of 4096 points in length, a 50% overlapping between adjacent windowed sections and a 8192-point FFT were used as computational parameters, thus providing a spectral resolution lower than 0.125 Hz. Regarding the selected frequency band, since most of the AA signal energy is contained in the 3–9 Hz band [116], SpecEn was computed only in this band.

Lempel-Ziv Complexity

Lempel-Ziv Complexity was introduced by Lempel and Ziv in 1976 [168] and is a non-parametric index of complexity for one-dimensional signals. LZC measures the number of different substrings and the rate of their appearance along the data. Larger values of this index imply more complexity in the time series. It is worth noting that LZC can be computed on short data segments [169].

In the context of biosignal analysis, LZC can be interpreted in terms of harmonic variability [169]. To this respect, LZC has been applied in the study of several physiological signals, including EEG recordings [170–172], intracranial pressure [173], heart rate variability [174, 175] and the detection of ventricular tachycardia and ventricular fibrillation from the surface ECG [176]. Regarding the application of LZC in the study of AF, this metric has been used to discriminate between atrial flutter and AF [33]. Moreover, the use of LZC as a predictor of AF termination has been proposed in a previous work [146]. Hence, the use of LZC could provide an estimation of AF organization.

In order to compute LZC, the first step is to transform the original signal $x(n)$ into a finite symbol sequence. Since the optimal symbol set for the study of AF organization through LZC has not been determined yet [146], two different sequence conversion methods were used:

1. Two-symbol sequence conversion, which is the most common choice for the analysis of biomedical signals [169]. The signal $x(n)$ is converted into a binary sequence defined by

$$s(i) = \begin{cases} 0 & \text{if } x(i) < x_m, \\ 1 & \text{if } x(i) \geq x_m, \end{cases}$$

   where x_m is the median of $x(n)$. The median was selected as a threshold, instead of the mean value, because its estimation is more robust to outliers [177].

2. Three-symbol sequence conversion, which was proposed in a previous pilot study [146] for the estimation of AF organization. The signal is converted into a 0-1-2 sequence defined by

$$s(i) = \begin{cases} 0 & \text{if } x(i) \leq T_{d1}, \\ 1 & \text{if } T_{d1} < x(i) < T_{d2}, \\ 2 & \text{if } x(i) \geq T_{d2}, \end{cases}$$

   the thresholds T_{d1} and T_{d2} being defined as $T_{d1} = x_m - |x_{min}|/16$ and $T_{d2} = x_m + |x_{max}|/16$, where x_{min} and x_{max} are the minimum and maximum values of $x(n)$, respectively [171]. Like in the previous case, the thresholds are defined using the median value in order to obtain a more robust conversion method.

Next, the sequence $s(n)$ is scanned from left to right. Every time a new sequence of consecutive symbols is detected, a complexity counter $c(n)$ is increased by one unit. Thereby, if two subsequences of $s(n)$ are denoted as P and Q and their concatenation is represented as PQ, the sequence $PQ\pi$ can be obtained by removing the last character of PQ and the vocabulary of $PQ\pi$ can be denoted as $v(PQ\pi)$. Then, $c(n)$ can be estimated as follows [169]:

1. The following initial values are assigned: $c(n) = 1$, $P = s(1)$, $Q = s(2)$.
2. In general, $P = s(1), s(2), ..., s(r)$ and $Q = s(r+1)$. Therefore, $PQ\pi = s(1), s(2), ..., s(r)$.
3. If Q belongs to $v(PQ\pi)$, its value is renewed to be $Q = s(r+1), s(r+2)$. Otherwise, a new subsequence has been found and thus $c(n)$ is increased by one.
4. The previous step is repeated while Q belongs to $v(PQ\pi)$.
5. Next, P is renewed to be $P = s(1), s(2), ..., s(r+i)$ and $Q = s(r+i+1)$ and the previous steps are repeated. This procedure is repeated until Q is the last character of $s(n)$.

Finally, $c(n)$ has to be normalized in order to obtain a complexity measure which does not depend on the data length. Thereby, for a symbol set of α different symbols and a sequence length N, it has been demonstrated [168] that the upper bound of $c(n)$ is given by

$$c(n) < \frac{N}{(1-\varepsilon)\log_\alpha(N)}, \tag{3.23}$$

where ε is a small number and $\varepsilon \to 0 (N \to \infty)$. As a rule, $N/\log_\alpha(N)$ is the upper bound of $c(n)$, where the base of the logarithm is the amount of different symbols in the symbol set, i.e.

$$\lim_{N\to\infty} c(n) = \frac{N}{\log_\alpha(N)} \tag{3.24}$$

and $c(n)$ can be normalized as

$$C(n) = \frac{c(n)}{\frac{N}{\log_\alpha(N)}}. \tag{3.25}$$

This normalized LZC, $C(n)$, reveals the occurrence rate of new substrings along with the sequence. Thus, its value is determined by the temporal structure of the signal and, therefore, it could provide an estimation of AF organization.

Hurst Exponent and its generalization

Hurst Exponents (H) [178] were originally developed to study the levels of the Nile river in order to determine the optimum sizes in a water reservoir system. To this respect, H estimates how fast the autocorrelation function decreases when the distance between observations increases [179]. Therefore, the scaling properties in time series can be quantified through H [179]. Scaling in data gives useful information on the underlying process and the analysis using Hurst Exponents examines if some statistical properties of a time series $x(n)$ scale with the observation period and the time resolution. Thus, H is commonly associated with the long-term statistical dependence of the signal and, therefore, quantifies the statistical self-similarity of time series, providing information on the recurrence rate of similar patterns in time series at different scales [180].

The study of scaling properties has been applied in the analysis of physiological signals, such as heart rate [181, 182], cerebral blood flow [183] and EEG recordings [184]. Moreover, H has been proposed as an estimation of Ventricular Fibrillation organization by Sherman et al. [185]. Furthermore, in this latter study H reflected the progressive organization deterioration following the onset of the arrythmia [185]. Hence, the use of Hurst Exponents could provide information about the atrial activation patterns regularity during AF and therefore it might provide an accurate estimation of AF organization. In this sense, a pilot study [186] analyzed the scaling properties of the atrial signal in AF and found differences between AF signals with different organization levels; however, no diagnostic accuracy was reported.

In order to estimate H from a time series, the fist step is to divide the data into segments X_n of length $n = N, N/2, N/4, ...$, where N represents the series total length. Next, the rescaled range $R(n)/S(n)$ is computed in each segment. For this purpose, the accumulated deviation from the mean value, denoted as $Y_n(t)$, $t = 1, 2, ..., n$, is calculated as

$$Y_n(t) = \sum_{i=1}^{t} \Big(X_n(i) - \bar{X}_n \Big), \tag{3.26}$$

where $\bar{X}_n$ represents the mean value of the segment. The range of this deviation, denoted as $R(n)$, can be defined as the difference between its maximum and minimum, i.e.

$$R(n) = \max(Y_n(t)) - \min(Y_n(t)). \tag{3.27}$$

and can be normalized by the standard deviation of each segment, $S(n)$, to obtain the rescaled range. Finally, H can be estimated as the slope of the line produced by $\ln\Big(R(n)/S(n)\Big)$ vs. $\ln(n)$. These estimates range between 0 and 1. Regarding the interpretation of this index, a value of 0.5 indicates no correlation in the time series and corresponds to a Brownian motion or random walk [179]. In contrast, a value between 0 and 0.5 denotes that the time series has long-range

anti-correlations, whereas values between 0.5 up to 1 evidence long-range correlations [180] and in this case the process is called persistent.

However, some time series, such as the heart rate [182], show a more complex behavior and, as a result, their characterization via H is not complete. Thus, a generalization of the approach proposed by Hurst in [178], known as the Generalized Hurst Exponents ($H(q)$) [187], is applied in the analysis of complex and inhomogeneous time series having many regions with different scaling properties. To this respect, $H(q)$ is associated with the scaling behavior of the q^{th} order moments of the signal's amplitude increments distribution. Thus, $H(q)$ is basically a tool to examine directly the scaling properties of the data via statistically significant properties of its amplitude increments [188]. Therefore, given a time series $x(n)$, the q-order moment of its increments distribution can be represented by the following expression

$$K_q(\tau) = \frac{1}{N-\tau+1} \sum_{i=1}^{N-\tau} |x(i+\tau) - x(i)|^q, \tag{3.28}$$

the time interval between observations, τ, being between 1 and N. Then, the scaling behavior of $K_q(\tau)$ can be assumed to follow the relation [188]

$$K_q(\tau) \propto \tau^{qH(q)}, \tag{3.29}$$

where $H(q)$ is the generalized Hurst exponent of order q.

Processes exhibiting this scaling behavior can be classified into two types:

1. Unifractal processes (also called uniscaling) are defined as processes in which $H(q)$ is independent of q. The scaling behavior of these processes is characterized by a single exponent, which is equal to the global Hurst exponent, H [187].

2. Multifractal processes (also known as multiscaling), in which $H(q)$ depends on the value of q and, therefore, each moment scales with a different exponent [187]. In this case, different values of q are associated with different characterizations of the multi-scaling behavior of the signal $x(n)$ and therefore the meaning of $H(q)$ varies with the value of q.

It should be noted that the exponents $H(1)$ and $H(2)$ have a special significance. $H(1)$ relates to the absolute values of the increments [189], while $H(2)$ is associated with the scaling of the autocorrelation function of the increments [189]. Thus, for the purposes of long-range dependence detection, the case of $q = 2$ has a particular importance. Hence, $H(1)$ and $H(2)$ have been considered as possible estimators of AF organization.

3.2.5 Application of the studied metrics

Firstly, the ability of the studied metrics in the classification between different AF organization degrees was evaluated. For this test, the studied metrics were applied to the immediate prediction of AF spontaneous termination. The results of the different metrics were compared and the metric which obtained the highest accuracy in the prediction was selected for the next tests. The best predictor of AF spontaneous termination could be considered as the most accurate in the estimation of AF organization because this index provided the most accurate classification between different AF organization levels. Next, the selected metric was applied to the estimation of AF organization in two different scenarios. The first one is the study of AF organization time course prior to PAF spontaneous termination in order to determine whether is possible to obtain a clinically useful prediction of PAF termination. This scenario was selected because the early prediction of AF spontaneous termination has never been attempted before. The second one is the classification between paroxysmal and persistent AF from short ECG recordings. This application of AF organization indices over short ECG recordings would be interesting in the clinical practice because, in the future, it could be an alternative to the use of Holter ECG recordings.

Prediction of AF termination

Previous studies have found that higher AF organization is associated with a higher likelihood of spontaneous termination in paroxysmal AF [16, 37]. Therefore, the ability of the indices presented in Section 3.2.4 to predict AF spontaneous termination will be tested. It is important to note that, since the DAF and SampEn are validated AF organization metrics, they were computed as references.

All the indices described in Section 3.2.4 were computed over the signals in the AFTDB, which has been described in Section 3.1.1, in order to evaluate their performance in the discrimination among different AF organization levels. For this purpose, a computational segment length of 10 seconds was chosen as a trade-off between robustness, time resolution and computational cost. Moreover, since ambulatory ECG recordings are usually of about 10 seconds in length, the use of this computational data length seems appropriate with regard to possible future clinical applications of the studied indices. Previous works have shown that this segment length is appropriate for SampEn [154]. Moreover, this segment length is also suitable for the DAF, while shorter ECG segments would not allow enough frequency resolution for an accurate estimation of this metric and, therefore, the comparison would not be fair. Hence, the studied metrics were computed over non-overlapped 10 second-length segments of the AA signals and then their average results were considered as an AF organization estimation. Since previous works showed that the MAW improves the performance of nonlinear indices, such as SampEn [16, 142], the use of the studied metrics on the MAW was also assessed. It is worth noting that, due to the existence of these previous results,

Sampen was computed only on the MAW. In addition, for a more exhaustive evaluation of the AF organization estimation given by each nonlinear metric, four different classification scenarios for AF termination prediction have been defined:

- Classification between groups N and T.
- Discrimination between groups N and S.
- Classification between groups S and T.
- Identification of all terminating episodes (group N vs groups S and T).

Finally, the classification results of the different studied metrics computed on the AA and the MAW, together with the DAF and SampEn, were compared. Additionally, a stepwise logistic regression analysis was performed in order to improve the classification accuracy attained by each individual index. This analysis combined the possible complementary information provided by each analyzed metric. Variable selection was performed by a forward stepwise approach including, at each step, the feature which led to the Wald statistic maximization.

Early prediction of AF termination

From a clinical point of view, the early prediction of paroxysmal AF termination is interesting because it could improve the current management of AF patients. For instance, patients with high probability of presenting long AF episodes could be identified and an aggressive therapy could be planned in order to avoid complications [2]. In contrast, a less aggressive treatment could be used in patients more likely to present short AF episodes. In that latter case, therapy could even be avoided. As a consequence, clinical costs and side effects for the patient would be reduced. To this respect, a previous work found that AF organization increases progressively within the last 2 minutes prior to the arrhythmia spontaneous termination [94]. Therefore, noninvasive AF organization estimators can be applied in the early prediction of AF spontaneous termination from the surface ECG.

However, most of the previous studies focused on AF spontaneous termination have only analyzed the AFTDB, which was described in section 3.1.1, and, thus, have analyzed only the last 2 minutes prior to the termination due to database limitations. Furthermore, the early prediction of AF termination has never been attempted before. Hence, in this work, the time course of AF organization has been estimated using the nonlinear metric that obtained the highest accuracy in the discrimination between different AF organization levels. First, the optimal computational parameters for the use of the selected nonlinear index as an estimator of AF organization have been determined. Then, this index has been applied to estimate the organization time course within the longest interval preceding AF termination in which AF organization changes indicative of the termination manifest. The DAF and SampEn have also been computed as reference metrics.

$H(2)$ was selected to estimate AF organization because this index yielded the best classification results (see Section 4.2 in the next chapter). Since no guidelines exist for the application of this index to AF signals, typical values of the computational parameters were considered in the study presented in the previous subsection. Thus, a computational segment length $L = 10$ seconds was considered, together with a sampling frequency of the recording $f_s = 1024$ Hz. On the other hand, the selected maximum value of τ (τ_{max}) was 20 ms [188]. Once this metric was selected for the next tests, the optimal computational parameters for the use of $H(2)$ were determined before the study of early prediction of AF termination in order to obtain the most accurate estimation of AF organization. Thereby, a systematic and thorough analysis about the effect of the computational parameters of $H(2)$ on the estimation of AF organization was developed, in the same way as with SampEn in a previous study [154]. It is important to note that a proper validation of the AF organization estimates obtained using different combinations of L, τ_{max} and f_s would require the use of synthetic AF signals with *a priori* defined organization. However, since the generation of such signals is not currently possible due to the lack of an appropriate method, real AF signals with different AF organization degrees were analyzed. For this purpose, the AFTDB was analyzed making use of the classification scenarios defined in the previous subsection.

Firstly, the effect of the computational data length (L) and the sampling rate (f_s) was studied. To this respect, the original signals were resampled to the rates of 64, 128, 256, 512, 1024 and 2048 Hz and $H(2)$ was computed for each f_s with variable values of L and a fixed value of $\tau_{max} = 20$ ms. Regarding the values of L, it has to be considered that too short intervals do not allow the quantification of long-range correlations. On the other hand, if the computational data length is too large, $H(2)$ loses its locality and may not quantify correlations whose characteristic range is much smaller than the interval length [190]. Taking into account these considerations, the variable L values were selected as non-overlapped intervals of 0.1, 0.2, 0.4, 0.8, 1, 5, 10, 15, 20, 30 and 60 seconds and averaged for the whole signal length for each analyzed f_s.

Next, the same computation was repeated with variable values of τ_{max} and f_s and a fixed value of L. In this case, the computational data length which provided the best classification results in the previous step was selected. Regarding the values of τ_{max}, no recommendations can be found in the literature. Thus, $H(2)$ was computed for τ_{max} values of 10, 15, 20, 25, 30, 50, 90, 100, 1000 and 2000 ms for each value of f_s. Finally, after the optimal value of f_s was found, the interdependence between L and τ_{max} for the optimal sampling rate was studied. Therefore, $H(2)$ was computed for every single pair of values of L and τ_{max} in the ranges specified above, respectively.

After determining the optimal use of $H(2)$, the early prediction of AF termination was studied analyzing the database described in Section 3.1.2. For this purpose, $H(2)$ was computed using the optimal parameters over all non-overlapping optimal length segments of the signals. Then, $H(2)$ values were compared with

optimal length ECG segments from the same patients selected 1 hour after AF onset using a paired t-test. The values of DAF and SampEn of each ECG segment were also computed as references.

Discrimination between paroxysmal and persistent AF

According to the literature, the outcome of AF therapies may be different for paroxysmal and persistent AF [2]. For instance, focal ablation is much more effective in paroxysmal AF than in persistent AF [66,191]. Besides, previous studies have found that the presence of AF alters the tissue electrophysiological properties in a way that promotes the arrhythmia perpetuation [7, 86]. In this sense, even a few minutes in AF are enough to shorten the atrial refractory period and reduce its adaptability to the heart rate changes [7, 86]. Moreover, a previous work analyzed the organization time course along successive AF episodes and reported that AF organization presented a decreasing trend in 63% of the studied patients, whereas the remaining 37% presented a stable AF organization level [145]. Furthermore, AF often progresses from short paroxysmal AF episodes to longer and more frequent episodes [2] and many patients eventually develop persistent AF [9]. In addition, since the arrhythmia is often asymptomatic, several AF episodes may occur before the arrhythmia is first diagnosed [2]. Therefore, an earlier intervention could be interesting in paroxysmal AF patients in order to maximize the probability of the therapy success [8]. Thus, the classification between both stages of the arrhythmia from ambulatory ECG recordings is interesting because it could contribute to make the appropriate decisions in the arrhythmia management without having to wait for a 24 or 48 hours Holter ECG recording.

Previous studies have reported organization differences between paroxysmal and persistent AF. For instance, Ravelli et al. [20] analyzed wave similarity maps obtained from invasive recordings and found high similarity regions in paroxysmal AF that were not present in persistent AF. In contrast, a recent study analyzed the dominant morphology of complex fractionated atrial electrograms and reported a higher spatiotemporal stability in persistent AF than in paroxysmal AF [192], thus suggesting the presence of more stable drivers in persistent AF. Moreover, high frequency activity regions with different distributions in paroxysmal and persistent AF patients were detected in a previous work through spectral analysis and frequency mapping of invasive atrial recordings [105]. In addition, Lazar et al. [106] found that paroxysmal AF presents a higher left-to-right atrial frequency gradient than persistent AF. Related to this latter finding, another invasive study found differences in the entropy values between both atria in paroxysmal AF patients that were not present in persistent AF [111]. With respect to noninvasive methods, previous works have demonstrated that persistent AF presents higher DAF values than paroxysmal AF [42, 43]. Furthermore, the application of noninvasive organization indices, such as DAF and SampEn, in ambulatory ECG recordings allows to classify between paroxysmal and persistent AF [44] regardless of the time instant in which the ECG was recorded [45].

Hence, the estimation of AF organization from the surface ECG is an interesting alternative to the use of Holter ECG recordings in the classification between paroxysmal and persistent AF patients. Thus, the metric that achieved the best classification results in the previous scenarios was applied in the discrimination between paroxysmal and persistent AF from short ECG recordings.

As before, $H(2)$ was selected for this scenario. $H(2)$ was computed over the MAW in order to improve its performance because in previous studies this strategy produced the best results (see Section 4.2 in the next chapter). Then, the performance of this metric in the classification between paroxysmal and persistent AF episodes was compared with two well-known AF organization metrics, such as DAF and SampEn. These three indices were computed over the whole 10 seconds signals in the database described in Section 3.1.3.

3.2.6 Statistical analysis

Nonlinearity and nonstationarity tests

The signals in the AFTDB were tested for stationarity using the runs test [193]. For this purpose, all non-overlapping 15 seconds segments of the recordings were divided into non-overlapping 0.5 seconds segments and the average value and standard deviation of the signal amplitude were computed on each segment. Then, the runs test was applied to each sequence in order to check whether the process could be considered as stationary.

Next, a study of surrogate data was performed in order to check whether the studied indices can detect a nonlinear behavior in the AF signals [194]. Since the signals showed a non-stationary behavior, the Truncated Fourier Transform method described in [195], which is a generalization of the Fourier Transform based surrogate data methods for its application in non-stationary time series, was selected. In this method, the phases above a certain cut-off frequency are randomized, leaving the low frequencies unaltered [195] in order to preserve the non-stationary behavior of the signal in the surrogates. Hence, surrogate data show the same linear and non-stationary properties than the original series, but not the possible nonlinear features. Thereby, significant differences between the values of any nonlinear index obtained from the two data sets will indicate that the signals are nonlinear [194]. Since the 3–9 Hz band contains most of the atrial activity energy during AF [149], a cut-off frequency of 3 Hz was selected for this method and 40 surrogate signals were generated both from each original AA and MAW extracted from the AFTDB. Figure 3.5 shows an example of original and surrogate signals. Next, the studied nonlinear indices were computed over each surrogate data set and compared with the values obtained from the corresponding original signals using a rank-order test [196]. Hence, the hypothesis of linearity was rejected if the original signal produced an index value that was either higher or lower than those of its corresponding surrogate data set.

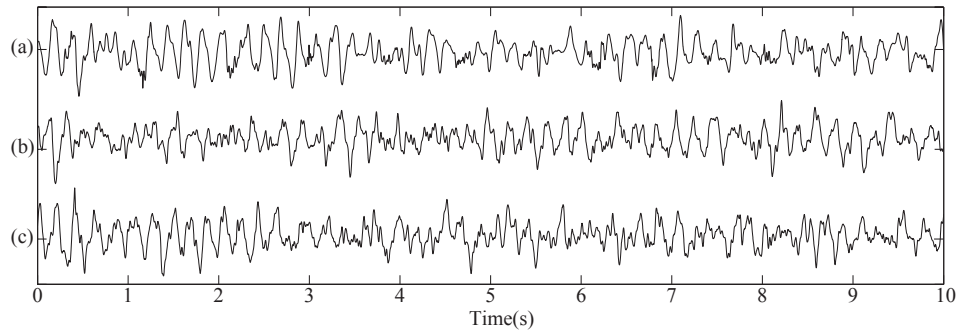

Figure 3.5. Example of surrogate data. (a) Original AA signal. (b), (c) Surrogate signals.

Classification performance and statistical significance

First, the distributions were tested for normality and homoscedasticity using the Kolmogorov-Smirnov and Levene tests. Then, the differences between groups were tested using a Student's t test when the distributions were normal; otherwise a Mann-Whitney U-test was carried out. In addition, when more than two groups were defined the differences among them were tested using a Kruskal-Wallis analysis of variance if the distributions were not normal and homoscedastic or an ANOVA analysis if the distributions were normal and homoscedastic. In both cases, a two-tailed value of $p < 0.05$ was considered as statistically significant.

Regarding the classification between pairs of groups, the receiver operating characteristics (ROC) curves were then computed in order to obtain the optimum threshold and the accuracy for each computed metric. In this analysis, the sensitivity value was defined as the fraction of true positives out of the positives and the specificity value was defined as the fraction of true negatives out of the negatives. The accuracy value was defined as the total number of AF episodes correctly classified. Then, the ROC curve was created by plotting the sensitivity versus 1-specificity for each possible threshold. The optimum threshold was selected as the point of the curve that maximized the accuracy. The area under the ROC curve (AROC), which represents a summary of the performance, was also computed. To this respect, a value of $AROC = 1$ corresponds to a perfect classification, whereas a random classifier would produce a value of $AROC = 0.5$, which is the worst possible case.

As for the study of the organization time course before AF termination, the existence of a significant trend in $H(2)$ values was tested using a non-parametric Kruskal–Wallis test because the distributions were not normal and homoscedastic. In addition, the differences among different time intervals were tested making use of a Wilcoxon T test for paired data. In both cases, a two-tailed value of $p < 0.05$ was considered as statistically significant

Finally, since the same data were used to define the classification thresholds and test the classification model, the obtained model can suffer from overfitting. Therefore, leave-one-out cross-validation was applied in order to improve the consistency of the classification. In this procedure, the classifier is trained using all cases but one and, then, the remaining case is classified. Next, this process is repeated for all cases.

Chapter 4

Results

In this chapter, the results of the studies described in Chapter 3 are presented. This chapter is structured as follows. First, the results of nonlinearity and non-stationarity tests are presented in section 4.1. Section 4.2 contains the comparative of the indices presented in Section 3.2.4 in the classification between different AF organization levels. Next, since $H(2)$ achieved the highest classification accuracy, the optimal parameters selection for this index is described in Section 4.3 and the study of early AF termination prediction results are shown in Section 4.4. Finally, the performance of $H(2)$ in the classification between paroxysmal and persistent AF episodes is presented in Section 4.5.

4.1 Nonlinearity and non-stationarity

The analyzed signals showed a non-stationary behavior. Moreover, statistically significant differences were found between the original and surrogate data for all the studied indices both from the AA and the MAW. To this respect, Figure 4.1 displays the values of SampEn, LZC and H computed over the original and surrogate AA signals extracted from the recordings in the AFTDB. It is interesting to note that the original signals produced lower SampEn and LZC values and higher H values than their corresponding surrogate data sets. Therefore, the original signals present higher pattern repetitiveness and higher self-similarity than the surrogate ones. A similar result was obtained for the MAW signals, as

can be observed in Figure 4.2 for SampEn, LZC and H. Although the differences between original and surrogate data were not as pronounced as in the case of the AA signals, statistically significant differences were found between original and surrogate MAW signals for most of the recordings. Although only the results of three indices have been displayed, all the studied metrics obtained similar results in the surrogate data test. Therefore, it can be concluded that AF responds to a nonlinear and non-stationary model. Hence, the use of nonlinear indices in the analysis of AA and MAW signals is appropriate.

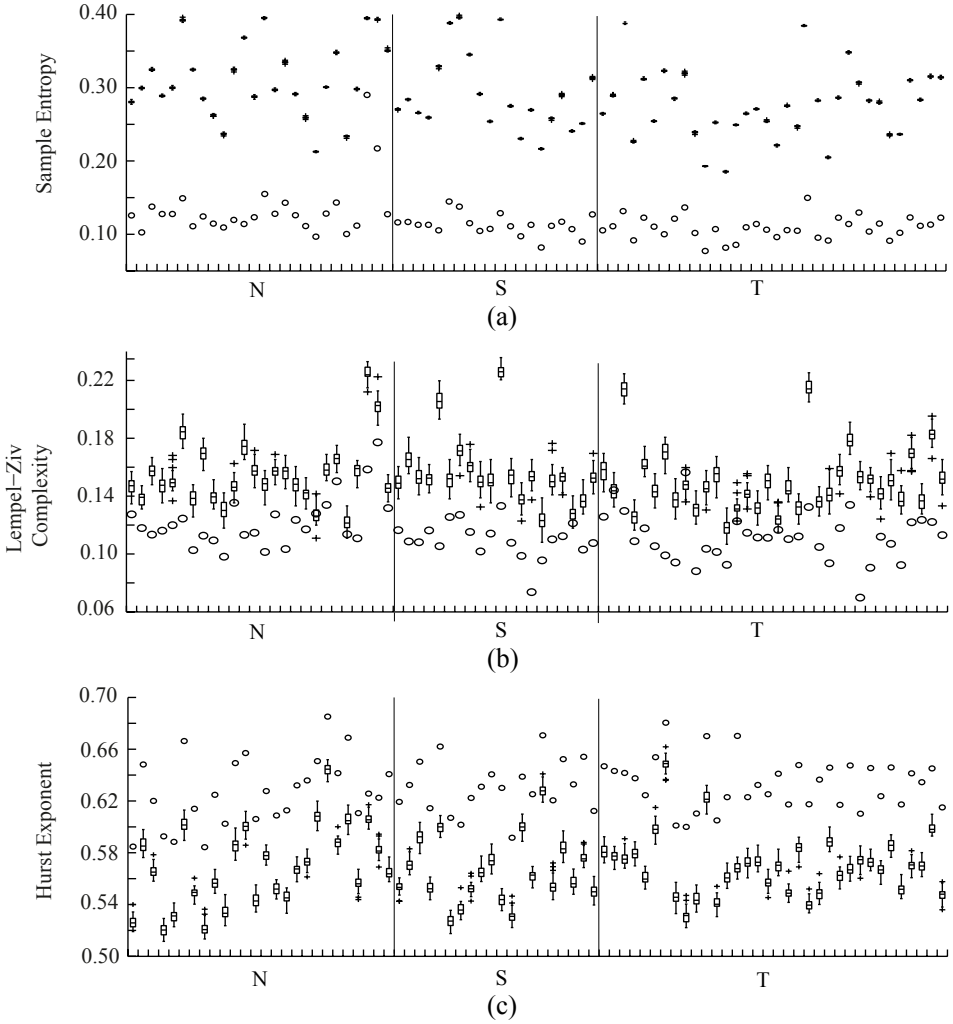

Figure 4.1. Results of the surrogate data test. Values of (a) SampEn, (b) LZC (two-symbol sequence conversion) and (c) H computed on the original AA signals extracted from the AFTDB (circles) and their corresponding surrogate data sets (boxplot).

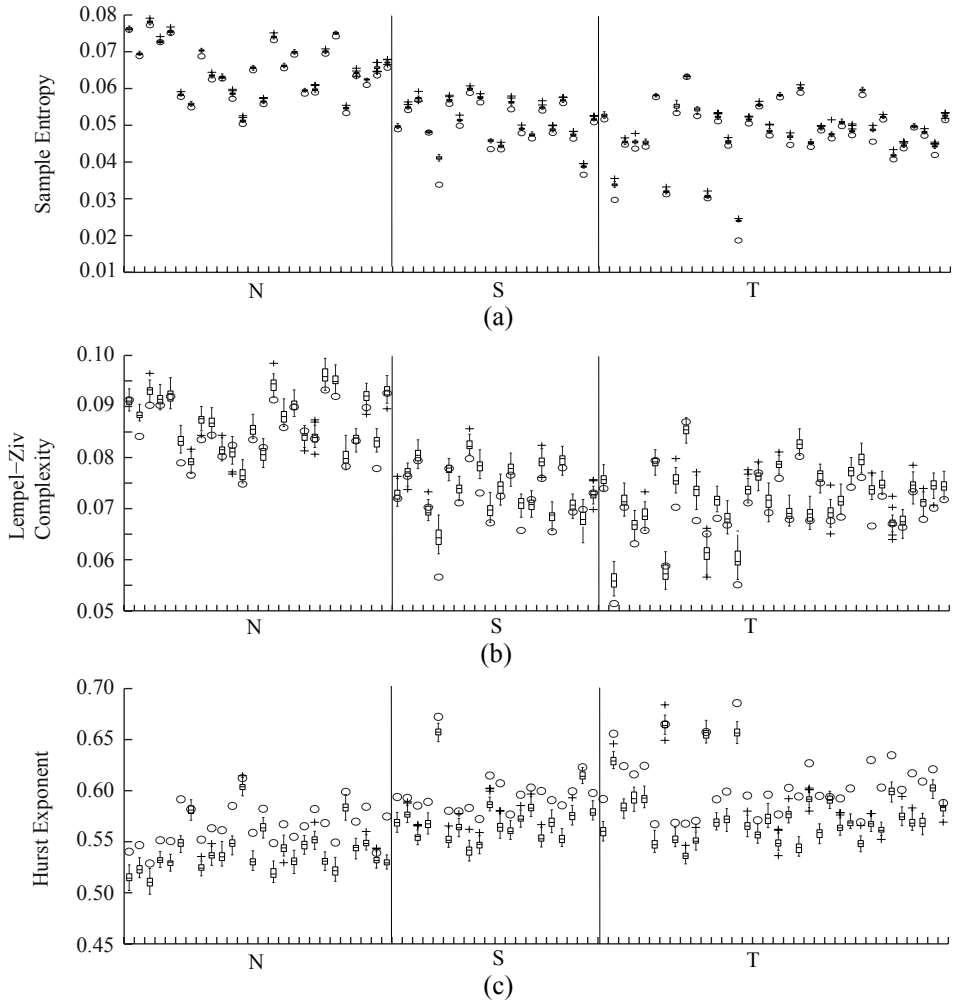

Figure 4.2. Results of the surrogate data test for the MAW signals extracted from all the recordings in the AFTDB. Values of (a) SampEn, (b) LZC (two-symbol sequence conversion) and (c) H computed on the original MAW signals (circles) and their corresponding surrogate data sets (boxplot).

4.2 Prediction of AF termination

The median values and interquartile ranges of the studied nonlinear metrics computed in the AA and the MAW for AFTDB groups N, S and T are shown in Tables 4.1 and 4.2. In addition, the median values and interquartile ranges of the reference metrics are displayed in Table 4.3. Note that all metrics computed on the MAW present increasing or decreasing median values from non-terminating to terminating AF episodes. This result suggests a coherent time course in AF organization prior to its spontaneous termination. However, only FuzzEn and H computed on the AA showed clear trends in median values from N to T episodes. Furthermore, these trends were more emphasized when the indices were calculated using the MAW instead of the AA. Besides, the MAW produced lower median FuzzEn, SpecEn and LZC values and higher $H(1)$ and $H(2)$ values than the AA signal, thus suggesting lower irregularity and complexity in the MAW than in the AA signal.

Table 4.1. Median and interquartile range of the nonlinear metrics computed for each group of episodes from the AA signal to predict AF termination from the AFTDB. The statistical significance p obtained with a Kruskal-Wallis analysis of variance is also presented.

	Group N		Group S		Group T		
	median	iqr	median	iqr	median	iqr	p-value
FuzzEn	0.0687	0.0191	0.0592	0.0142	0.0574	0.0159	< 0.03
SpecEn	0.9393	0.0304	0.8767	0.0670	0.8814	0.0862	< 0.001
LZC (2 Sym)	0.1174	0.0171	0.1094	0.0115	0.1117	0.0207	0.034
LZC (3 Sym)	0.1408	0.0227	0.1250	0.0114	0.1289	0.0263	0.044
H	0.6252	0.0395	0.6306	0.0285	0.6355	0.0284	0.164
$H(1)$	0.9617	0.0180	0.9549	0.0099	0.9544	0.0124	0.089
$H(2)$	0.9539	0.0347	0.9429	0.0121	0.9447	0.0223	0.105

Table 4.2. Median and interquartile range of the nonlinear metrics computed for each group of episodes from the MAW to predict AF termination from the AFTDB. The statistical significance p obtained with a Kruskal-Wallis analysis of variance is also presented.

	Group N		Group S		Group T		
	median	iqr	median	iqr	median	iqr	p-value
FuzzEn	0.0370	0.0111	0.0221	0.0060	0.0215	0.0060	< 0.001
SpecEn	0.9110	0.0258	0.8507	0.0519	0.8471	0.0959	< 0.001
LZC (2 sym)	0.0848	0.0098	0.0719	0.0079	0.0704	0.0069	< 0.001
LZC (3 sym)	0.0990	0.0120	0.0839	0.0084	0.0814	0.0090	< 0.001
H	0.5641	0.0314	0.5933	0.0171	0.5999	0.0324	< 0.001
$H(1)$	0.9959	0.0014	0.9973	0.0007	0.9976	0.0006	< 0.001
$H(2)$	0.9958	0.0015	0.9972	0.0007	0.9975	0.0006	< 0.001

Regarding the differences among groups, all the metrics obtained from the MAW provided statistically significant differences among groups ($p < 0.01$). On the other hand, when computing the nonlinear indices on the AA, only FuzzEn, SpecEn and LZC presented statistically significant differences among groups.

Table 4.3. Median and interquartile range of the DAF and SampEn, computed as reference parameters, to predict AF termination from the AFTDB. The statistical significance p obtained with a Kruskal-Wallis analysis of variance is also presented.

	Group N		Group S		Group T		
	median	iqr	median	iqr	median	iqr	p-value
DAF (Hz)	6.583	0.8799	5.1906	0.8265	5.0584	0.6053	< 0.001
SampEn	0.0642	0.0108	0.0494	0.0087	0.0473	0.0075	< 0.001

However, the differences found with all the metrics between groups S and T were not statistically significant.

With respect to the discrimination accuracy of the metrics, Tables 4.4 and 4.5 contain the accuracy values of the metrics computed on the AA and the MAW, respectively, and the diagnostic accuracy of the reference metrics is presented in Table 4.6. Moreover, cross-validation results are presented in Table 4.7. Finally, the values of the indices computed on the AA and the MAW, together with the ROC curves and classification thresholds obtained for each studied scenario are displayed in Figures 4.3, 4.4, 4.5, 4.6, 4.7, 4.8, and 4.9. In addition, the values of the reference metrics and their corresponding ROC curves and classification thresholds are shown in Figure 4.10. As can be seen in these tables and figures, the classification among groups was more accurate when the nonlinear indices were computed on the MAW, which is in agreement with previous studies. In this sense, all the metrics computed on the MAW, excepting H, achieved a higher discrimination accuracy than the reference metrics. Thus, improvements in the diagnostic accuracy with regard to SampEn as far as 6.5%, 6%, 5.5% and 2.5% were observed in the four classification scenarios, respectively. In contrast, none of the metrics applied to the AA yielded better classification results than the DAF and SampEn. To this respect, only the SpecEn from the AA reached a slightly lower discriminant ability than the DAF in the four considered classification scenarios, being more than 75% of cross-validated grouped cases properly identified in scenarios N vs. T, N vs. S and N vs. (S & T).

Finally, a stepwise logistic regression analysis was performed using all the studied metrics in order to improve the discrimination accuracy obtained from each individual index. However, this analysis did not improve the best classification accuracy provided by a single parameter. In fact, for every considered classification scenario, this analysis produced a discriminant model composed only by the parameter $H(2)$, computed from the MAW. In connection with this result, is important to note that a statistically significant Spearman correlation was noticed among all the studied indices computed on both the AA and the MAW. Thus, for metrics computed over the AA a minimum correlation value of 0.46 was observed, whereas this value increased up to 0.58 for the metrics computed over the MAW. Moreover, correlation values higher than 0.90 were noticed among the indices FuzzEn, LZC, $H(1)$, $H(2)$ and SampEn computed over the MAW.

Table 4.4. Classification results provided by each single nonlinear metric computed from the AA signals extracted from the recordings in the AFTDB for each scenario described in Section 3.2.5 for the prediction of AF termination.

	N vs. T				N vs. S			
	Sp	Se	Acc	p	Sp	Se	Acc	p
FuzzEn	61.76%	84.62%	71.67%	0.008	73.08%	65.00%	69.57%	0.135
SpecEn	92.31%	82.35%	86.69%	< 0.001	92.31%	85.00%	89.13%	< 0.001
LZC (2 sym)	58.82%	69.23%	63.33%	0.028	65.00%	73.08%	69.57%	0.011
LZC (3 sym)	55.88%	76.92%	65.00%	0.023	85.00%	76.92%	80.43%	0.009
H	38.46%	85.29%	65.00%	0.329	90.00%	34.62%	58.70%	0.584
$H(1)$	88.24%	50.00%	71.67%	0.072	80.00%	57.69%	69.57%	0.044
$H(2)$	82.35%	57.69%	71.67%	0.077	85.00%	61.54%	71.74%	0.064
	S vs. T				N vs. (S & T)			
	Sp	Se	Acc	p	Sp	Se	Acc	p
FuzzEn	47.06%	80.00%	59.26%	0.316	61.54%	75.93%	71.25%	0.003
SpecEn	40.00%	76.47%	62.98%	0.474	92.31%	83.33%	86.25%	< 0.001
LZC (2 sym)	60.00%	55.88%	57.41%	0.589	59.26%	73.08%	63.75%	0.059
LZC (3 sym)	60.00%	61.76%	61.11%	0.838	66.67%	76.92%	70.00%	0.015
H	65.00%	52.94%	57.41%	0.539	15.38%	98.15%	71.25%	0.353
$H(1)$	45.00%	67.65%	59.26%	0.642	75.93%	61.54%	71.25%	0.027
$H(2)$	85.00%	41.18%	57.41%	0.616	85.19%	57.69%	76.25%	0.038

Table 4.5. Classification results provided by each single nonlinear metric computed from the MAW signals extracted from the recordings in the AFTDB for each scenario described in Section 3.2.5 for the prediction of AF termination.

	N vs. T				N vs. S			
	Sp	Se	Acc	p	Sp	Se	Acc	p
FuzzEn	85.29%	96.15%	90.00%	< 0.001	88.46%	95.00%	91.30%	< 0.001
SpecEn	88.24%	96.15%	91.67%	< 0.001	90.00%	88.46%	89.13%	< 0.001
LZC (2 sym)	94.12%	92.31%	93.34%	< 0.001	88.46%	95.00%	91.30%	< 0.001
LZC (3 sym)	88.24%	92.31%	90.00%	< 0.001	85.00%	96.15%	91.30%	< 0.001
H	79.41%	88.46%	83.33%	< 0.001	88.46%	75.00%	82.61%	< 0.001
$H(1)$	96.15%	94.12%	95.00%	< 0.001	95.00%	88.46%	91.30%	< 0.001
$H(2)$	92.30%	94.12%	93.34%	< 0.001	100.00%	85.00%	93.48%	< 0.001
	S vs. T				N vs. (S & T)			
	Sp	Se	Acc	p	Sp	Se	Acc	p
FuzzEn	35.00%	85.29%	66.67%	0.152	80.77%	98.15%	92.50%	< 0.001
SpecEn	80.00%	41.18%	55.56%	0.513	87.04%	96.15%	90.00%	< 0.001
LZC (2 sym)	45.00%	85.29%	70.37%	0.103	94.44%	88.46%	92.50%	< 0.001
LZC (3 sym)	40.00%	82.35%	66.67%	0.078	88.89%	92.59%	90.00%	< 0.001
H	45.00%	76.47%	64.81%	0.237	57.69%	98.15%	85.00%	< 0.001
$H(1)$	55.00%	73.53%	66.67%	0.072	96.15%	90.74%	92.50%	< 0.001
$H(2)$	55.00%	73.53%	66.67%	0.067	96.15%	90.74%	92.50%	< 0.001

Table 4.6. Classification results provided by DAF and SampEn, computed as reference parameters on the AFTDB, for each scenario described in Section 3.2.5 for the prediction of AF termination provided by DAF and SampEn, computed as reference parameters.

	N vs. T				N vs. S			
	Sp	Se	Acc	p	Sp	Se	Acc	p
DAF	82.35%	96.15%	88.33%	< 0.001	85.00%	80.77%	82.61%	< 0.001
SampEn	82.35%	96.15%	88.33%	< 0.001	95.00%	84.62%	89.13%	< 0.001
	S vs. T				N vs. (S & T)			
	Sp	Se	Acc	p	Sp	Se	Acc	p
DAF	55.00%	67.65%	62.96%	0.118	81.48%	96.15%	86.25%	< 0.001
SampEn	35.00%	82.35%	64.81%	0.159	92.59%	88.46%	91.25%	< 0.001

Table 4.7. Accuracy values obtained in leave-one-out cross-validation results for the reference metrics and the nonlinear indices computed on both the AA and MAW signals extracted from the recordings in the AFTDB for each scenario described in Section 3.2.5 for the prediction of AF termination.

	N vs. T	N vs. S	T vs. S	N vs. (T & S)
DAF	85.00%	78.26%	57.41%	82.50%
SampEn-MAW	85.00%	89.13%	54.00%	86.25%
FuzzEn-AA	63.33%	69.57%	53.70%	63.75%
SpecEn-AA	76.67%	86.96%	48.15%	75.00%
LZC-AA (2 sym)	66.67%	65.22%	51.85%	62.50%
LZC-AA (3 sym)	63.33%	78.26%	57.41%	68.75%
H-AA	56.67%	52.17%	53.70%	54.30%
$H(1)$-AA	60.00%	60.87%	55.56%	62.50%
$H(2)$-AA	66.67%	67.39%	53.70%	71.25%
FuzzEn-MAW	88.33%	86.96%	53.70%	90.00%
SpecEn-MAW	88.33%	86.96%	48.15%	87.50%
LZC-MAW (2 sym)	91.67%	89.13%	55.56%	90.00%
LZC-MAW (3 sym)	90.00%	89.13%	59.26%	88.75%
H-MAW	81.67%	78.26%	50.00%	78.75%
$H(1)$-MAW	91.67%	86.96%	58.00%	91.25%
$H(2)$-MAW	91.67%	89.13%	57.41%	91.25%

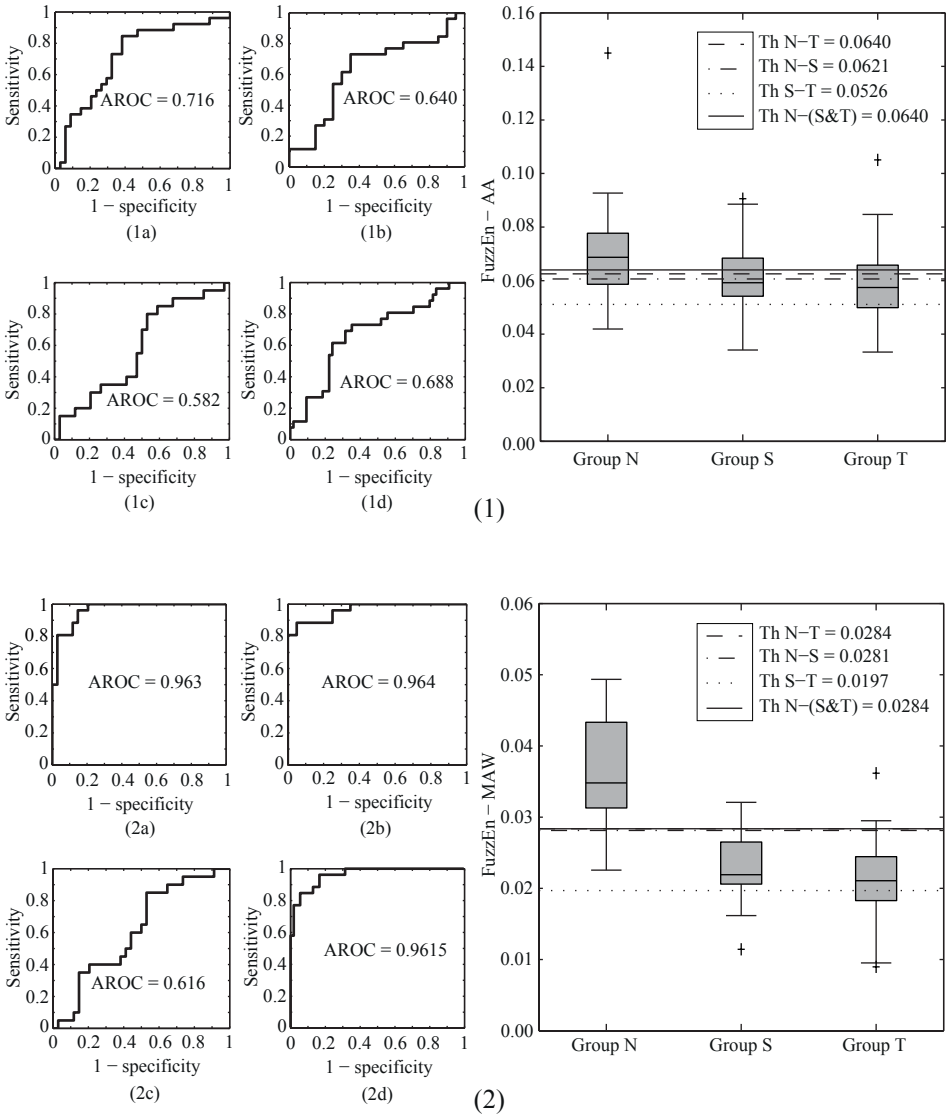

Figure 4.3. Results of FuzzEn computed on the AA signals (1) and MAW signals (2) in the prediction of AF termination using the AFTDB. ROC curves calculated for each of the four considered scenarios: N vs. T (a), N vs. S (b), S vs. T (c) and N vs. S and T (d). The values of FuzzEn for each group and optimum classification thresholds are also displayed.

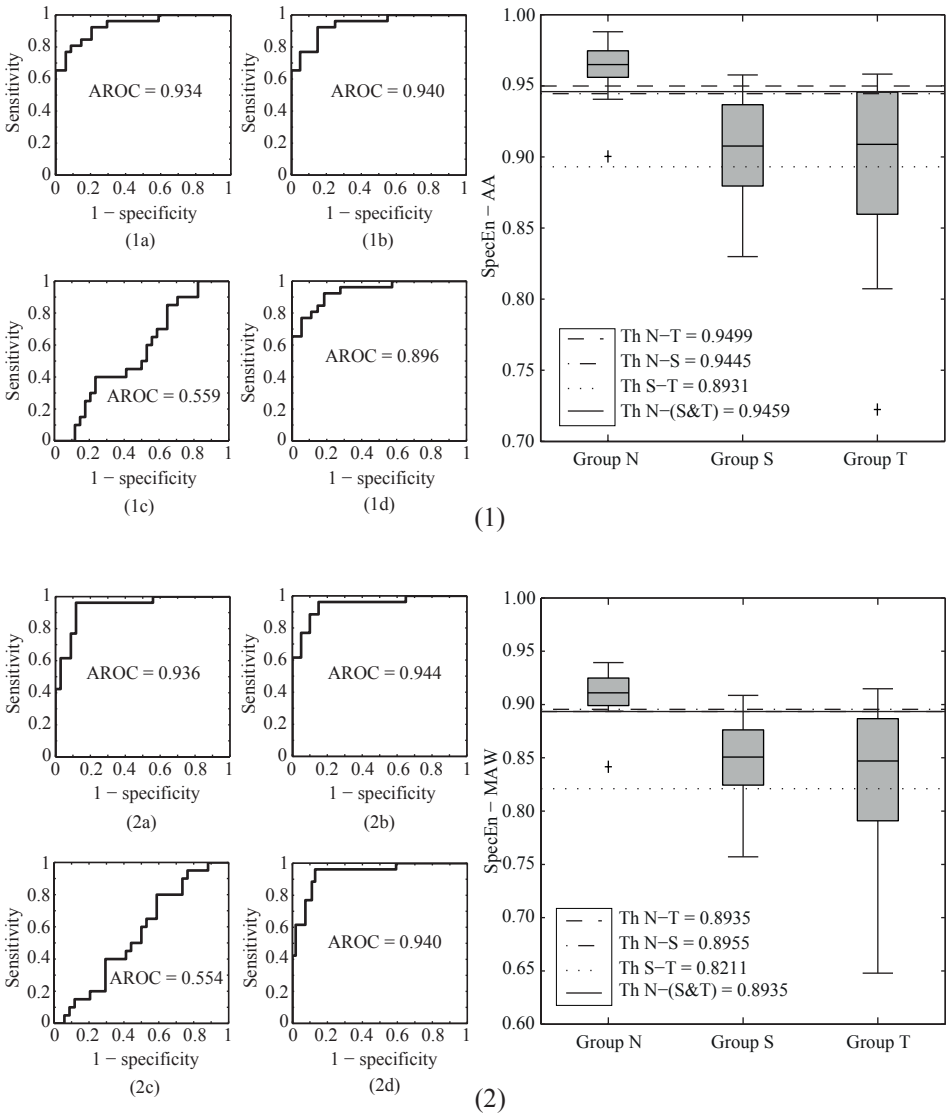

Figure 4.4. Performance of SpecEn computed on the AA signals (1) and MAW signals (2) in the prediction of AF termination from the AFTDB. The ROC curves obtained in the four considered classification scenarios are displayed: N vs. T (a), N vs. S (b), S vs. T (c) and N vs. S and T (d). The values of SpecEn for each group in the database and the optimum classification thresholds are also shown.

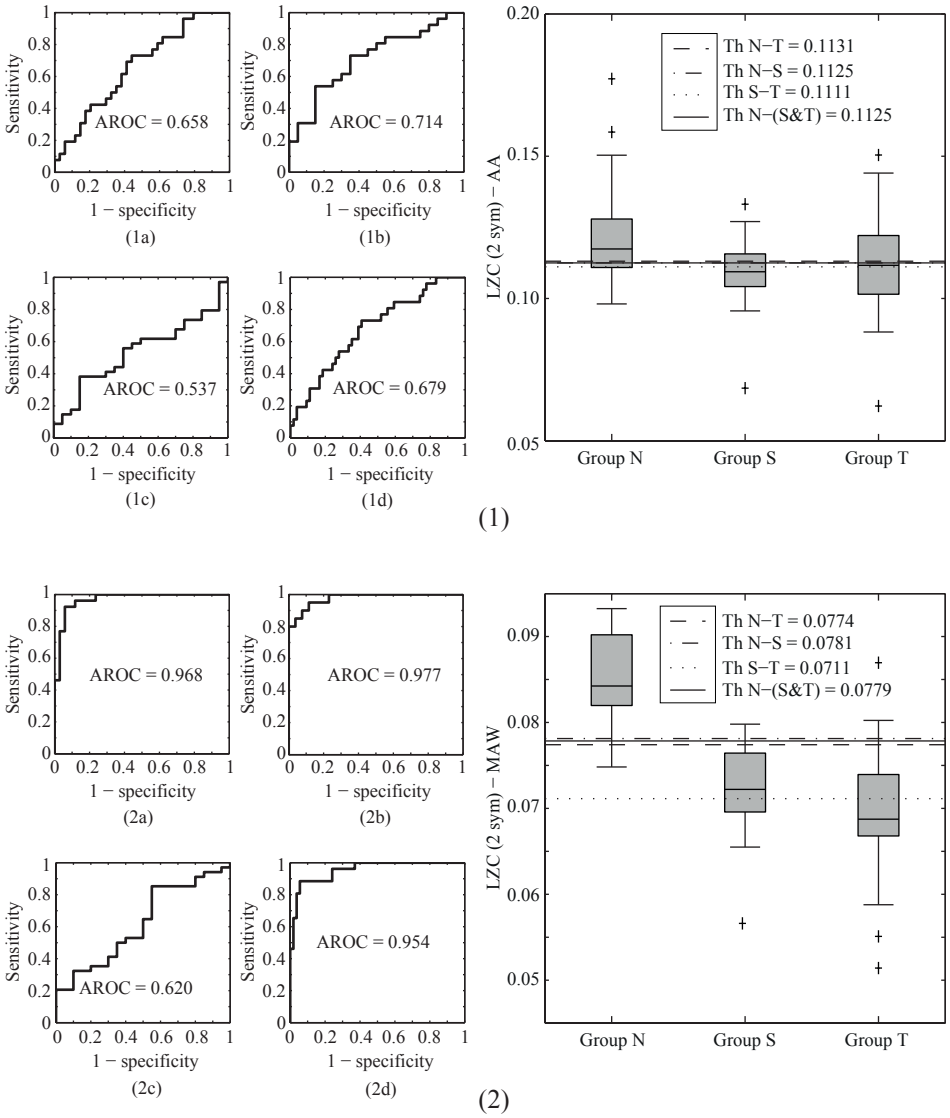

Figure 4.5. Results of LZC computed using the binary conversion in the prediction of AF termination using the AFTDB. The ROC curves obtained for LZC computed on the AA signals (1) and MAW signals (2), the values of LZC and the optimum classification thresholds are shown. The four considered classification scenarios are displayed: N vs. T (a), N vs. S (b), S vs. T (c) and N vs. S and T (d).

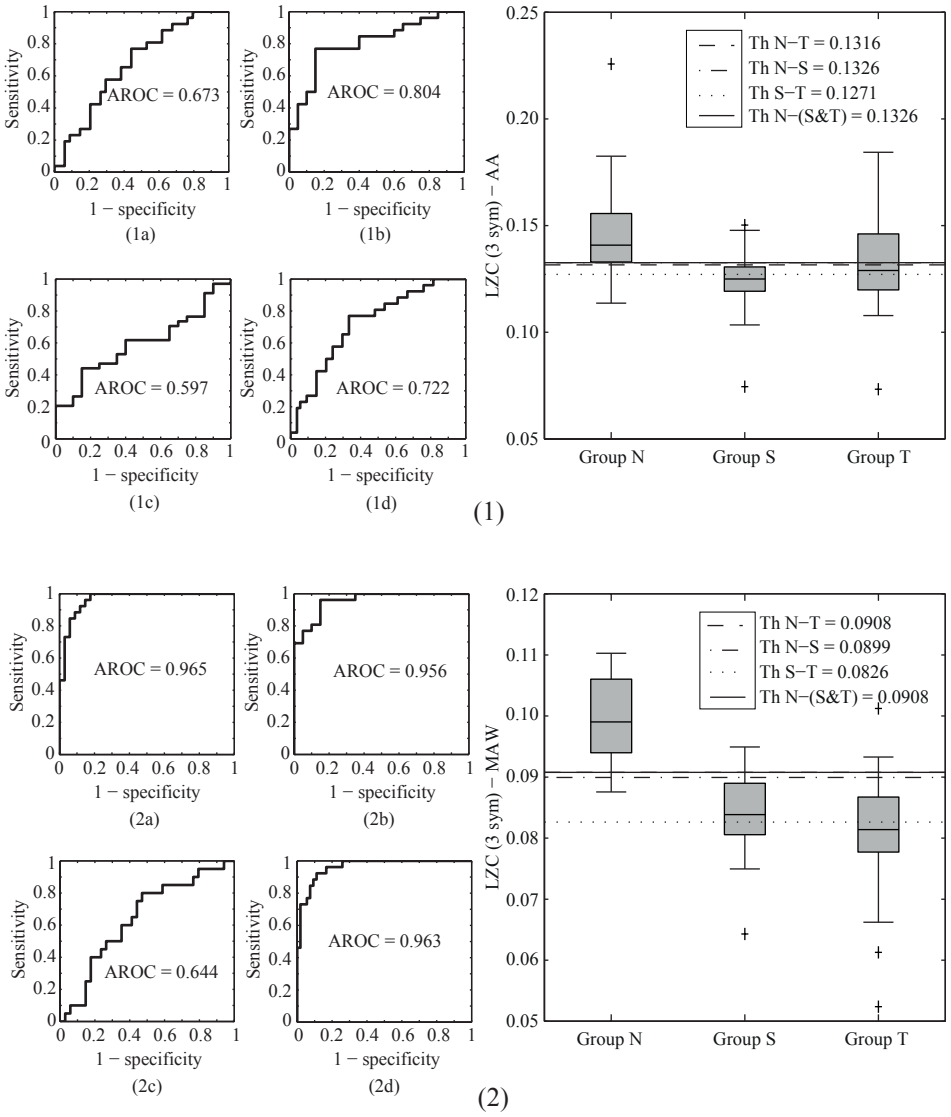

Figure 4.6. Performance of LZC computed using the three-symbol conversion on the AA signals (1) and MAW signals (2) in the prediction of AF termination from the AFTDB. The curves corresponding to the four considered classification scenarios are shown: (a) N vs. T, (b) N vs. S, (c) S vs. T and (d) N vs. S and T. The values of LZC in each group and the optimum classification thresholds are also displayed.

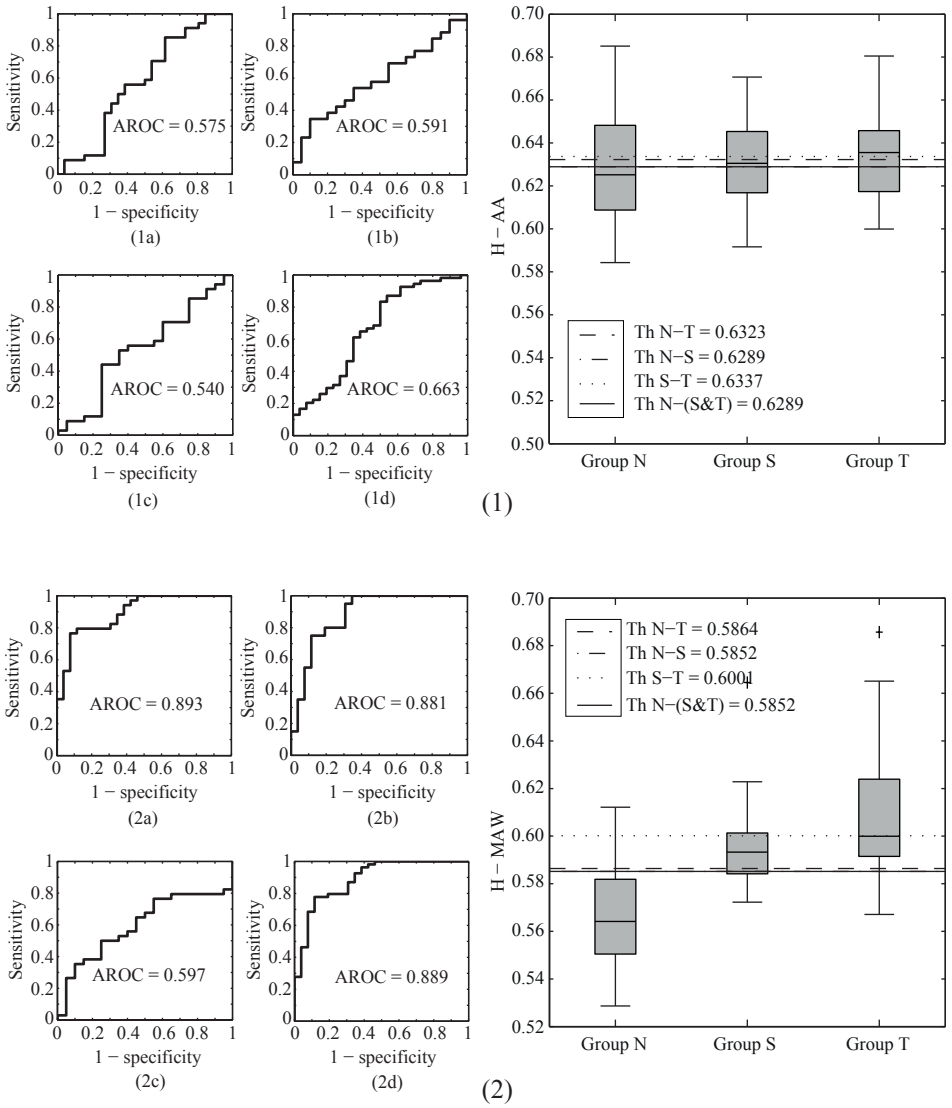

Figure 4.7. Results of H computed on the AA signals (1) and MAW signals (2) in the prediction of AF termination. ROC curves, values of H in each group of the AFTDB and optimum classification thresholds are displayed. The ROC curves corresponding to the four considered classification scenarios are presented: N vs. T (a), N vs. S (b), S vs. T (c) and N vs. S and T (d).

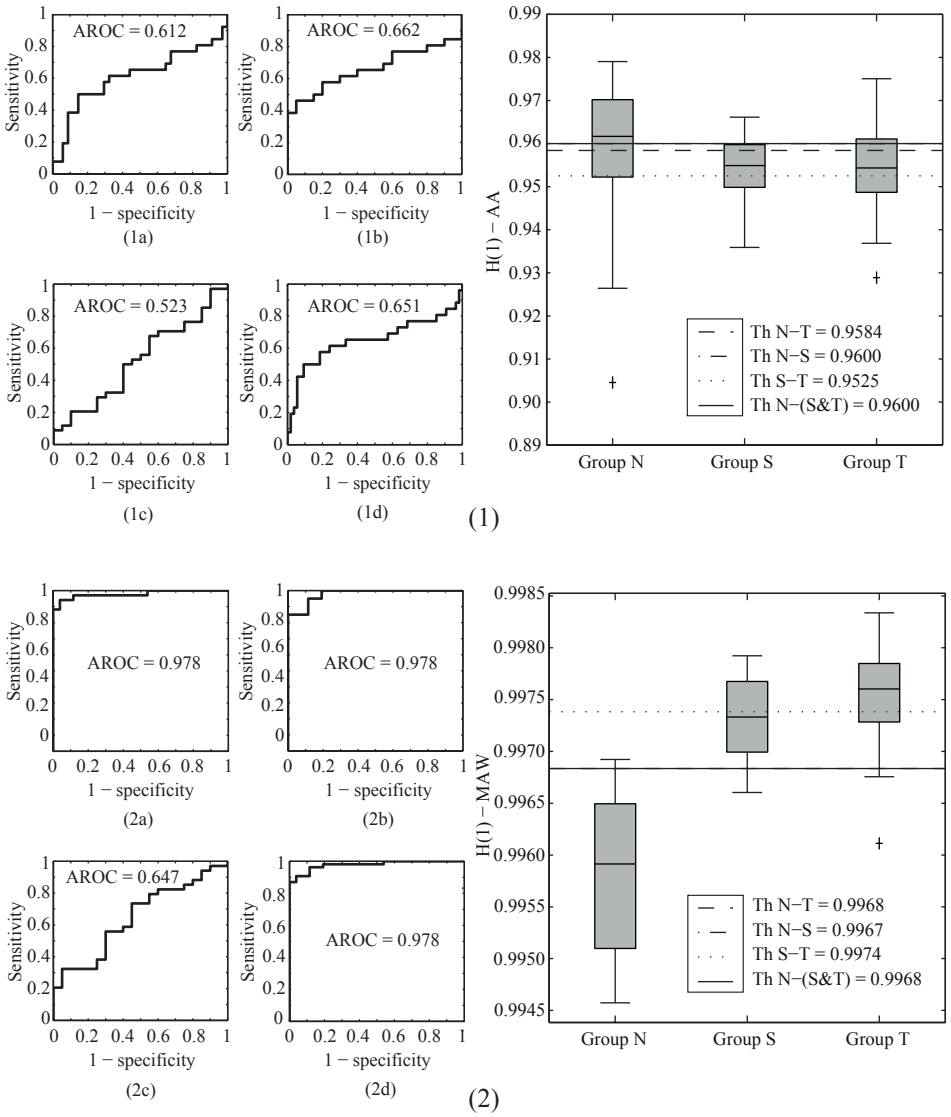

Figure 4.8. Prediction of AF termination using $H(1)$ computed on the AA signals (1) and MAW signals (2) extracted from the AFTDB. The ROC curves corresponding to the four considered classification scenarios are displayed: N vs. T (a), N vs. S (b), S vs. T (c) and N vs. S and T (d). The values of $H(1)$ in each group and the optimum classification thresholds are also shown.

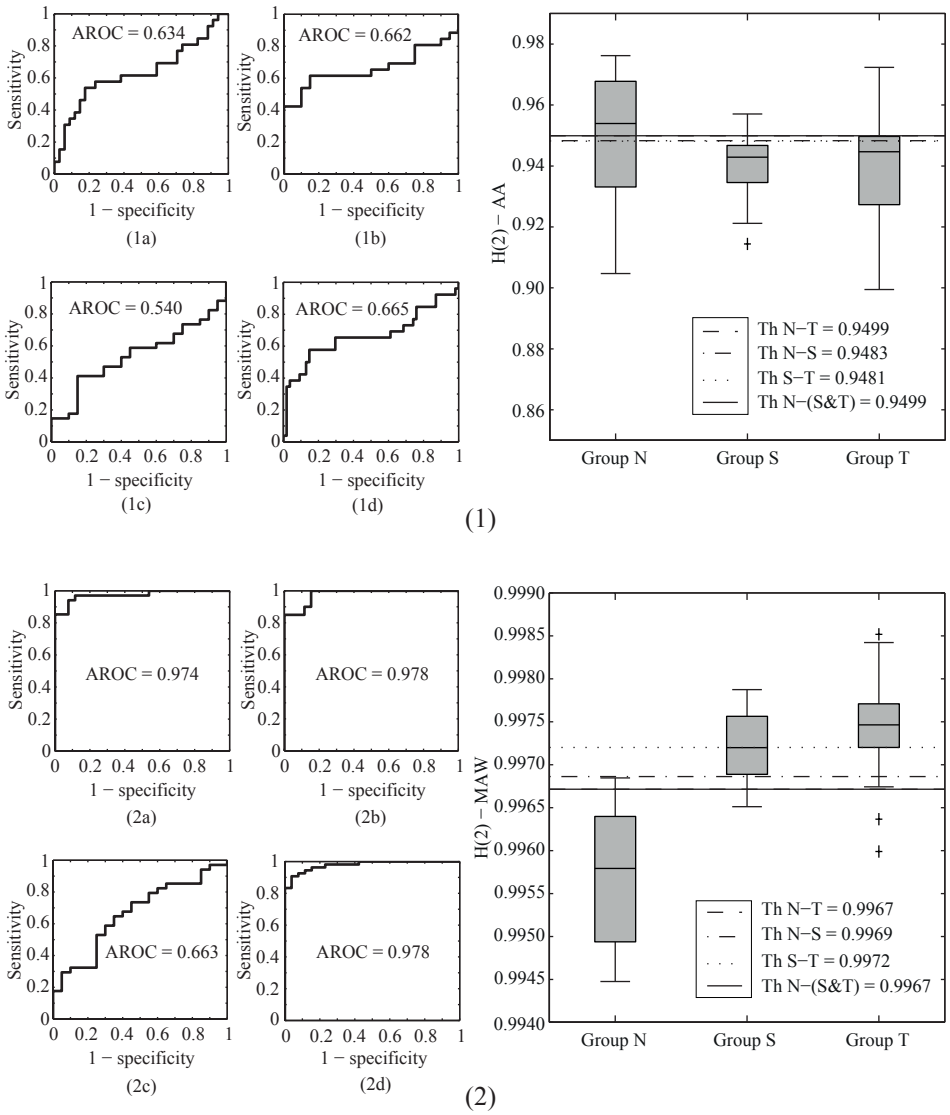

Figure 4.9. Performance of $H(2)$ computed on the AA signals (1) and MAW signals (2) in the prediction of AF termination using the AFTDB. The ROC curves corresponding to the four considered classification scenarios are presented: N vs. T (a), N vs. S (b), S vs. T (c) and N vs. S and T (d). The values of $H(2)$ in each group of the database and the optimum classification thresholds are also displayed.

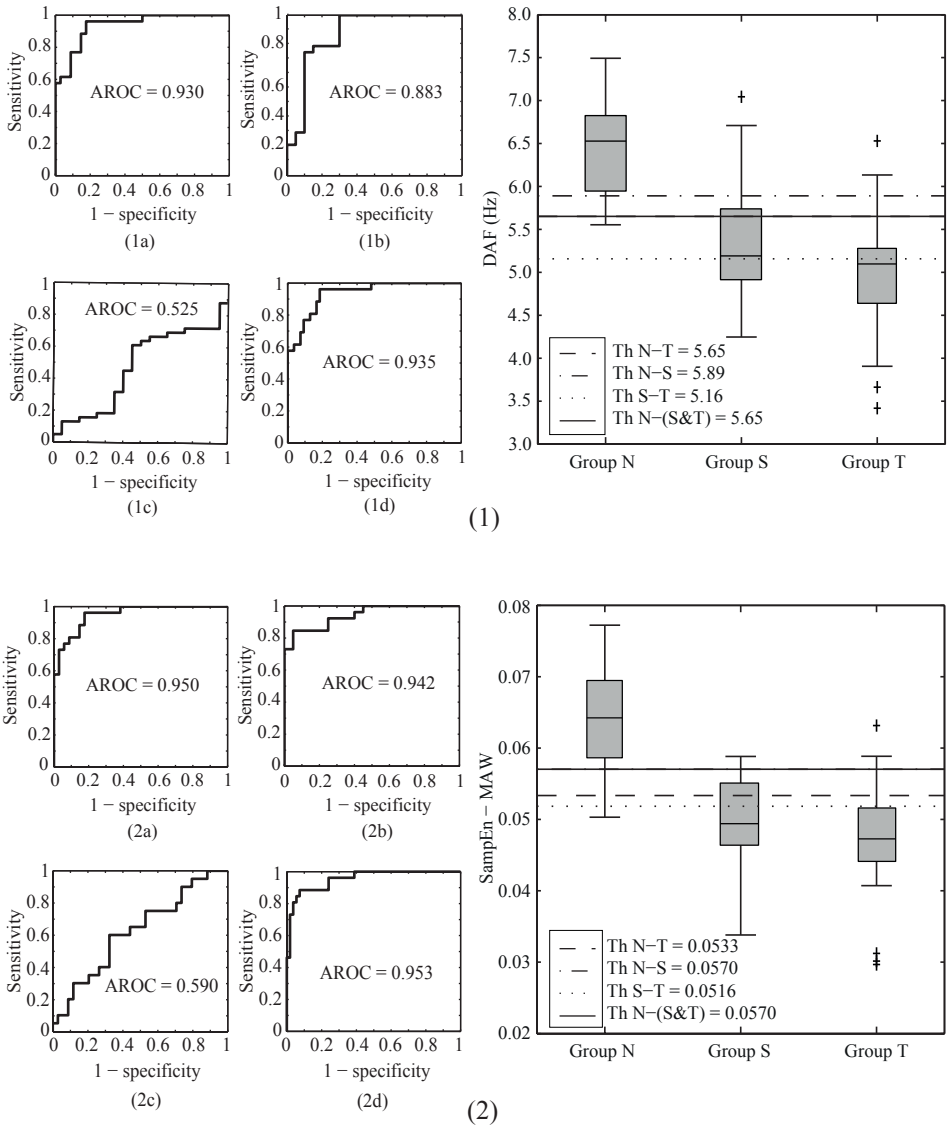

Figure 4.10. Results of the reference metrics, namely, DAF computed on the AA signals (1) and SampEn computed on the MAW (2) in the prediction of AF termination from the AFTDB. The ROC curves, the values of DAF and SampEn in each group of the database and the optimum classification thresholds are presented. The ROC curves corresponding to the four considered classification scenarios are shown: N vs. T (a), N vs. S (b), S vs. T (c) and N vs. S and T (d).

4.3 Optimal computational parameters for $H(2)$

$H(2)$ was selected for the estimation of AF organization in the next studies because of its high accuracy in the prediction of AF termination, as has been shown in results presented in the previous section. Hence, a systematic study of the optimal values of its computational parameters was performed in order to improve the performance of this index in the estimation of AF organization. For this study, the AFTDB was analyzed and the scenarios for discriminating between N, S and T episodes for the prediction of AF termination presented in Section 3.2.5 were considered.

The classification accuracy values of $H(2)$ in each scenario computed using all the combinations of L and f_s values are shown in Figure 4.11. As can be seen in this Figure, relevant differences were observed among the accuracy values. The highest accuracy values were obtained for f_s values between 128 Hz and 1024 Hz and L values of 400 ms or longer. Moreover, several combinations of L and f_s values provided the highest classification accuracy and AROC values in each scenario. Nevertheless, the highest AROC values were obtained for $L = 15$ seconds and $f_s = 1024$ Hz in every classification scenario. More concretely, the AROC for N vs. T, N vs. S, S vs. T and N vs. S and T was 0.9796, 0.9827, 0.6632 and 0.9793, respectively. This pair of values also produced the highest statistical differences between groups. To this respect, the values of p obtained for each scenario were 2.66×10^{-10}, 2.85×10^{-8}, 0.0905 and 4.25×10^{-12}, respectively. Thus, a segment length of 15 seconds was chosen for the next step, where all combinations of τ_{max} and f_s values were studied.

Figure 4.12 displays the classification accuracy values obtained for each pair of τ_{max} and f_s values. The pair of values $\tau_{max} = 20$ ms and $f_s = 1024$ Hz yielded the best classification results in all the studied scenarios. In addition, this pair of values also produced the highest statistical differences between groups. Hence, a sampling rate of 1024 Hz was selected as optimal value.

Finally, Figure 4.13 presents the classification accuracy obtained for each pair of L and τ_{max} values. Once more, several pairs of values produced the highest classification accuracy in each scenario. However, the values of $L = 15$ seconds and $\tau_{max} = 20$ ms produced the highest AROC values and statistical differences between groups in every scenario. Note that this outcome is in complete agreement with the recommendation of the authors who introduced the index [188]. Considering all these results, the optimal values of $L = 15$ seconds, $f_s = 1024$ Hz and $\tau_{max} = 20$ ms were selected for the application of $H(2)$ in any other scenario dealing with atrial activity signals from patients in AF. The ROC curves obtained for $H(2)$ computed using the selected computational values in each of the considered classification scenarios are shown in Figure 4.14.

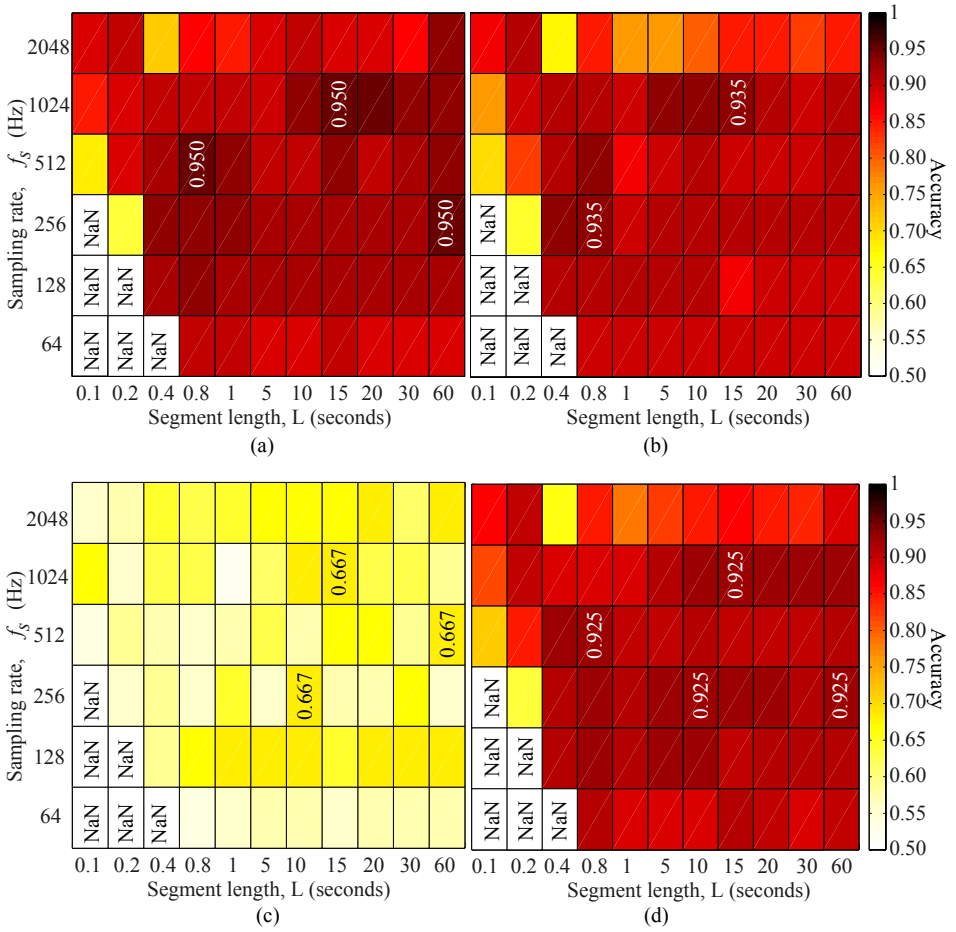

Figure 4.11. Optimal parameters determination for $H(2)$. Effect of the sampling frequency f_s and the analyzed segment length L on the classification accuracy with a reference value of $\tau_{max} = 20$ ms in the four considered classification scenarios for the prediction of AF termination from the AFTDB: (a) N vs. T, (b) N vs. S, (c) S vs. T and (d) N vs S and T. The highest accuracies are indicated in the corresponding square. NaN in some cells stands for Not a Number because $H(2)$ could not be computed in such a short time series.

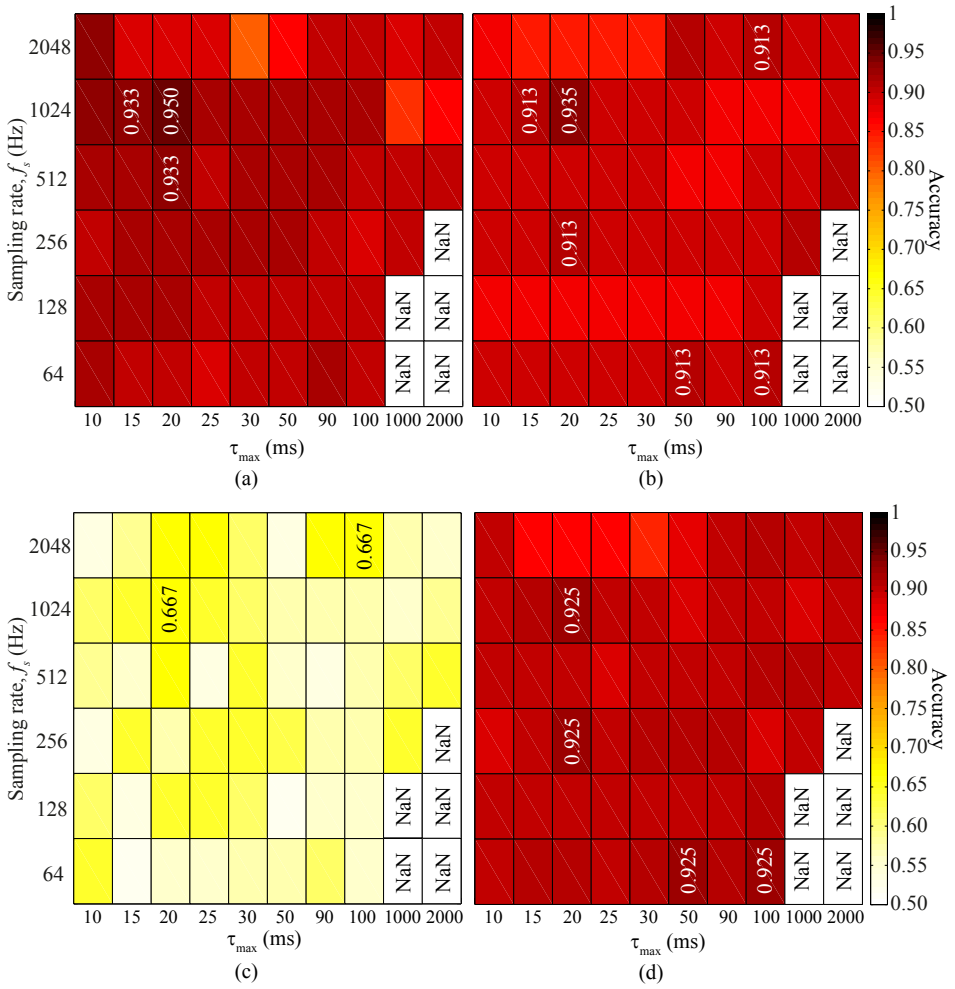

Figure 4.12. Optimal parameters determination for $H(2)$. Classification accuracy obtained for each pair of sampling frequency f_s and τ_{max} values with a reference value of $L = 15$ s in the four considered classification scenarios for the prediction of AF termination from the AFTDB: (a) N vs. T, (b) N vs. S, (c) S vs. T and (d) N vs S and T. The highest accuracies are indicated in the corresponding square. NaN stands for impossible computations.

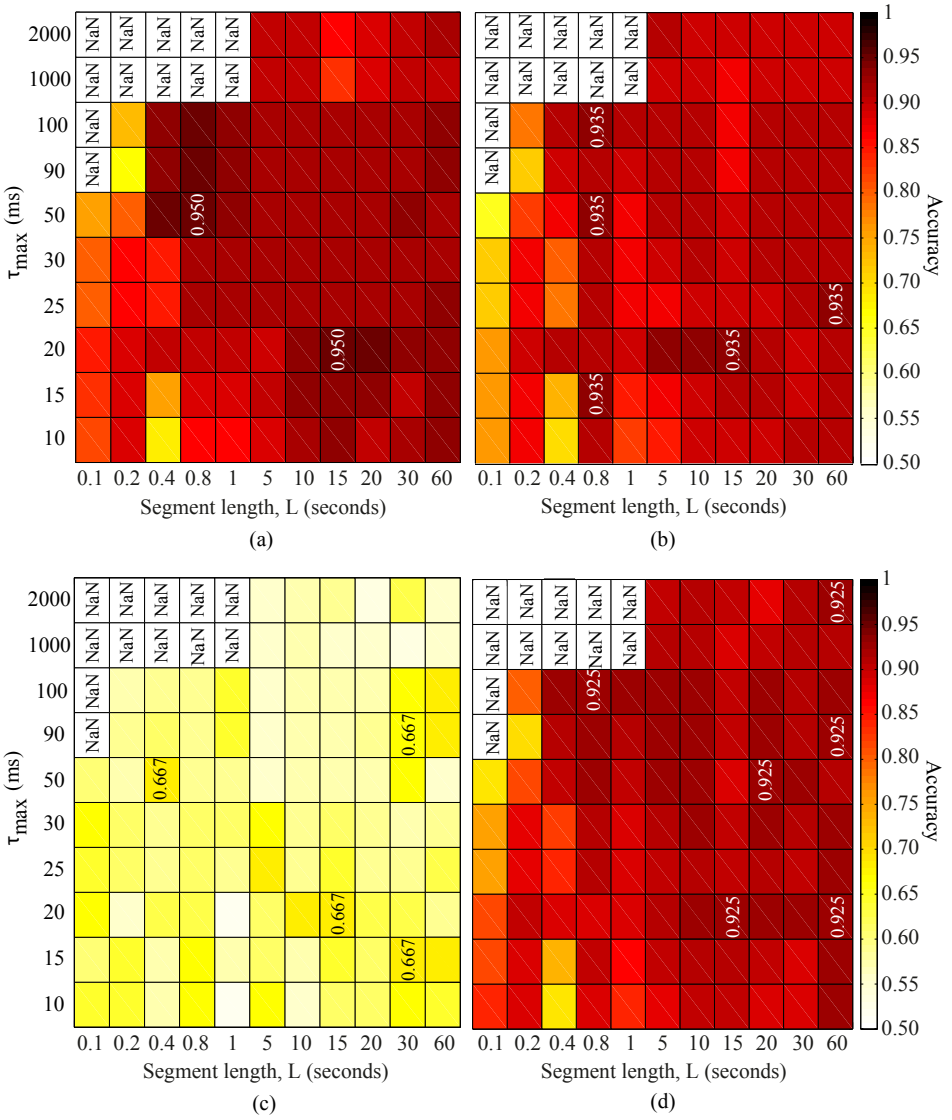

Figure 4.13. Optimal parameters determination for $H(2)$. Effect of the analyzed segment length L and τ_{max} on the classification performance with the optimal $f_s = 1024$ Hz in the four considered classification scenarios for the prediction of AF termination from the AFTDB: (a) N vs. T, (b) N vs. S, (c) S vs. T and (d) N vs S and T. The highest accuracies are indicated in the corresponding square. NaN in some cells stands for Not a Number because $H(2)$ could not be computed for these combinations of L and τ_{max} values.

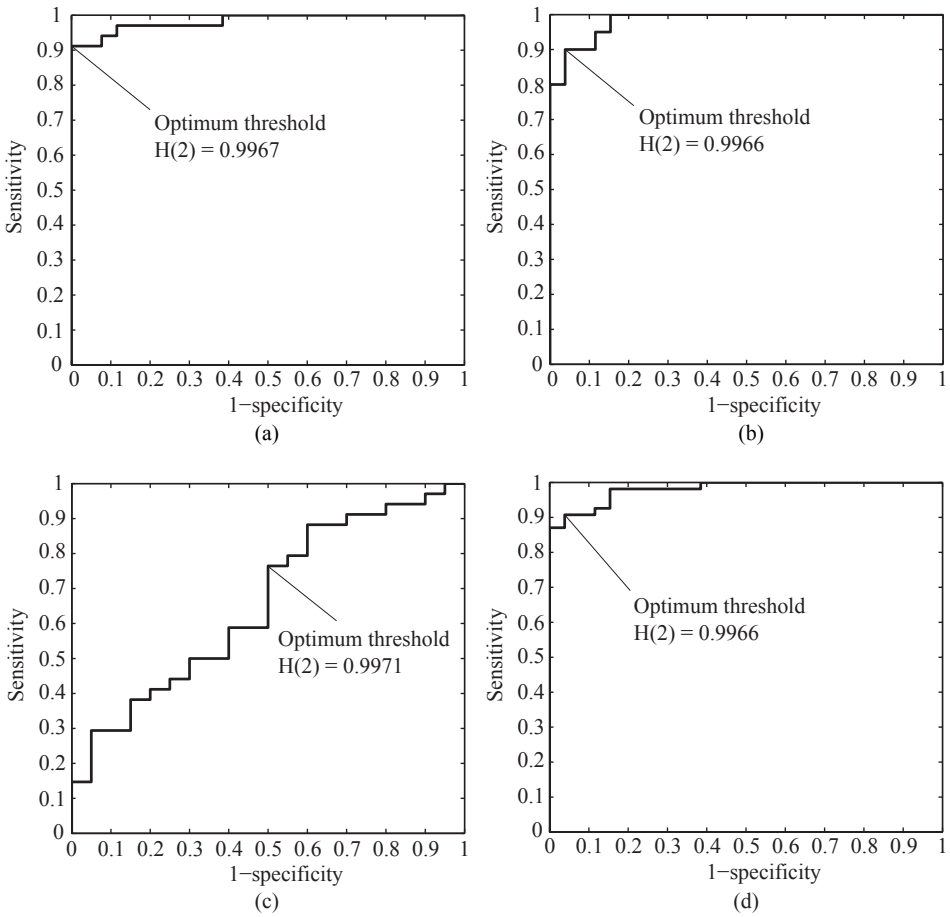

Figure 4.14. Performance of $H(2)$ computed using the optimal computational parameters values $f_s = 1024$ Hz, $L = 15$ s and $\tau_{max} = 20$ ms in the prediction of PAF termination from the AFTDB. ROC curves and classification thresholds obtained for each of the four studied scenarios: (a) N vs. T, (b) N vs. S, (c) S vs. T and (d) N vs S and T.

4.4 Early prediction of AF termination

Once the optimal values of the computational parameters for $H(2)$ were obtained, the time course of $H(2)$ prior to paroxysmal AF spontaneous termination was computed making use of the database assembled for this purpose described in Section 3.1.2. Figure 4.15 shows the evolution of $H(2)$, DAF and SampEn computed on all the signals in the database and averaged for each minute preceding AF termination. These results show that all three parameters can be considered stable until the last three minutes. DAF and SampEn values decrease progressively in the last three minutes before PAF termination, whilst $H(2)$ values increase, thus suggesting a progressive organization of the atrial activity. Moreover, statistically significant differences ($p < 0.05$) between the second-to-last (0.9971 ± 0.0005) and the last minute (0.9973 ± 0.0005) and between the third-to-last (0.9969 ± 0.0006) and the second-to-last minutes. Similarly to $H(2)$, DAF and SampEn also presented statistically significant differences ($p < 0.05$) between third-to-last and second-to-last minutes and between second-to-last and last minutes before the termination. In contrast, no statistically significant differences were found between any other two consecutive minutes ($p > 0.05$). Moreover, statistically significant differences were found between each of the last two minutes before AF termination and any other minute of the recordings for all three indices.

Regarding the prediction results, the AROC values decreased as moving away from the termination, as is shown in Figure 4.16, which indicates a progressive deterioration of the prediction capability of $H(2)$. As can be seen in this Figure, the classification given by DAF and SampEn also became progressively less accurate as moving away from the termination. Regarding the accuracy of the prediction, all indices reached the highest accuracy values in the last minute before AF termination, which were 92.86%, 88.10% and 83.33% for $H(2)$, SampEn and DAF, respectively. In contrast, the accuracy yielded by all three indices outside the last three minutes preceding the termination, whose values were around 60.0–70.0%, was notably lower.

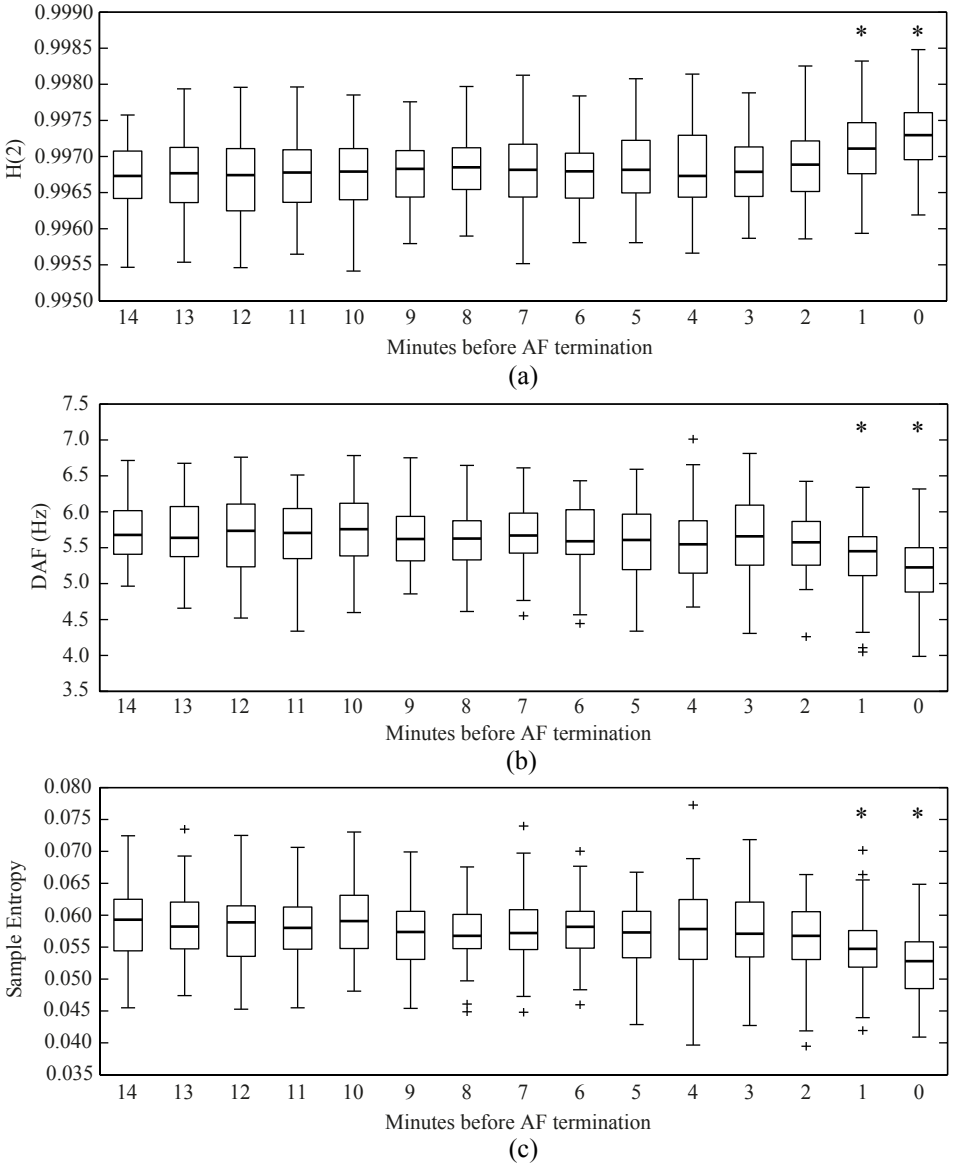

Figure 4.15. Results of the study of the early prediction of AF spontaneous termination. Variation of $H(2)$ (a), DAF (b) and SampEn (c) average values computed from the signals in the database described in 3.1.2 over non-overlapping 15 seconds segments within the last 15 minutes before AF spontaneous termination is presented. The mark * indicates the existence of statistically significant differences between the signed minute and the preceding one.

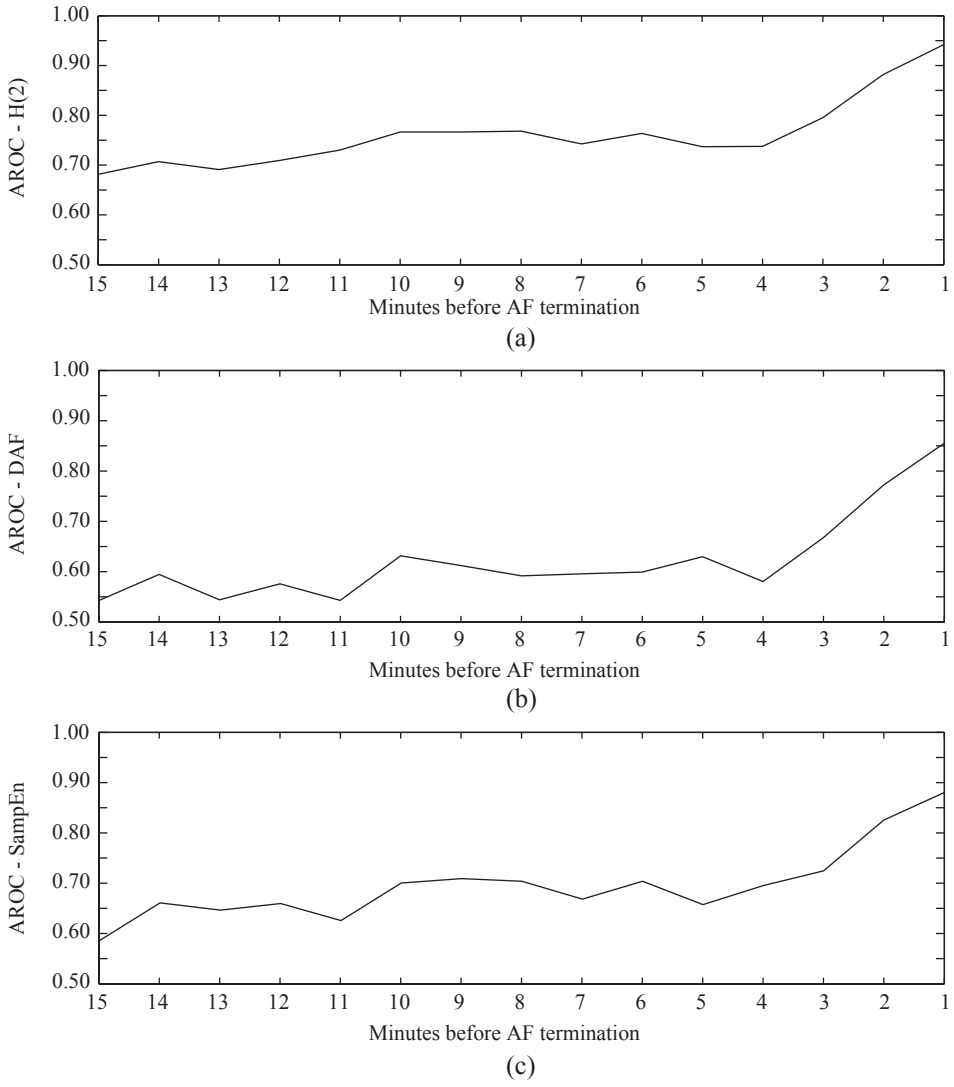

Figure 4.16. Results of the study of the early prediction of AF spontaneous termination. Variation of AROC values obtained from $H(2)$ (a), DAF (b) and SampEn (c) computed from the signals in the database described in 3.1.2 within the last 15 minutes before AF spontaneous termination.

4.5 Paroxysmal vs. persistent AF discrimination

Table 4.8 contains the mean and standard deviation of the studied metrics computed on the database assembled for the classification between paroxysmal and persistent AF episodes described in Section 3.1.3. As can be seen in table 4.8, paroxysmal AF episodes presented lower DAF and SampEn than persistent AF, which indicates that AF organization is higher in PAF than in persistent AF. In contrast, paroxysmal AF segments presented higher $H(2)$ values than persistent AF.

Table 4.8. Mean and standard deviation of the indices computed on the database described in Section 3.1.3 for paroxysmal and persistent AF episodes. Student's t test p value is also included.

	Paroxysmal AF	Persistent AF	p value
DAF (Hz)	5.0436 ± 0.6644	6.9125 ± 0.5819	< 0.001
SampEn	0.0545 ± 0.0078	0.0770 ± 0.0082	< 0.001
$H(2)$	0.9975 ± 0.0007	0.9953 ± 0.0009	< 0.001

Regarding the diagnostic accuracy of the metrics, the parameters obtained from the ROC curves and leave-one-out cross-validation for each studied metric are presented in Table 4.9. In addition, the ROC curves and values of each index for paroxysmal and persistent AF episodes, together with the corresponding optimum classification thresholds, are displayed in Figure 4.17. $H(2)$ achieved the best classification results, as is shown in Table 4.9, obtaining an accuracy value of 95% in cross-validation. Moreover, all the metrics yielded statistically significant differences between paroxysmal and persistent AF, with p values lower than 0.001 in all cases.

Table 4.9. Parameters obtained from the ROC curves for all the studied metrics computed on the database described in Section 3.1.3 in the classification between paroxysmal and persistent AF. The accuracy values obtained in leave-one-out cross-validation are also presented

	Sp	Se	Acc	AROC	Threshold	Acc crossval.
DAF	88.0%	93.0%	90.5%	0.9592	6.2103	91.0%
SampEn	90.0%	94.0%	92.0%	0.9692	0.0655	92.5%
$H(2)$	98.0%	92.0%	95.0%	0.9788	0.9962	95.0%

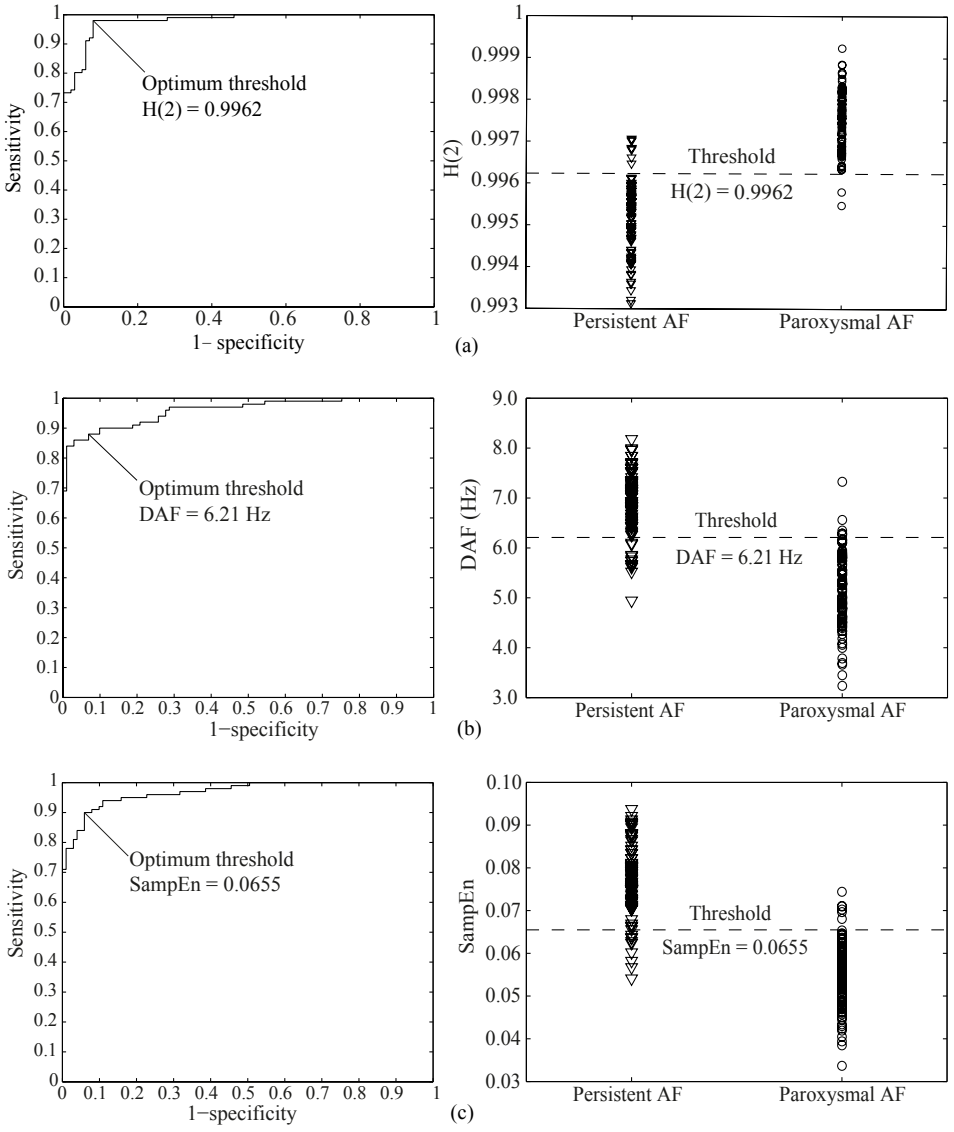

Figure 4.17. Discrimination between paroxysmal and persistent AF episodes. Selection of the optimum classification threshold for each index using the ROC curves, values of each studied metric for paroxysmal and persistent AF episodes and optimum thresholds. (a) $H(2)$ computed on the MAW. (b) DAF values. (c) SampEn computed on the MAW.

Chapter 5

Discussion

In this chapter, the meaning and clinical implications of the results presented in the previous chapter are analyzed in light of the findings reported in the literature which are related to this research. This chapter is structured as follows. Section 5.1 addresses the performance of the different tested indices in the classification among AF organization degrees. On the other hand, the study of AF termination early prediction results are analyzed in Section 5.3 and the use of $H(2)$ in the discrimination between paroxysmal and persistent AF is discussed in Section 5.4. Finally, the last Section of this chapter examines the limitations of this study.

5.1 Prediction of AF termination

5.1.1 Comparison with previous predictors of AF termination

Several previous works have proposed different strategies based on the use of nonlinear indices to estimate AF organization from the surface ECG in order to predict the arrhythmia spontaneous termination. In this sense, Table 5.1 summarizes these methods, which include both single predictors [123, 125, 126] and combinations of several metrics using an advanced classifier [32, 117, 197–199]. It is worth noting that most of these studies have analyzed the database described in Section 3.1.1 and, thus, only the last two minutes prior to AF spontaneous termination were considered. With respect to the classification among groups, all these previous studies have found statistically significant differences between non-terminating and immediately terminating AF episodes. In addition, some of them have also reported significant differences between non-terminating and soon-terminating groups [32, 117, 199] or between soon-terminating and immediately terminating groups [197–199].

Regarding the classification performance of the methods proposed in previous works, similar diagnostic accuracy values to the ones presented in Chapter 4 were reported in these studies, but notably more complex strategies were used to extract the information. In this sense, the single predictors of AF spontaneous termination which have yielded the highest accuracy are the central tendency measure from the first differences scatter plot of the wavelet transform coefficients (96%) [126] and Wavelet Entropy (95%) [125]. These two methods are based on the use of the wavelet transform and therefore they require a good match between the wavelet scale and AF frequencies, otherwise their performance would be reduced [125, 126]. Besides, the need to transform the AA signal to a set of scaled wavelet coefficient vectors, which contain simultaneous time and frequency information [126], can also make difficult the interpretation of the results in comparison with the direct application of nonlinear metrics to the AA or its spectrum, such as in the present work. On the other hand, the methods presented by Sun and Wang in [32] and [198] attained a higher classification accuracy than any of the single parameters proposed in other studies. In these works, recurrence and Poincaré plots were analyzed in order to characterize the nonlinear dynamics of the atrial [32] and ventricular [198] activities. In both cases, several different features were extracted, selected by means of a sequential forward search algorithm and combined by using an advanced classifier, such as a multilayer perceptron neural network and a fuzzy support vector machine, respectively. However, the use of this type of classifiers makes difficult the interpretation of the results from a clinical point of view because the meaning of each parameter is blurred within the classification approach. Besides, since Sun and Wang's methods do not provide an organization index, they cannot be applied in the study of AF organization time course.

Table 5.1. Comparison among recent studies predicting PAF termination from the surface ECG. Note that, from this doctoral thesis, only the results for the most accurate index, namely, $H(2)$ with its optimized computational parameters, are displayed.

Study	Database	Methods	Classification accuracy
This work	AFTDB	Estimation of the MAW regularity via Generalized Hurst Exponents	95% (N-T) 93% (N-S)
Mohebbi & Ghassemian 2014 [199]	AFTDB	Combination of Heart Rate Variability and spectral analysis of the atrial activity	93%
Alcaraz & Rieta 2012 [126]	AFTDB	CTM from the first differences scatter plot of the wavelet coefficient vector associated to the AF frequency scale of the AA	96%
Alcaraz & Rieta 2012 [125]	AFTDB	Assessment of the AA regularity in time and frequency domains through Wavelet Entropy	95%
Alcaraz & Rieta 2009 [123]	AFTDB	Estimation of the MAW regularity via Sample Entropy	93%
Sun & Wang 2009 [198]	AFTDB	Combination of features extracted from the RR intervals Poincaré plot using a fuzzy support vector machine	100% (N-T) 95% (N-S) 100% (S-T)
Sun & Wang 2008 [32]	AFTDB	Combination of features extracted from the signal's recurrence plot using a multilayer perceptron neural network	96%
Alcaraz & Rieta 2008 [124]	AFTDB	Regularity analysis of the AA in time and wavelet domains via Sample Entropy	93%
Alcaraz et al 2008 [144]	Own database (50 episodes)	Analysis of time and frequency parameters of the AA and Heart Rate Variability	92%
Chiarugi et al 2007 [117]	AFTDB	Combination of Heart Rate Variability and spectral analysis of the AA using stepwise discriminant analysis	94% (N-T) 91% (N-S)
Nilsson et al 2006 [91]	AFTDB	Analysis of time and frequency parameters and nonlinear metrics obtained from the AA	90%
Petrutiu et al 2004 [197]	AFTDB	Combination of DAF and the evolution of the AA peak power within the 2 last seconds	93%

5.1.2 Performance of the studied metrics

To the best of our knowledge, this study presents for the first time the successful application of several nonlinear metrics, such as FuzzEn, SpecEn, LZC, H, $H(1)$ and $H(2)$ to the atrial activity and its fundamental waveform, the MAW, in an attempt to estimate AF organization from the single-lead ECG. In this sense, while only FuzzEn, SpecEn and LZC reported statistically significant differences among groups when computed on the AA signals obtained from the AFTDB, all the studied metrics computed on the MAW provided statistical significance values lower than 0.01. Moreover, all the studied indices yielded a higher diagnostic

accuracy when computed over the MAW than from the AA. These findings are consistent with a previous work [123], which reported the effect of noise and ventricular residuals in the performance of SampEn as an estimator of AF organization from the surface ECG. This previous study also showed that the extraction of the MAW improved significantly the classification accuracy of SampEn. Thus, it can be concluded that the use of a previous band-pass filtering step is necessary in order to obtain a reliable noninvasive AF organization estimation through the use of the studied nonlinear indices.

According to the results presented in Tables 4.1 and 4.4, SpecEn yielded the highest discriminant accuracy and statistical difference among groups of all the metrics computed on the AA. Therefore, this metric seems the most insensitive to ventricular residuals and noise of all the proposed nonlinear indices. However, this result is in contrast with a previous study by Nilsson et al [91], in which SpecEn computed on the AA did not present statistically significant differences between terminating and non-terminating nor between soon-terminating and immediately terminating episodes. A possible explanation for these results could be that in the present work SpecEn was computed within the 3–9 Hz frequency band. In fact, ventricular residuals in the AA signal seem to be mainly concentrated in frequencies lower than 3 Hz [123]. However, high frequency components of the QRST residuals can also be found on the AA [147], which could explain the discrimination accuracy improvement when SpecEn was computed over the MAW. Besides, in this work the signal's PSD was estimated with a higher frequency resolution than in [91].

Regarding the results obtained by Hurst Exponents, the generalized exponents $H(1)$ and $H(2)$ showed a higher diagnostic accuracy than the global exponent H. Indeed, the improvement rate reached by $H(1)$ and $H(2)$ with respect to the global exponent was higher than 5% and 8%, when computed on both the AA and the MAW, respectively, excepting the classification scenario S vs. T. This outcome could be justified by the fact that the first and second moments are less sensitive to outliers than the maxima and minima [188]. Furthermore, after the optimization of its computational parameters, $H(2)$ has achieved a higher accuracy than most of the methods previously applied in the prediction of AF termination, as can be seen in Table 5.1. Moreover, $H(2)$, as a single organization estimator, has an easier clinical interpretation than the combination of several metrics proposed in other works [32,117,197,198] and, additionally, it allows to study the arrhythmia organization time course. Furthermore, since the analysis of short ECG segments yielded high accuracy values in the classification between groups (see Figures 4.11 and 4.13), this index can be applied in the study of AF organization from ambulatory ECG recordings. Thus, the Generalized Hurst Exponents could be considered as a promising tool for the study of AF organization. Besides, it is also interesting to note that remarkable differences between H, $H(1)$ and $H(2)$ values were observed, thus suggesting that both the AA and the MAW may be considered as multi-scaling time series. This finding is in agreement with previous works proving that physiological control systems generate non-stationary and inhomogeneous time series which present multi-scaling behavior [182].

On the other hand, LZC obtained a higher classification accuracy with the binary conversion than when a three-symbol conversion was used. This result is in agreement with previous works which have claimed that a two-symbol sequence conversion is enough to study the dynamic complexity of other physiological signals [170]. A possible explanation for this outcome could be that more information from the signals is kept during the coarse-graining process when a binary conversion is used. However, the results obtained in the present doctoral thesis are in contrast with a previous study [146], in which the highest accuracy in the classification between AF organization degrees was obtained using the three-symbol sequence conversion. Nonetheless, in neither of both studies estimating AF organization through LZC were appreciated significant differences with respect to the use of a three-symbol sequence conversion. Therefore, results were not conclusive about the optimal use of LZC in the study of AF organization and therefore further analysis with wider databases are needed to determine which symbol conversion choice is the most suitable in this context.

With respect to FuzzEn, this metric has been proposed in previous studies as a more accurate regularity estimator than SampEn [200]. According to its authors, FuzzEn not only presents stronger relative consistency and less dependence on the computational data length, which means less bias, but also achieves continuity, freer parameter selections and more robustness to noise than SampEn [200]. The results obtained in this work are consistent with these claims. Indeed, FuzzEn computed on the AA signal showed statistically significant differences among groups N, S and T. Moreover, the use of Fuzzen on the MAW achieved a higher accuracy than SampEn in all the considered classification scenarios. Nevertheless, all the nonlinear indices computed over the MAW, excepting H and SpecEn, reached a similar diagnostic accuracy or slightly higher than FuzzEn and, therefore, higher than SampEn and the DAF.

5.1.3 Interpretation of the studied metrics results

In view of the results related to the prediction of AF termination (see Section 4.2), it can be concluded that all the analyzed metrics provide evidences on the existence of repetitive patterns in the MAW. This result is consistent with the reported observations about a progressive wavelet fusion, which would produce simpler wavefronts in the AA, thus turning irregular f-waves to regular P waves on the ECG [6]. This could explain the notable correlation observed among all the studied metrics. It is interesting to note that, according to previous works, LZC relates to the spectral features of the signal [169] and, thus, is affected by signal bandwith changes in stochastic processes and is sensitive to changes in the variability of signal harmonics in quasi-periodic signals. In addition, it should be noticed that $H(2)$ is related to the autocorrelation function of the signal and, therefore, to its power spectrum [188]. Anyway, these findings could justify the logistic regression analysis outcome, which highlights the absence of complementary information among the AF organization estimates provided by the tested metrics.

With respect to the values of the indices for each group in the AFTDB, all the analyzed metrics computed on the MAW presented clear trends in median values from non-terminating to terminating episodes. This result suggests a progressive increase in AF global organization before AF termination. In addition, some of the indices computed on the AA also presented these trends. Moreover, similar trends were observed in the study of AF organization time course presented in 4.4 for the values of DAF, SampEn and $H(2)$ computed over the database studied in the early prediction of AF termination, described in Section 3.1.2. This observation is also in agreement with previous works providing evidences of a progressive merging of wavelets into one massive wavefront prior to AF termination [71, 127]. To this respect, Ndrepepa et al. [127] analyzed the spontaneous termination of induced AF episodes from invasive recordings and reported a progressive increase of the atrial cycle length within the last 4 seconds before the termination. In addition, Kneller et al. [71] studied the effect of antiarrhythmic drugs both from simulation and animal models and found that AF termination was preceded by a slowing of the fibrillatory rate and a decreased number of rotors and daughter wavelets in the atria. Regarding the results presented in Section 4.2, the median values of FuzzEn, SpecEn and LZC were higher for non-terminating episodes than for the terminating ones. Similarly, these values were higher for soon terminating than for immediately terminating episodes. Thus, these indices reported less time irregularity, lower spectral irregularity and lower complexity in the signal as AF termination approximated. Similarly, Hurst Exponents showed an increasing trend in median values through non-terminating, soon-terminating and immediately terminating episodes, thus presenting higher statistical self-similarity in the MAW signal prior to AF termination. Therefore, FuzzEn, SpecEn, LZC, $H(1)$ and $H(2)$ could be considered as promising tools for the study of AF organization from the surface ECG.

5.1.4 Statistical analysis considerations

Finally, it is worth noting that a freely available database was selected to assess the performance of the studied nonlinear indices, thus avoiding any bias in the analysis. In the Computers in Cardiology Challenge 2004 [92], the database was divided into a training set, composed by ten recordings from each of the three groups (N, S and T), and two testing data sets: test A, containing 16 non-terminating and 14 immediately terminating recordings and test B, containing ten pairs of soon-terminating and terminating recordings from the same AF episode. However, as is described in Section 3.2.5, in this work that division was not maintained in order to avoid the bias introduced for the test set B and reach a more exhaustive analysis in the classification of AF organization degrees. More precisely, in the present study a resubstitution validation approach was used for all the considered classification scenarios, each single metric being learned from all the available data and then tested on the same dataset. Then, a leave-one-out cross-validation approach was used in order to improve the consistency of the results by avoiding the possible over-fitting of the resubstitution process. For this

reason, slight differences can be appreciated between the classification accuracy values attained by SampEn in this work and in previous studies, such as [16]. Moreover, since the observations were not independent in the S vs. T and N vs. (S & T) cases, the statistical analysis was repeated for these scenarios using only one recording per patient in order to ensure its validity. Although a certain bias could be appreciated, when the results from this analysis were compared with those obtained from the whole database, the average accuracy variation was lower than 1% in both cases (0.74% and 0.20%, respectively). Therefore, since in previous works no recordings were excluded from the analysis, the results obtained from the study of the whole database have been presented in Chapter 4.

Regarding the cross-validation results presented in Table 4.7, the obtained classification rates were only slightly lower than with the resubstitution approach in all the studied scenarios. However, whereas more than 63% and 72% of cross-validated grouped cases were properly classified for the discrimination between non-terminating and any of the terminating groups both for AA and MAW signals, respectively, more than 50% in both cases were inappropriately identified in the scenario S vs. T. This result suggests the absence of bias in the studied classifications excepting the scenario S vs. T. In agreement with this finding, the differences observed between groups S and T when analyzing the whole database with any studied metric were not statistically significant. Moreover, previous works making use of the same database division reported a similar outcome [117, 198]. However, this result is also in contrast with some previous works which only made use of the test set B [32, 197] and reported classification rates higher than 85%. Nevertheless, it has to be remarked that, when only the signals corresponding to the test set B were analyzed, all the tested nonlinear metrics computed on the MAW also provided diagnostic accuracy values higher than 85% and statistically significant differences between groups.

5.2 Optimal computational parameters for $H(2)$

Prior to the study of AF organization time course before the termination, the effect of the parameters needed for $H(2)$ computation was assessed in order to optimize the estimation of AF organization given by $H(2)$. This nonlinear index was selected because it achieved outstanding results in the prediction of AF termination from the AFTDB. With respect to the effect of the computational parameters values, the classification results of $H(2)$ in each of the scenarios for the prediction of AF termination from the AFTDB showed substantial differences depending on the values of f_s, L and τ_{max}. However, in view of the results presented in Figures 4.11, 4.12 and 4.13, it can be concluded that there is a variety of values which could provide good classification results. More concretely, L values between 0.4 and 60 seconds yielded good classification results (see Figures 4.11 and 4.13). Larger values of L were not tested in order to avoid a possible loss of locality. However, since high accuracy values were obtained for $L = 60$ s, larger values of L could also provide an accurate estimation of AF organization.

In the same way, f_s can be selected between 256 and 1024 Hz. Finally, the interval in which τ_{max} provided high classification results was between 15 and 100 ms (see Figures 4.12 and 4.13). Nevertheless, the highest discriminatory ability was reached for the combination $f_s = 1024$ Hz, $L = 15$ s and $\tau_{max} = 20$ ms. Besides, the values of these parameters also had a significant effect on the computational burden of $H(2)$. For instance, the time elapsed in $H(2)$ computation using a value of $\tau_{max} = 20$ ms over a single 15 seconds signal segment sampled at $f_s = 1024$ Hz was around 150 ms in a normal PC. In contrast, this computation took about 70 seconds on the same PC when a value of $\tau_{max} = 2000$ ms was used. Therefore, since the values of f_s, L and τ_{max} can play a critical role in the outcome of $H(2)$, as well as in its computational burden, the proper selection of these parameters should be studied when applying $H(2)$ to other physiological signals. In that case, the development of a similar study would be highly recommended.

5.3 Early prediction of AF termination

In spite of all the research that has been carried out in recent years, the mechanisms leading to the spontaneous termination of this arrhythmia are still unknown. To date, few studies have tried to address this question by analyzing the last seconds before AF termination from invasive recordings [40, 42, 94, 201]. Hence, the study of AF organization time course within a time interval long enough to detect the earliest changes that will lead to AF termination has been analyzed for the first time in this doctoral thesis. For this purpose, the nonlinear metric which yielded the best classification results in the prediction of AF termination from the AFTDB, $H(2)$, was selected as an estimator of AF organization.

5.3.1 Comparison with previous studies

Once the optimal values were selected, AF organization time course within a time interval long enough to detect the earliest sings leading to AF termination was estimated through $H(2)$. To this respect, the results presented in Figure 4.15 show a stable organization time course up to three minutes before the arrhythmia termination, followed by a progressive increase in $H(2)$ values together with a decrease in DAF and SampEn values. In this sense, the last minute before termination presents the highest $H(2)$ mean value and the lowest DAF and SampEn mean values. In fact, ROC analysis between the central minute and the ones before PAF termination only improved notably for the last 2 minutes. This finding is in agreement with some previous works. For instance, previous studies have found that AF termination by anti-fibrillatory drugs is preceded by a progressive slowing of the DAF during few minutes, which implies a gradual increase in AF organization [39, 202]. Regarding PAF spontaneous termination, another study [42] also reported lower DAF values in the last minute prior to the termination than five minutes after AF onset for episodes lasting more than 15 minutes. Addition-

ally, no differences were reported among DAF values from different time instants sufficiently far from both onset and termination. However, the time interval between 15 minutes after AF onset and the last minute prior to AF termination were not analyzed in that work. Moreover, a more recent study reported a progressive decrease in SampEn values within the last two minutes of several PAF episodes, which implies a gradual AF organization increase [94]. However, only the last two minutes before the arrhythmia termination were analyzed in that work.

The observed time course of $H(2)$, DAF and SampEn suggest a progressive AF organization increase before the termination. According to its definition, AF organization provides a quantitative estimation of the amount of simultaneous reentries existing in the atria (see Section 3.2.1). In this sense, previous studies have associated a higher variability of the atrial activations recorded on unipolar electrograms with the presence of a higher number of reentries [23, 69, 203]. Moreover, a direct relationship between the f-waves recorded on surface lead V_1 and the electrical activations of the right atrium has been reported in a previous study [115]. Therefore, higher values of $H(2)$ could suggest the presence of fewer simultaneous reentries. In this sense, the observed time course of $H(2)$ could be indicative of a progressive fusion of reentries into one massive wavefront during the last three minutes before AF termination. This progressive merging of wavefronts has been described in the literature [71, 127].

In contrast, several previous studies [40, 127, 128, 201, 204] have described paroxysmal AF spontaneous termination as a short process, lasting only few seconds. Those works have suggested that the reentries are simultaneously annihilated just before the arrhythmia termination. For instance, during a mapping study of induced AF using a basket catheter, the earliest detectable event was found within the last 4 seconds before the termination [127]. Moreover, a recent invasive study by Tso et al [128] reported that the activity in the SA node region presented a lower dominant frequency than the rest of the right atrium within the last 2 seconds prior to AF spontaneous termination. Similarly, Petrutiu et al. [201] analyzed the last 2 minutes prior to AF termination from noninvasive ECG recordings and found a significant difference between the DAF values in the last 2 seconds before the termination. Moreover, another noninvasive study analyzing induced AF episodes obtained similar results [40]. Finally, a recent computer simulation study by Uldry et al. [204] reported two different ways of AF spontaneous termination, both lasting less than 4 seconds, which depended on the amount of existing wavelets in the atria. To this respect, the spontaneous termination of low complexity AF episodes could be identified 3.2 seconds in advance, but in the case of high complexity AF the termination could only be detected 1.6 seconds before its occurrence.

Nonetheless, it is worth noting that remarkable differences can be found between the AF episodes analyzed in the aforementioned works and those included in this study. On one hand, the duration of the episodes was different. Indeed, whilst in the present study the last 15 minutes prior to spontaneous termination of AF episodes lasting for more than 2 hours have been analyzed, previous

works only studied short AF episodes, lasting from some seconds to few minutes [40, 127, 128, 201, 204]. To this respect, the episode duration could have a significant influence on its termination mechanisms. Indeed, Bollmann et al. [42] found significant differences between the DAF values of the first and last minute of episodes longer than 15 minutes, while these differences were not statistically significant for shorter AF episodes. Furthermore, several previous studies have also related higher AF duration with lower organization [42, 145, 205]. Nevertheless, further research is needed in order to determine the influence of the episode duration on the mechanisms leading to AF termination. On the other hand, most of the studies cited above analyzed simulated [204] or induced [40, 127, 128] AF, whereas spontaneous PAF has been analyzed here. To this respect, it is still unknown whether the the type of episode (spontaneous or induced) could have an influence on the termination mechanisms.

5.3.2 Clinical implications of the results

According to the results presented in this thesis and in a previous study [94], the increase of the signal regularity prior to AF spontaneous termination happens within the last 2–3 minutes. Moreover, the previous studies cited in Table 5.1 have reported that AF termination can be predicted within the last 2 minutes, although the termination process itself is seemingly abrupt [127, 201, 204]. Therefore, the results presented in Section 4.4 together with the findings reported in previous studies suggest that the early prediction of AF spontaneous termination is not possible with the current methods. This fact implies that, from a clinical point of view, the prediction of PAF termination is not useful because it is obtained too late for an appropriate action. To this respect, several previous studies have proposed different strategies for the prediction of AF spontaneous termination from the ECG, as can be seen in Table 5.1. However, although several of those methods were able to classify between non-terminating and immediately-terminating AF episodes with high accuracy, this application of AF organization estimation does not seem interesting for the clinical practice. Nevertheless, the use of those methods in the study of other events related to AF organization, such as the outcome of the therapies, might provide valuable clinical information. On the other hand, since the mechanisms causing PAF spontaneous termination are still not fully explained [11], further studies are needed in order to improve our current understanding of this arrhythmia.

Although the early prediction of AF spontaneous termination does not seem possible, the application of $H(2)$ in the estimation of AF organization may improve the current treatment of AF. For instance, $H(2)$ could be applied in real-time continuous AF organization monitoring because there are efficient algorithms for its computation [206]. Since moments of high organization without termination were occasionally detected, this kind of analysis might detect optimal instants for intervention. To this respect, previous studies have reported that treatments like electrical cardioversion present higher success rates in more

organized arrhythmias [108, 207]. Moreover, the application of catheter ablation during high organization time instants could reduce the duration of the procedure and the extension of atrial lesions, thus reducing the risk of collateral damages [208]. Nevertheless, further research would be needed in order to test this possible use of $H(2)$.

5.4 Paroxysmal vs. persistent AF classification

5.4.1 Comparison with previous works

Several previous works, analyzing both invasive [20,105,106] and noninvasive [42, 43] recordings, have reported organization differences between paroxysmal and persistent AF. Regarding the invasive studies, Ravelli et al. [20] reported different patterns in wave similarity maps for paroxysmal and persistent AF that were stable in time. More concretely, they found high similarity regions in PAF that were not present in persistent AF. In a different study dealing with AF spatiotemporal organization, Sanders et al. [105], found that high frequency sites were more frequent in PAF than in persistent AF, thus suggesting that focal mechanisms are more important in paroxysmal AF than in sustained stages of the arrhythmia. In this sense, high frequency sites were more frequent in the PV in paroxysmal AF patients. In addition, persistent AF presented higher fibrillatory rates than PAF. Besides, Lazar et al. [106] found that PAF patients presented a frequency gradient between both atria that was not detected in persistent AF. Similar gradients in several entropy measures were reported by Cervigón et al. [111] for PAF patients, whereas no such differences were detected in persistent AF. Finally, Ciaccio et al. [192] analyzed the dominant morphologies in complex fractionated atrial electrograms and found that persistent AF patients had more stable morphologies than PAF patients, thus suggesting the existence of more stable drivers in persistent AF.

With respect to the noninvasive study of AF organization, previous studies have reported higher DAF values in paroxysmal AF than in persistent AF [42,43]. However, to the best of our knowledge, only three previous studies [44, 45, 209] have reported the diagnostic capability of their methods. To this respect, in the present thesis the metrics DAF and SampEn have shown a similar performance than in a previous study [44]. Moreover, another previous study [45] analyzed the use of subband sample entropy and classified between both stages of the arrhythmia using the combination of the information extracted from different frequency bands, thus obtaining high sensitivity and specificity values. Furthermore, this latter study demonstrated that the discrimination between paroxysmal and persistent AF from ambulatory ECG recordings is possible regardless of the time instant when the signal was recorded with respect to the onset and termination of the AF episode. Therefore, the application of AF organization estimation to classify between paroxysmal and persistent AF patients from ambulatory ECG

recordings is an interesting alternative to the use of Holter ECG recordings. Finally, Ortigosa et al. [209] performed a time-frequency analysis of ECG recordings of paroxysmal and persistent AF and obtained a classification accuracy of approximately 80%. It is interesting to note that a notably more complex strategy than the one presented in this thesis was proposed in that study, because it involved the combination of several features using a support vector machine.

Regarding the results of classification between paroxysmal and persistent AF presented in Section 4.5, $H(2)$ has yielded a higher classification accuracy than DAF and SampEn. Moreover, $H(2)$ has achieved the best diagnostic ability in the discrimination between paroxysmal and persistent AF reported to this date for a single parameter. In this sense, the use of a single metric is interesting because it allows a more direct clinical interpretation than the combination of several parameters, such as in two of the aforementioned studies [45,209]. In addition, previous studies have demonstrated that paroxysmal AF shows higher organization near its onset and termination [94,95], and therefore the results presented in this thesis correspond to a worst case scenario. Hence, the same or higher accuracy can be expected in the use of this method in ambulatory ECG recordings.

5.4.2 Clinical interpretation of the results

As for the clinical interpretation of the results, paroxysmal AF episodes produced lower mean DAF and SampEn values than persistent AF episodes, which indicates a higher organization in paroxysmal AF. Note that this result is consistent with previous works [44]. Regarding $H(2)$ computed on the MAW, this metric presents a higher mean value in paroxysmal AF than in persistent AF. Moreover, the results of the AF spontaneous termination study presented in Sections 4.2 and 4.4 show that $H(2)$ presents higher values near AF termination than far from the termination. Therefore, higher $H(2)$ values correspond to higher AF organization levels.

Regarding the clinical applications of this method, the classification between paroxysmal and persistent AF from short ECG recordings could be an alternative to the use of long Holter ECG recordings. This use of AF organization estimation could allow an earlier intervention, which might improve the likelihood of therapy success because atrial remodeling would be in a less advanced state [7,8].

5.5 Limitations of the study

Finally, this study presents some limitations. Firstly, only lead V_1 was analyzed and, thus, the information contained in the other two leads of the Holter recordings was not considered. However, lead V_1 is a common choice in the analysis of AF [6] due to the higher amplitude of the atrial activity in this lead with respect to the ventricular activity. In this sense, previous studies have found that the DAF

obtained from lead V_1 reflects the fibrillatory rate of the right atrium [114]. Similarly, the values of SampEn computed on the MAW in lead V_1 present a significant correlation with those obtained from invasive recordings of the right atrium [115]. Therefore, the analysis of this lead can provide valuable information for an accurate estimation of AF temporal organization. The second limitation is that a correct determination of the DAF is needed to obtain the MAW. Otherwise, the performance of the nonlinear metrics applied on the MAW would be reduced. Besides, although the analysis of the MAW improved the performance of the studied metrics, the information contained in the harmonics of the atrial activity was not considered in the present thesis. According to a previous study, the analysis of the atrial harmonics could provide complementary information, thus improving the diagnostic accuracy obtained with an AF organization estimator [45]. Therefore, it would be interesting to address this topic in future studies.

On the other hand, the study of the effect of the computational parameters was only performed for $H(2)$ because this metric achieved the best prediction of AF termination from the AFTDB. However, the results presented in Section 4.3 for $H(2)$ and a previous optimization study for SampEn [154] show that there can be wide ranges in the parameters values which produce an accurate classification between different AF organization degrees. Nevertheless, a similar study on the optimal use of FuzzEn, LZC and SpecEn would be recommended in order to determine their optimum use because these indices obtained promising results in the first part of this study.

Regarding the analysis of AF organization time course, AF organization progression over the whole PAF episodes was not studied in this doctoral thesis. However, AF organization variation during the first minutes after AF onset has been studied previously [94, 95] and a progressive deterioration of AF organization within the first three minutes was reported. Additionally, in the present study no significant differences were observed further than 3 minutes from the termination. Besides, it is worth noting that the amount of analyzed signals is not very large and, therefore, the results should be considered with caution. Finally, since only surface ECG recordings were studied, the assumptions regarding the involved physiological mechanisms must be considered as speculative.

Chapter 6

Conclusions, Future Lines and Contributions

This final chapter contains the main conclusions derived from the research work carried out in this doctoral thesis. In addition, since the clinical application of the proposed methods would require further studies, some future lines of research based on the results obtained in this thesis that could be developed in the future are suggested. Finally, the scientific publications derived from this study are presented in the last section of this chapter.

6.1 Conclusions

In the present doctoral thesis, the ability of several nonlinear metrics to estimate AF organization from single-lead ECG recordings has been demonstrated through their application in the classification of events related to AF organization. In this sense, a higher level of AF organization is related to lower LZC, SpecEn and FuzzEn values, whereas higher Hurst Exponents values correspond to higher AF organization levels. Moreover, most of these indices have reached a higher accuracy in the classification among different AF organization degrees than the most well-known organization estimators, such as the DAF and SampEn. On the other hand, the extraction of the MAW by selective filtering has been found to be mandatory in order to obtain an accurate estimation of AF organi-

zation through the use of the studied nonlinear indices. Apart from their high accuracy in the discrimination between different AF organization levels, the indices studied in this doctoral thesis are efficient because they can be applied both in short ECG recordings and in long Holter recordings. Moreover, the use of a single metric has an easier clinical interpretation than a combination of several indices through an advanced classifier. Hence, the nonlinear metrics studied in this thesis can be considered as promising tools for the study of AF organization from the surface ECG.

In particular, $H(2)$ has achieved the highest accuracy published to this date for a single index in the classification between paroxysmal and persistent AF episodes. Moreover, this index has also yielded a higher accuracy in the prediction of AF spontaneous termination than most of the previously published methods. Thus, further research on the use of this method to estimate AF organization in different scenarios would be especially recommendable.

Regarding the study of the early prediction of AF spontaneous termination, AF organization time course prior to AF termination has been estimated for the first time in this doctoral thesis. According to the results presented in Section 4.4, AF $H(2)$ mean values increase progressively within the last 3 minutes before the termination. On the contrary, DAF and SampEn values decrease within this same time interval. Moreover, none of the studied indices presented significant variations outside the last 3 minutes prior to the termination. This result is consistent with previous works which reported an increase in AF organization within the last 2 minutes preceding AF termination. As a consequence, although several previous studies have suggested the possibility of an early prediction of PAF spontaneous termination, it is not possible with the present signal analysis methods. Thus, since the anticipation with which PAF spontaneous termination can be detected is very reduced, this application of AF organization estimation is not clinically useful.

On the other hand, since the use of nonlinear indices depends on the values of their computational parameters, a systematic analysis of the effect of those parameters is fundamental for their application in the analysis of biosignals. To this respect, a similar optimization strategy to the one presented in this doctoral thesis for $H(2)$ would be recommendable for any other nonlinear method applied to physiological time series.

The use of the studied nonlinear indices may contribute in the future to make more appropriate decisions on the patient's management, thus improving the efficacy of the current therapies and reducing their associate costs. For instance, the use of $H(2)$ to classify between paroxysmal and persistent AF patients from ambulatory ECG recordings could allow an early intervention in the case of paroxysmal AF patients, thus avoiding the arrhythmia chronification. Nevertheless, further studies are required to validate the robustness and repeatability of these results on wider and independent databases and to determine the optimal application of these metrics to AF signals.

6.2 Future Lines

Although the nonlinear indices studied in the present work allow to classify among AF organization levels, the optimal use of several of these metrics, such as LZC and FuzzEn, has not been determined. Therefore, it would be interesting to study the effect of computational parameters, such as the computational data length, in the performance of these nonlinear indices. Moreover, the use of a different sequence conversion strategy for the computation of LZC might produce a higher diagnostic accuracy. In this sense, the analysis of a wider database could determine which sequence conversion produces the most accurate AF organization estimation through LZC. Similarly, the optimal values of the parameters m, r and n for FuzzEn computation could be determined in further studies.

Another interesting future line could be the application of these new AF organization estimators in the prediction of the therapy outcome. For instance, the studied metrics could be applied in the prediction of the outcome of therapies such as electrical of pharmacological cardioversion, ablation and surgery in order to select the best option for the patient.

On the other hand, in this work the study of the last 15 minutes prior to AF spontaneous termination has been presented. Related to that study, the analysis of the AF organization time course along the whole paroxysmal AF episodes could be addressed in future works. This study could be interesting in order to improve the current knowledge about the arrhythmia spontaneous behavior.

Finally, since only lead V_1 has been analyzed in this work, the analysis of different ECG leads could be interesting in order to determine whether they contain complementary information that could improve the diagnostic accuracy of the studied metrics. Besides, the analysis of the atrial harmonics could also provide complementary information and, therefore, it might improve the classification accuracy yielded by the application of studied indices on the MAW.

6.3 Contributions

6.3.1 Publications

The comparative study of nonlinear indices was published in the journal *Computers in Biology and Medicine*:

- Matilde Julián, Raúl Alcaraz, and José J Rieta, Comparative Assessment of Nonlinear Metrics to Quantify Organization-Related Events in Surface Electrocardiograms of Atrial Fibrillation, *Computers in Biology and Medicine*, 2014, 48C, 66-76.

A paper describing the optimization strategy followed for $H(2)$ and its application in the study of AF organization prior to PAF spontaneous termination is currently under review to be published in the journal *Physiological Measurement*:

- Matilde Julián, Raúl Alcaraz, and José J Rieta, Application of Hurst Exponents to Assess Atrial Reverse Remodeling in Paroxysmal Atrial Fibrillation, *Physiological Measurement*.

The study of the early prediction of AF spontaneous termination through $H(2)$, DAF and SampEn has been submitted to the journal *Pacing and Clinical Electrophysiology* and is currently under review:

- Matilde Julián, Raúl Alcaraz, and José J Rieta, How Long Can Atrial Fibrillation Be Predicted before it Happens?, *Pacing and Clinical Electrophysiology*.

The study of the application of $H(2)$ in the discrimination between paroxysmal and persistent AF from the ECG is currently under review to be published in the journal *Annals of Biomedical Engineering*:

- Matilde Julián, Raúl Alcaraz, and José J Rieta, Hurst Exponents as a Tool for Discriminating Between Paroxysmal and Persistent Atrial Fibrillation, *Annals of Biomedical Engineering*.

In addition, some of the main contributions of this thesis have been presented in international conferences:

- M. Julián, R. Alcaraz, and J.J. Rieta, Comparative study of nonlinear metrics to discriminate atrial fibrillation events from the surface ECG, *Computing in Cardiology (CinC), 2012*, 2012, p. 197-200
- M. Julián, R. Alcaraz, and J.J. Rieta, Study on the Optimal Use of Generalized Hurst Exponents for Noninvasive Estimation of Atrial Fibrillation Organization, *Computing in Cardiology (CinC), 2013*, 2013, p. 1039-1042.
- M. Julián, R. Alcaraz, and J.J. Rieta, Generalized Hurst Exponents as a Tool to Estimate Atrial Fibrillation Organization from the Surface ECG, *Computing in Cardiology (CinC), 2013*, 2013, p. 1199-1202.
- M. Julián, R. Alcaraz, and J.J. Rieta, Study on Atrial Arrhythmias Optimal Organization Assessment with Generalized Hurst Exponents. *XIII Mediterranean Conference on Medical and Biological Engineering and Computing 2013. Springer International Publishing*, 2014. p. 1013-1016.
- M. Julián, R. Alcaraz, and J.J. Rieta, Paroxysmal Atrial Fibrillation Termination Prognosis through the Application of Generalized Hurst Exponents. *XIII Mediterranean Conference on Medical and Biological Engineering and Computing 2013. Springer International Publishing*, 2014. p. 973-976.

and in national conferences:

- M. Julián, R. Alcaraz, and J.J. Rieta, Comparativa de Estimadores No Lineales en el Estudio de Eventos en Fibrilación Auricular Mediante el ECG de Superficie, *XXX Congreso Anual de la Sociedad Española de Ingeniería Biomédica (CASEIB 2012) (ISSN 978-84-616-2147-7)*, 2012
- M. Julián, F. Hornero, R. Alcaraz, and J.J. Rieta, Medida de la organización en registros de superficie de fibrilación auricular mediante exponentes generalizados de Hurst, *Rev Esp Cardiol. 2012;66 Supl 1:459*, 2013

6.3.2 Funding

This work has been funded by the following research incentive programs: TEC2010–20633 from the Spanish Ministry of Science and Innovation and PPII11–0194–8121 from Junta de Comunidades de Castilla-La Mancha.

Bibliography

[1] Y. Yap and J. Camm, "Epidemiology of atrial fibrillation," in *Essentials of Atrial Fibrillation*, pp. 1–5, Springer Healthcare Ltd., 2014.

[2] A. J. Camm, G. Y. Lip, R. De Caterina, I. Savelieva, D. Atar, S. H. Hohnloser, G. Hindricks, P. Kirchhof, , J. J. Bax, H. Baumgartner, C. Ceconi, V. Dean, C. Deaton, R. Fagard, C. Funck-Brentano, D. Hasdai, A. Hoes, P. Kirchhof, J. Knuuti, P. Kolh, T. McDonagh, C. Moulin, B. A. Popescu, Ž. Reiner, U. Sechtem, P. A. Sirnes, M. Tendera, A. Torbicki, A. Vahanian, S. Windecker, , P. Vardas, N. Al-Attar, O. Alfieri, A. Angelini, C. Blömstrom-Lundqvist, P. Colonna, J. De Sutter, S. Ernst, A. Goette, B. Gorenek, R. Hatala, H. Heidbüchel, M. Heldal, S. D. Kristensen, P. Kolh, J.-Y. Le Heuzey, H. Mavrakis, L. Mont, P. P. Filardi, P. Ponikowski, B. Prendergast, F. H. Rutten, U. Schotten, I. C. Van Gelder, and F. W. Verheugt, "2012 focused update of the ESC guidelines for the management of atrial fibrillation," *European Heart Journal*, vol. 33, no. 21, pp. 2719–2747, 2012.

[3] J. Ball, M. J. Carrington, J. J. McMurray, and S. Stewart, "Atrial fibrillation: profile and burden of an evolving epidemic in the 21st century," *International journal of cardiology*, vol. 167, no. 5, pp. 1807–1824, 2013.

[4] C. B. Lundqvist, G. Y. H. Lip, and P. Kirchhof, "What are the costs of atrial fibrillation?," *Europace*, vol. 13 Suppl 2, pp. ii9–12, May 2011.

[5] A. M. Gillis, A. D. Krahn, A. C. Skanes, and S. Nattel, "Management of atrial fibrillation in the year 2033: new concepts, tools, and applications leading to personalized medicine," *Can J Cardiol*, vol. 29, pp. 1141–6, Oct 2013.

[6] S. Petrutiu, J. Ng, G. M. Nijm, H. Al-Angari, S. Swiryn, and A. V. Sahakian, "Atrial fibrillation and waveform characterization," *Engineering in Medicine and Biology Magazine, IEEE*, vol. 25, no. 6, pp. 24–30, 2006.

[7] M. C. Wijffels, C. J. Kirchhof, R. Dorland, and M. A. Allessie, "Atrial fibrillation begets atrial fibrillation a study in awake chronically instrumented goats," *Circulation*, vol. 92, no. 7, pp. 1954–1968, 1995.

[8] A. Bollmann and F. Lombardi, "Electrocardiology of atrial fibrillation," *Engineering in Medicine and Biology Magazine, IEEE*, vol. 25, no. 6, pp. 15–23, 2006.

[9] A. Jahangir, V. Lee, P. A. Friedman, J. M. Trusty, D. O. Hodge, S. L. Kopecky, D. L. Packer, S. C. Hammill, W.-K. Shen, and B. J. Gersh, "Long-term progression and outcomes with aging in patients with lone atrial fibrillation a 30-year follow-up study," *Circulation*, vol. 115, no. 24, pp. 3050–3056, 2007.

[10] S. Nattel, E. Guasch, I. Savelieva, F. G. Cosio, I. Valverde, J. L. Halperin, J. M. Conroy, S. M. Al-Khatib, P. L. Hess, P. Kirchhof, J. De Bono, G. Y. H. Lip, A. Banerjee, J. Ruskin, D. Blendea, and A. J. Camm, "Early management of atrial fibrillation to prevent cardiovascular complications," *European Heart Journal*, vol. 35, no. 22, pp. 1448–1456, 2014.

[11] J. L. Anderson, J. L. Halperin, N. M. Albert, B. Bozkurt, R. G. Brindis, L. H. Curtis, and et al, "Management of patients with atrial fibrillation (compilation of 2006 ACCF/AHA/ESC and 2011 ACCF/AHA/HRS recommendations): a report of the american college of cardiology/american heart association task force on practice guidelines," *J Am Coll Cardiol*, vol. 61, pp. 1935–44, May 2013.

[12] J. Dunning, M. Nagendran, O. R. Alfieri, S. Elia, A. P. Kappetein, U. Lockowandt, G. E. Sarris, P. H. Kolh, and O. behalf of the EACTS Clinical Guidelines Committee, "Guideline for the surgical treatment of atrial fibrillation," *European Journal of Cardio-Thoracic Surgery*, 2013.

[13] R. Alcaraz and J. J. Rieta, "Review: Application of non-linear methods in the study of atrial fibrillation organization," *Journal of Medical and Biological Engineering*, vol. 33, no. 3, pp. 239–252, 2013.

[14] L. Faes, G. Nollo, R. Antolini, F. Gaita, and F. Ravelli, "A method for quantifying atrial fibrillation organization based on wave-morphology similarity," *Biomedical Engineering, IEEE Transactions on*, vol. 49, no. 12, pp. 1504–1513, 2002.

[15] H. J. Sih, D. P. Zipes, E. J. Berbari, and J. E. Olgin, "A high-temporal resolution algorithm for quantifying organization during atrial fibrillation," *Biomedical Engineering, IEEE Transactions on*, vol. 46, no. 4, pp. 440–450, 1999.

[16] R. Alcaraz and J. J. Rieta, "A review on sample entropy applications for the non-invasive analysis of atrial fibrillation electrocardiograms," *Biomedical Signal Processing and Control*, vol. 5, no. 1, pp. 1–14, 2010.

[17] K. T. Konings, J. L. Smeets, O. C. Penn, H. J. Wellens, and M. A. Allessie, "Configuration of unipolar atrial electrograms during electrically induced atrial fibrillation in humans," *Circulation*, vol. 95, pp. 1231–41, Mar 1997.

[18] L. Sörnmo, M. Stridh, D. Husser, A. Bollmann, and S. B. Olsson, "Analysis of atrial fibrillation: from electrocardiogram signal processing to clinical

management," *Philosophical Transactions of the Royal Society A: Mathematical, Physical and Engineering Sciences*, vol. 367, no. 1887, pp. 235–253, 2009.

[19] G. Nollo, M. Marconcini, L. Faes, F. Bovolo, F. Ravelli, and L. Bruzzone, "An automatic system for the analysis and classification of human atrial fibrillation patterns from intracardiac electrograms," *Biomedical Engineering, IEEE Transactions on*, vol. 55, no. 9, pp. 2275–2285, 2008.

[20] F. Ravelli, L. Faes, L. Sandrini, F. Gaita, R. Antolini, M. Scaglione, and G. Nollo, "Wave similarity mapping shows the spatiotemporal distribution of fibrillatory wave complexity in the human right atrium during paroxysmal and chronic atrial fibrillation," *Journal of cardiovascular electrophysiology*, vol. 16, no. 10, pp. 1071–1076, 2005.

[21] B. P. T. Hoekstra, C. G. H. Diks, M. A. Allessie, and J. DeGoede, "Nonlinear analysis of epicardial atrial electrograms of electrically induced atrial fibrillation in man," *Journal of Cardiovascular Electrophsiology*, vol. 6 No. 6, pp. 419–440, 1995.

[22] F. Censi, V. Barbaro, P. Bartolini, G. Calcagnini, A. Michelucci, and S. Cerutti, "Non-linear coupling of atrial activation processes during atrial fibrillation in humans," *Biological Cybernetics*, vol. 85, no. 3, pp. 195–201, 2001.

[23] M. Masè, L. Faes, R. Antolini, M. Scaglione, and F. Ravelli, "Quantification of synchronization during atrial fibrillation by shannon entropy: validation in patients and computer model of atrial arrhythmias," *Physiological measurement*, vol. 26, no. 6, p. 911, 2005.

[24] F. Censi, V. Barbaro, P. Bartolini, G. Calcagnini, A. Michelucci, G. Gensini, and S. Cerutti, "Recurrent patterns of atrial depolarization during atrial fibrillation assessed by recurrence plot quantification," *Annals of biomedical engineering*, vol. 28, no. 1, pp. 61–70, 2000.

[25] J. Ng, D. Gordon, R. S. Passman, B. P. Knight, R. Arora, and J. J. Goldberger, "Electrogram morphology recurrence patterns during atrial fibrillation," *Heart Rhythm*, vol. 11, no. 11, pp. 2027 – 2034, 2014.

[26] M. S. Guillem, A. M. Climent, F. Castells, D. Husser, J. Millet, A. Arya, C. Piorkowski, and A. Bollmann, "Noninvasive mapping of human atrial fibrillation," *Journal of Cardiovascular Electrophysiology*, vol. 20, no. 5, pp. 507–513, 2009.

[27] M. Stridh, L. Sörnmo, C. J. Meurling, and S. B. Olsson, "Sequential characterization of atrial tachyarrhythmias based on ECG time-frequency analysis," *Biomedical Engineering, IEEE Transactions on*, vol. 51, no. 1, pp. 100–114, 2004.

[28] S. M. Narayan, G. K. Feld, A. Hassankhani, and V. Bhargava, "Quantifying intracardiac organization of atrial arrhythmias using temporospatial phase

of the electrocardiogram," *Journal of Cardiovascular Electrophysiology*, vol. 14 no. 9, pp. 971–981, 2003.

[29] R. Alcaraz, F. Hornero, A. Martínez, and J. J. Rieta, "Short-time regularity assessment of fibrillatory waves from the surface ECG in atrial fibrillation," *Physiological Measurement*, vol. 33, no. 6, p. 969, 2012.

[30] R. Alcaraz, F. Hornero, and J. J. Rieta, "Dynamic time warping applied to estimate atrial fibrillation temporal organization from the surface electrocardiogram," *Medical engineering & physics*, vol. 35, no. 9, pp. 1341 – 1348, 2013.

[31] B. Taha, S. Reddy, Q. Xue, and S. Swiryn, "Automated discrimination between atrial fibrillation and atrial flutter in the resting 12-lead electrocardiogram," *Journal of Electrocardiology*, vol. 33, Supplement 1, no. 0, pp. 123 – 125, 2000.

[32] R. Sun and Y. Wang, "Predicting termination of atrial fibrillation based on the structure and quantification of the recurrence plot," *Med Eng Phys*, vol. 30, pp. 1105–11, Nov 2008.

[33] T. Kao, Y. Su, H. Tso, Y. Lin, S. Chen, and C. Tai, "Nonlinear analysis of human atrial flutter and fibrillation using surface electrocardiogram," in *Computers in Cardiology, 2004*, pp. 441–444, IEEE, 2004.

[34] L. Uldry, J. Van Zaen, Y. Prudat, L. Kappenberger, and J.-M. Vesin, "Measures of spatiotemporal organization differentiate persistent from longstanding atrial fibrillation," *Europace*, vol. 14, no. 8, pp. 1125–1131, 2012.

[35] M. Meo, V. Zarzoso, O. Meste, D. G. Latcu, and N. Saoudi, "Catheter ablation outcome prediction in persistent atrial fibrillation using weighted principal component analysis," *Biomedical Signal Processing and Control*, vol. 8, no. 6, pp. 958 – 968, 2013.

[36] P. Bonizzi, M. de la Salud Guillem, A. Climent, J. Millet, V. Zarzoso, F. Castells, and O. Meste, "Noninvasive assessment of the complexity and stationarity of the atrial wavefront patterns during atrial fibrillation," *Biomedical Engineering, IEEE Transactions on*, vol. 57, no. 9, pp. 2147–2157, 2010.

[37] A. Bollmann, D. Husser, L. Mainardi, F. Lombardi, P. Langley, A. Murray, J. J. Rieta, J. Millet, S. B. Olsson, M. Stridh, and L. Sörnmo, "Analysis of surface electrocardiograms in atrial fibrillation: techniques, research, and clinical applications," *Europace*, vol. 8, pp. 911–26, Nov 2006.

[38] R. Alcaraz, J. J. Rieta, and F. Hornero, "Non-invasive atrial fibrillation organization follow-up under successive attempts of electrical cardioversion," *Medical & biological engineering & computing*, vol. 47, no. 12, pp. 1247–1255, 2009.

[39] A. Bollmann, N. K. Kanuru, K. K. McTeague, P. F. Walter, D. B. DeLurgio, and J. J. Langberg, "Frequency analysis of human atrial fibrillation using the surface electrocardiogram and its response to ibutilide," *Am J Cardiol*, vol. 81, pp. 1439–45, Jun 1998.

[40] A. Fujiki, M. Sakabe, K. Nishida, K. Mizumaki, and H. Inoue, "Role of fibrillation cycle length in spontaneous and drug-induced termination of human atrial fibrillation," *Circ J*, vol. 67, pp. 391–5, May 2003.

[41] A. Hernández, R. Alcaraz, F. Hornero, and J. J. Rieta, "Preoperative study of the surface ecg for the prognosis of atrial fibrillation maze surgery outcome at discharge," *Physiological Measurement*, vol. 35, no. 7, p. 1409, 2014.

[42] A. Bollmann, K. Sonne, H. D. Esperer, I. Toepffer, J. J. Langberg, and H. U. Klein, "Non-invasive assessment of fibrillatory activity in patients with paroxysmal and persistent atrial fibrillation using the holter ecg," *Cardiovasc Res*, vol. 44, pp. 60–6, Oct 1999.

[43] Q. Xi, A. V. Sahakian, T. G. Frohlich, J. Ng, and S. Swiryn, "Relationship between pattern of occurrence of atrial fibrillation and surface electrocardiographic fibrillatory wave characteristics," *Heart Rhythm*, vol. 1, no. 6, pp. 656–663, 2004.

[44] R. Alcaraz and J. J. Rieta, "The application of nonlinear metrics to assess organization differences in short recordings of paroxysmal and persistent atrial fibrillation," *Physiological measurement*, vol. 31, no. 1, p. 115, 2010.

[45] R. Alcaraz, F. Sandberg, L. Sörnmo, and J. J. Rieta, "Classification of paroxysmal and persistent atrial fibrillation in ambulatory ECG recordings," *Biomedical Engineering, IEEE Transactions on*, vol. 58, no. 5, pp. 1441–1449, 2011.

[46] S. M. Pincus and A. L. Goldberger, "Physiological time-series analysis: what does regularity quantify?," *American Journal of Physiology-Heart and Circulatory Physiology*, vol. 266, no. 4, pp. H1643–H1656, 1994.

[47] H. Stanley, L. N. Amaral, A. Goldberger, S. Havlin, P. C. Ivanov, and C.-K. Peng, "Statistical physics and physiology: monofractal and multifractal approaches," *Physica A: Statistical Mechanics and its Applications*, vol. 270, no. 1, pp. 309–324, 1999.

[48] D. M. Bers and E. Grandi, "Human atrial fibrillation: insights from computational electrophysiological models," *Trends Cardiovasc Med*, vol. 21, pp. 145–50, Jul 2011.

[49] Z. Qu, "Chaos in the genesis and maintenance of cardiac arrhythmias," *Progress in Biophysics and Molecular Biology*, vol. 105, no. 3, pp. 247 – 257, 2011.

[50] A. Katz, *Physiology of the Heart*. Wolters Kluwer Health, 2011.

[51] R. E. Klabunde, *Cardiovascular physiology concepts*. Wolters Kluwer Health, 2011.

[52] L. H. Opie, *Heart physiology: from cell to circulation*. Wolters Kluwer Health, 2004.

[53] D. Sigg, P. A. Iaizzo, and Y.-F. Xiao, *Cardiac electrophysiology methods and models*. Springer, 2010.

[54] J. Jalife, M. Delmar, J. Anumonwo, O. Berenfeld, and J. Kalifa, *Impulse Initiation and Propagation in Cardiac Muscle*, pp. 92–120. Wiley-Blackwell, 2009.

[55] J. Malmivuo and R. Plonsey, *Bioelectromagnetism: Principles and Applications of Bioelectric and Biomagnetic Fields*. Oxford University Press, 1995.

[56] A. L. Goldberger, *Clinical electrocardiography: a simplified approach*. Elsevier Health Sciences, 2012.

[57] A. B. De Luna, *Clinical electrocardiography: a textbook*. John Wiley & Sons Incorporated, 2012.

[58] A. S. Go, E. M. Hylek, K. A. Phillips, Y. Chang, L. E. Henault, J. V. Selby, and D. E. Singer, "Prevalence of diagnosed atrial fibrillation in adults," *JAMA: the journal of the American Medical Association*, vol. 285, no. 18, pp. 2370–2375, 2001.

[59] M. W. Rich, "Epidemiology of atrial fibrillation," *Journal of interventional cardiac electrophysiology*, vol. 25, no. 1, pp. 3–8, 2009.

[60] F. Rahman, G. F. Kwan, and E. J. Benjamin, "Global epidemiology of atrial fibrillation," *Nat Rev Cardiol*, vol. 11, pp. 639–654, Nov 2014.

[61] S. Nattel, "New ideas about atrial fibrillation 50 years on," *Nature*, vol. 415, no. 6868, pp. 219–226, 2002.

[62] P. Kirchhof, A. Auricchio, J. Bax, H. Crijns, J. Camm, H.-C. Diener, A. Goette, G. Hindricks, S. Hohnloser, L. Kappenberger, K.-H. Kuck, G. Y. Lip, B. Olsson, T. Meinertz, S. Priori, U. Ravens, G. Steinbeck, E. Svernhage, J. Tijssen, A. Vincent, and G. Breithardt, "Outcome parameters for trials in atrial fibrillation: Recommendations from a consensus conference organized by the german atrial fibrillation competence network and the european heart rhythm association," *Europace*, vol. 9, no. 11, pp. 1006–1023, 2007.

[63] M. Rienstra, S. A. Lubitz, S. Mahida, J. W. Magnani, J. D. Fontes, M. F. Sinner, I. C. Van Gelder, P. T. Ellinor, and E. J. Benjamin, "Symptoms and functional status of patients with atrial fibrillation: State of the art and future research opportunities," *Circulation*, vol. 125, no. 23, pp. 2933–2943, 2012.

[64] R. J. Sung and M. R. Lauer, "Atrial fibrillation: Can we cure it if we can't explain it?," *Journal of cardiovascular electrophysiology*, vol. 16, no. 5, pp. 505–507, 2005.

[65] M. Haissaguerre, P. Jaïs, D. C. Shah, A. Takahashi, M. Hocini, G. Quiniou, S. Garrigue, A. Le Mouroux, P. Le Métayer, and J. Clémenty, "Spontaneous initiation of atrial fibrillation by ectopic beats originating in the pulmonary veins," *New England Journal of Medicine*, vol. 339, no. 10, pp. 659–666, 1998.

[66] H. Oral, B. P. Knight, H. Tada, M. Özaydın, A. Chugh, S. Hassan, C. Scharf, S. W. Lai, R. Greenstein, F. Pelosi, *et al.*, "Pulmonary vein isolation for paroxysmal and persistent atrial fibrillation," *Circulation*, vol. 105, no. 9, pp. 1077–1081, 2002.

[67] G. K. Moe, "On the multiple wavelet hypothesis of atrial fibrillation," *Arch Int Pharmacodyn Ther*, vol. 140, pp. 183–188, 1962.

[68] U. Schotten, S. Verheule, P. Kirchhof, and A. Goette, "Pathophysiological mechanisms of atrial fibrillation: A translational appraisal," *Physiological Reviews*, vol. 91, no. 1, pp. 265–325, 2011.

[69] K. Konings, C. Kirchhof, J. Smeets, H. Wellens, O. C. Penn, and M. A. Allessie, "High-density mapping of electrically induced atrial fibrillation in humans.," *Circulation*, vol. 89, no. 4, pp. 1665–1680, 1994.

[70] M. A. Allessie, W. J. E. P. Lammers, F. I. M. Bonke, and J. Hollen, "Experimental evaluation of Moe's multiple wavelet hypothesis of atrial fibrillation," in *Cardiac Electrophysiology and Arrhythmias* (D. P. Zipes and J. Jalife, eds.), pp. 265–275, Orlando, FL.: Grune & Stratton, 1985.

[71] J. Kneller, J. Kalifa, R. Zou, A. V. Zaitsev, M. Warren, O. Berenfeld, E. J. Vigmond, L. J. Leon, S. Nattel, and J. Jalife, "Mechanisms of atrial fibrillation termination by pure sodium channel blockade in an ionically-realistic mathematical model," *Circ Res*, vol. 96, pp. e35–47, Mar 2005.

[72] Y. Takahashi, P. Sanders, P. Jais, M. Hocini, R. Dubois, M. Rotter, T. Rostock, C. J. Nalliah, F. Sacher, J. Clémenty, *et al.*, "Organization of frequency spectra of atrial fibrillation: relevance to radiofrequency catheter ablation," *Journal of cardiovascular electrophysiology*, vol. 17, no. 4, pp. 382–388, 2006.

[73] J. Jalife, O. Berenfeld, and M. Mansour, "Mother rotors and fibrillatory conduction: a mechanism of atrial fibrillation," *Cardiovascular Research*, vol. 54, no. 2, pp. 204–216, 2002.

[74] S. V. Pandit and J. Jalife, "Rotors and the dynamics of cardiac fibrillation," *Circulation Research*, vol. 112, no. 5, pp. 849–862, 2013.

[75] S. Zlochiver, M. Yamazaki, J. Kalifa, and O. Berenfeld, "Rotor meandering contributes to irregularity in electrograms during atrial fibrillation," *Heart Rhythm*, vol. 5, no. 6, pp. 846 – 854, 2008.

[76] M. Yamazaki and J. Jalife, "Pathophysiology of atrial fibrillation: From initiation to maintenance," *Journal of Arrhythmia*, vol. 28, no. 3, pp. 129–139, 2012.

[77] S. M. Narayan, K. Shivkumar, D. E. Krummen, J. M. Miller, and W.-J. Rappel, "Panoramic electrophysiological mapping but not electrogram morphology identifies stable sources for human atrial fibrillation: Stable af rotors and focal sources relate poorly to fractionated electrograms," *Circulation: Arrhythmia and Electrophysiology*, 2013.

[78] S. M. Narayan, D. E. Krummen, and W.-J. Rappel, "Clinical mapping approach to diagnose electrical rotors and focal impulse sources for human atrial fibrillation," *Journal of cardiovascular electrophysiology*, vol. 23, no. 5, pp. 447–454, 2012.

[79] M. Vaquero, D. Calvo, and J. Jalife, "Cardiac fibrillation: From ion channels to rotors in the human heart," *Heart Rhythm*, vol. 5, no. 6, pp. 872 – 879, 2008.

[80] M. Allessie and N. de Groot, "Crosstalk opposing view: Rotors have not been demonstrated to be the drivers of atrial fibrillation," *The Journal of Physiology*, vol. 592, no. 15, pp. 3167–3170, 2014.

[81] N. M. de Groot, R. P. Houben, J. L. Smeets, E. Boersma, U. Schotten, M. J. Schalij, H. Crijns, and M. A. Allessie, "Electropathological substrate of longstanding persistent atrial fibrillation in patients with structural heart disease: Epicardial breakthrough," *Circulation*, vol. 122, no. 17, pp. 1674–1682, 2010.

[82] M. A. Allessie, N. M. de Groot, R. P. Houben, U. Schotten, E. Boersma, J. L. Smeets, and H. J. Crijns, "Electropathological substrate of long-standing persistent atrial fibrillation in patients with structural heart disease: Longitudinal dissociation," *Circulation: Arrhythmia and Electrophysiology*, vol. 3, no. 6, pp. 606–615, 2010.

[83] S. Verheule, J. Eckstein, D. Linz, B. Maesen, E. Bidar, A. Gharaviri, and U. Schotten, "Role of endo-epicardial dissociation of electrical activity and transmural conduction in the development of persistent atrial fibrillation," *Progress in Biophysics and Molecular Biology*, vol. 115, no. 2 - 3, pp. 173 – 185, 2014. Novel Technologies as Drivers of Progress in Cardiac Biophysics.

[84] S. Verheule, E. Tuyls, A. van Hunnik, M. Kuiper, U. Schotten, and M. Allessie, "Fibrillatory conduction in the atrial free walls of goats in persistent and permanent atrial fibrillation," *Circulation: Arrhythmia and Electrophysiology*, vol. 3, no. 6, pp. 590–599, 2010.

[85] J. Eckstein, S. Zeemering, D. Linz, B. Maesen, S. Verheule, A. van Hunnik, H. Crijns, M. A. Allessie, and U. Schotten, "Transmural conduction is the predominant mechanism of breakthrough during atrial fibrillation: Evidence from simultaneous endo-epicardial high density activation mapping," *Circulation: Arrhythmia and Electrophysiology*, 2013.

[86] E. G. Daoud, F. Bogun, R. Goyal, M. Harvey, K. C. Man, S. A. Strickberger, and F. Morady, "Effect of atrial fibrillation on atrial refractoriness in humans," *Circulation*, vol. 94, no. 7, pp. 1600–1606, 1996.

[87] B. Burstein, B. S. Stanley, and M. D. Nattel, "Atrial fibrosis: Mechanisms and clinical relevance in atrial fibrillation," *Journal of the American College of Cardiology*, vol. 51, no. 8, pp. 802–809, 2008.

[88] A. J. Camm and I. Savelieva, "Atrial fibrillation: the rate versus rhythm management controversy," *The journal of the Royal College of Physicians of Edinburgh*, vol. 42 Suppl 18, pp. 23–34, 2012.

[89] Y. Yap and J. Camm, "Rate and rhythm control strategies for atrial fibrillation," in *Essentials of Atrial Fibrillation*, pp. 21–36, Springer Healthcare Ltd., 2014.

[90] H. Calkins, K. H. Kuck, R. Cappato, J. Brugada, A. J. Camm, S.-A. Chen, H. J. Crijns, R. J. Damiano, D. W. Davies, J. DiMarco, *et al.*, "2012 HRS/EHRA/ECAS expert consensus statement on catheter and surgical ablation of atrial fibrillation: recommendations for patient selection, procedural techniques, patient management and follow-up, definitions, endpoints, and research trial design," *Europace*, vol. 14, no. 4, pp. 528–606, 2012.

[91] F. Nilsson, M. Stridh, A. Bollmann, and L. Sörnmo, "Predicting spontaneous termination of atrial fibrillation using the surface ECG," *Med Eng Phys*, vol. 28, pp. 802–8, Oct 2006.

[92] G. Moody, "Spontaneous termination of atrial fibrillation: a challenge from physionet and computers in cardiology 2004," *Computers in cardiology*, vol. 31, p. 101, 2004.

[93] A. L. Goldberger, L. A. Amaral, L. Glass, J. M. Hausdorff, P. C. Ivanov, R. G. Mark, J. E. Mietus, G. B. Moody, C. K. Peng, and H. E. Stanley, "Physiobank, physiotoolkit, and physionet: components of a new research resource for complex physiologic signals.," *Circulation*, vol. 101, pp. E215–E220, Jun 2000.

[94] R. Alcaraz and J. J. Rieta, "Non-invasive organization variation assessment in the onset and termination of paroxysmal atrial fibrillation," *Computer methods and programs in biomedicine*, vol. 93, no. 2, pp. 148–154, 2009.

[95] F. Ravelli, M. Masè, M. d. Greco, L. Faes, and M. Disertori, "Deterioration of organization in the first minutes of atrial fibrillation: A beat-to-beat analysis of cycle length and wave similarity," *Journal of cardiovascular electrophysiology*, vol. 18, no. 1, pp. 60–65, 2007.

[96] H. J. Sih, D. P. Zipes, E. J. Berbari, D. E. Adams, and J. E. Olgin, "Differences in organization between acute and chronic atrial fibrillation in dogs," *J. Am. Coll. Cardiol.*, vol. 36, no. 3, pp. 924–931, 2000.

[97] M. S. Guillem, A. M. Climent, F. Castells, D. Husser, J. Millet, A. Arya, C. Piorkowski, and A. Bollmann, "Noninvasive mapping of human atrial fibrillation," *Journal of cardiovascular electrophysiology*, vol. 20, no. 5, pp. 507–513, 2009.

[98] W. G. Stevenson and K. Soejima, "Recording techniques for clinical electrophysiology," *Journal of cardiovascular electrophysiology*, vol. 16, no. 9, pp. 1017–1022, 2005.

[99] R. Alcaraz and J. J. Rieta, "The contribution of nonlinear methods in the understanding of atrial fibrillation," in *Atrial Fibrillation - Mechanisms and Treatment*, ch. 8, pp. 181 – 204, InTech, 2013.

[100] J. L. Wells, R. B. Karp, N. T. Kouchoukos, W. A. MacLean, T. N. James, and A. L. Waldo, "Characterization of atrial fibrillation in man: Studies following open heart surgery*," *Pacing and Clinical Electrophysiology*, vol. 1, no. 4, pp. 426–438, 1978.

[101] V. Barbaro, P. Bartolini, G. Calcagnini, S. Morelli, A. Michelucci, and G. Gensini, "Automated classification of human atrial fibrillation from intraatrial electrograms," *Pacing and Clinical Electrophysiology*, vol. 23, no. 2, pp. 192–202, 2000.

[102] G. W. Botteron and J. M. Smith, "A technique for measurement of the extent of spatial organization of atrial activation during atrial fibrillation in the intact human heart," *Biomedical Engineering, IEEE Transactions on*, vol. 42, no. 6, pp. 579–586, 1995.

[103] L. Faes and F. Ravelli, "A morphology-based approach to the evaluation of atrial fibrillation organization," *Engineering in Medicine and Biology Magazine, IEEE*, vol. 26, no. 4, pp. 59–67, 2007.

[104] P. Jais, M. Haissaguerre, D. C. Shah, S. Chouairi, and J. Clementy, "Regional disparities of endocardial atrial activation in paroxysmal atrial fibrillation," *Pacing and clinical electrophysiology*, vol. 19, no. 11, pp. 1998–2003, 1996.

[105] P. Sanders, O. Berenfeld, M. Hocini, P. Jaïs, R. Vaidyanathan, L.-F. Hsu, S. Garrigue, Y. Takahashi, M. Rotter, F. Sacher, *et al.*, "Spectral analysis identifies sites of high-frequency activity maintaining atrial fibrillation in humans," *Circulation*, vol. 112, no. 6, pp. 789–797, 2005.

[106] S. Lazar, S. Dixit, F. E. Marchlinski, D. J. Callans, and E. P. Gerstenfeld, "Presence of left-to-right atrial frequency gradient in paroxysmal but not persistent atrial fibrillation in humans," *Circulation*, vol. 110, no. 20, pp. 3181–3186, 2004.

[107] K. M. Ropella, A. V. Sahakian, J. M. Baerman, and S. Swiryn, "The coherence spectrum. a quantitative discriminator of fibrillatory and nonfibrillatory cardiac rhythms.," *Circulation*, vol. 80, no. 1, pp. 112–9, 1989.

[108] T. H. Everett, L. C. Kok, R. H. Vaughn, J. R. Moorman, and D. E. Haines, "Frequency domain algorithm for quantifying atrial fibrillation organization to increase defibrillation efficacy.," *IEEE Trans. Biomed. Eng.*, vol. 48, no. 9, pp. 969–978, 2001.

[109] A. Porta, M. Di Rienzo, N. Wessel, and J. Kurths, "Addressing the complexity of cardiovascular regulation," *Philos Transact A Math Phys Eng Sci*, vol. 367, pp. 1215–8, Apr 2009.

[110] H. F. Pitschner, A. Berkovic, S. Grumbrecht, and J. Neuzner, "Multielectrode basket catheter mapping for human atrial fibrillation.," *Journal of cardiovascular electrophysiology*, vol. 9, no. 8 Suppl, pp. S48–S56, 1998.

[111] R. Cervigón, J. Moreno, R. Reilly, J. Millet, J. Pérez-Villacastín, and F. Castells, "Entropy measurements in paroxysmal and persistent atrial fibrillation," *Physiological measurement*, vol. 31, no. 7, p. 1011, 2010.

[112] J. Ng, A. I. Borodyanskiy, E. T. Chang, R. Villuendas, S. Dibs, A. H. Kadish, and J. J. Goldberger, "Measuring the complexity of atrial fibrillation electrograms," *Journal of cardiovascular electrophysiology*, vol. 21, no. 6, pp. 649–655, 2010.

[113] L. T. Mainardi, V. D. Corino, L. Lombardi, C. Tondo, M. Mantica, F. Lombardi, S. Cerutti, *et al.*, "Assessment of the dynamics of atrial signals and local atrial period series during atrial fibrillation: effects of isoproterenol administration," *Biomed. Eng. Online*, vol. 3, p. 37, 2004.

[114] D. Husser, M. Stridh, D. S. Cannom, A. K. Bhandari, M. J. Girsky, S. Kang, L. Sörnmo, S. Bertil Olsson, and A. Bollmann, "Validation and clinical application of time-frequency analysis of atrial fibrillation electrocardiograms," *Journal of cardiovascular electrophysiology*, vol. 18, no. 1, pp. 41–46, 2007.

[115] R. Alcaraz, F. Hornero, and J. J. Rieta, "Assessment of non-invasive time and frequency atrial fibrillation organization markers with unipolar atrial electrograms," *Physiological measurement*, vol. 32, no. 1, p. 99, 2011.

[116] M. Holm, S. Pehrson, M. Ingemansson, L. Sörnmo, R. Johansson, L. Sandhall, M. Sunemark, B. Smideberg, C. Olsson, and S. B. Olsson, "Noninvasive assessment of the atrial cycle length during atrial fibrillation in man: introducing, validating and illustrating a new ECG method," *Cardiovasc Res*, vol. 38, pp. 69–81, Apr 1998.

[117] F. Chiarugi, M. Varanini, F. Cantini, F. Conforti, and G. Vrouchos, "Noninvasive ECG as a tool for predicting termination of paroxysmal atrial fibrillation," *Biomedical Engineering, IEEE Transactions on*, vol. 54, no. 8, pp. 1399–1406, 2007.

[118] A. Bollmann, M. Mende, A. Neugebauer, and D. Pfeiffer, "Atrial fibrillatory frequency predicts atrial defibrillation threshold and early arrhythmia recurrence in patients undergoing internal cardioversion of persistent atrial fibrillation," *Pacing and clinical electrophysiology*, vol. 25, no. 8, pp. 1179–1184, 2002.

[119] F. Holmqvist, M. Stridh, J. E. Waktare, L. Sörnmo, S. B. Olsson, and C. J. Meurling, "Atrial fibrillatory rate and sinus rhythm maintenance in patients undergoing cardioversion of persistent atrial fibrillation," *European heart journal*, vol. 27, no. 18, pp. 2201–2207, 2006.

[120] M. Stridh, L. Sörnmo, C. J. Meurling, and S. B. Olsson, "Characterization of atrial fibrillation using the surface ECG: time-dependent spectral properties," *Biomedical Engineering, IEEE Transactions on*, vol. 48, no. 1, pp. 19–27, 2001.

[121] V. D. Corino, L. T. Mainardi, M. Stridh, and L. Sörnmo, "Improved time–frequency analysis of atrial fibrillation signals using spectral modeling," *Biomedical Engineering, IEEE Transactions on*, vol. 55, no. 12, pp. 2723–2730, 2008.

[122] F. Sandberg, M. Stridh, and L. Sörnmo, "Frequency tracking of atrial fibrillation using hidden markov models," *Biomedical Engineering, IEEE Transactions on*, vol. 55, no. 2, pp. 502–511, 2008.

[123] R. Alcaraz and J. J. Rieta, "Surface ECG organization analysis to predict paroxysmal atrial fibrillation termination," *Comput Biol Med*, vol. 39, pp. 697–706, Aug 2009.

[124] R. Alcaraz and J. J. Rieta, "Wavelet bidomain sample entropy analysis to predict spontaneous termination of atrial fibrillation," *Physiological measurement*, vol. 29, no. 1, p. 65, 2008.

[125] R. Alcaraz and J. J. Rieta, "Application of wavelet entropy to predict atrial fibrillation progression from the surface ECG," *Computational and mathematical methods in medicine*, vol. 2012, 2012.

[126] R. Alcaraz, J. J. Rieta, *et al.*, "Central tendency measure and wavelet transform combined in the non-invasive analysis of atrial fibrillation recordings," *Biomedical engineering online*, vol. 11, no. 1, pp. 1–19, 2012.

[127] G. Ndrepepa, S. Weber, M. R. Karch, M. A. E. Schneider, J. ü. Schreieck J, A. Schömig, and C. Schmitt, "Electrophysiologic characteristics of the spontaneous onset and termination of atrial fibrillation," *Am J Cardiol*, vol. 90, pp. 1215–20, Dec 2002.

[128] H.-W. Tso, Y.-J. Lin, C.-T. Tai, S.-A. Chen, and T. Kao, "Characteristics of fibrillatory activities during spontaneous termination of paroxysmal atrial fibrillation: New insight from high-density right atrium frequency mapping," *Canadian Journal of Cardiology*, vol. 28, no. 1, pp. 87 – 94, 2012.

[129] B. Hoekstra, C. G. Diks, M. A. Allessie, and J. DeGoede, "Nonlinear analysis of the pharmacological conversion of sustained atrial fibrillation in conscious goats by the class ic drug cibenzoline," *Chaos: An Interdisciplinary Journal of Nonlinear Science*, vol. 7, no. 3, pp. 430–446, 1997.

[130] J. Slocum, A. Sahakian, and S. Swiryn, "Diagnosis of atrial fibrillation from surface electrocardiograms based on computer-detected atrial activity," *Journal of Electrocardiology*, vol. 25, no. 1, pp. 1 – 8, 1992.

[131] J. Pan and W. J. Tompkins, "A real-time qrs detection algorithm," *Biomedical Engineering, IEEE Transactions on*, vol. BME-32, no. 3, pp. 230–236, 1985.

[132] I. Dotsinsky and T. Stoyanov, "Optimization of bi-directional digital filtering for drift suppression in electrocardiogram signals," *Journal of Medical Engineering & Technology*, vol. 28, no. 4, pp. 178–180, 2004.

[133] Y. Sun, K. L. Chan, and S. M. Krishnan, "ECG signal conditioning by morphological filtering," *Computers in biology and medicine*, vol. 32, no. 6, pp. 465–479, 2002.

[134] S. M. Martens, M. Mischi, S. G. Oei, and J. W. Bergmans, "An improved adaptive power line interference canceller for electrocardiography," *Biomedical Engineering, IEEE Transactions on*, vol. 53, no. 11, pp. 2220–2231, 2006.

[135] J. Slocum, E. Byrom, L. McCarthy, A. Sahakian, and S. Swiryn, "Computer detection of atrioventricular dissociation from surface electrocardiograms during wide QRS complex tachycardias.," *Circulation*, vol. 72, no. 5, pp. 1028–1036, 1985.

[136] R. Alcaraz and J. J. Rieta, "Adaptive singular value cancelation of ventricular activity in single-lead atrial fibrillation electrocardiograms," *Physiological measurement*, vol. 29, no. 12, p. 1351, 2008.

[137] M. Stridh and L. Sörnmo, "Spatiotemporal QRST cancellation techniques for analysis of atrial fibrillation," *Biomedical Engineering, IEEE Transactions on*, vol. 48, no. 1, pp. 105–111, 2001.

[138] J. Rieta, F. Castells, C. Sanchez, V. Zarzoso, and J. Millet, "Atrial activity extraction for atrial fibrillation analysis using blind source separation," *Biomedical Engineering, IEEE Transactions on*, vol. 51, no. 7, pp. 1176–1186, 2004.

[139] P. Langley, J. Rieta, M. Stridh, J. Millet, L. Sörnmo, and A. Murray, "Comparison of atrial signal extraction algorithms in 12-lead ECGs with atrial fibrillation," *Biomedical Engineering, IEEE Transactions on*, vol. 53, no. 2, pp. 343–346, 2006.

[140] S. Cerutti, L. Mainardi, and L. Sörnmo, *Understanding atrial fibrillation: The signal processing contribution*. Morgan & Claypool, San Rafael, CA, 2008.

[141] F. Castells, C. Mora, J. Rieta, D. Moratal-Perez, and J. Millet, "Estimation of atrial fibrillatory wave from single-lead atrial fibrillation electrocardiograms using principal component analysis concepts," *Medical and Biological Engineering and Computing*, vol. 43, no. 5, pp. 557–560, 2005.

[142] R. Alcaraz and J. J. Rieta, "Sample entropy of the main atrial wave predicts spontaneous termination of paroxysmal atrial fibrillation," *Medical engineering & physics*, vol. 31, no. 8, pp. 917–922, 2009.

[143] R. Alcaraz, F. Hornero, and J. J. Rieta, "Noninvasive time and frequency predictors of long-standing atrial fibrillation early recurrence after electrical cardioversion," *Pacing and Clinical Electrophysiology*, vol. 34, no. 10, pp. 1241–1250, 2011.

[144] R. Alcaraz, J. J. Rieta, and F. Hornero, "Non-invasive characterization of atrial activity immediately prior to termination of paroxysmal atrial fibrillation," *Revista Española de Cardiología (English Edition)*, vol. 61, no. 2, pp. 154–160, 2008.

[145] R. Alcaraz, F. Hornero, and J. J. Rieta, "Surface ECG organization time course analysis along onward episodes of paroxysmal atrial fibrillation," *Medical engineering & physics*, vol. 33, no. 5, pp. 597–603, 2011.

[146] D. Abásolo, R. Alcaraz, J. J. Rieta, and R. Hornero, "Lempel-Ziv complexity analysis for the evaluation of atrial fibrillation organization," in *Proceedings of the 8th IASTED International Conference on Biomedical Engineering, Biomed 2011*, pp. 30–35, 2011.

[147] L. Sörnmo and P. Laguna, *Bioelectrical signal processing in cardiac and neurological applications [electronic resource]*. Academic Press, 2005.

[148] L. Rabiner, J. McClellan, and T. Parks, "FIR digital filter design techniques using weighted chebyshev approximation," *Proceedings of the IEEE*, vol. 63, no. 4, pp. 595–610, 1975.

[149] A. Bollmann, D. Husser, M. Stridh, L. Sörnmo, M. Majic, H. U. Klein, and S. B. Olsson, "Frequency measures obtained from the surface electrocardiogram in atrial fibrillation research and clinical decision-making," *Journal of cardiovascular electrophysiology*, vol. 14, no. s10, pp. S154–S161, 2003.

[150] M. Najim, *Modeling, Estimation and Optimal Filtration in Signal Processing*, vol. 25. John Wiley & Sons, 2010.

[151] P. Welch, "The use of fast fourier transform for the estimation of power spectra: a method based on time averaging over short, modified periodograms," *Audio and Electroacoustics, IEEE Transactions on*, vol. 15, no. 2, pp. 70–73, 1967.

[152] J. S. Richman and J. R. Moorman, "Physiological time-series analysis using approximate entropy and sample entropy," *American Journal of Physiology-Heart and Circulatory Physiology*, vol. 278, no. 6, pp. H2039–H2049, 2000.

[153] S. M. Pincus, "Assessing serial irregularity and its implications for health," *Annals of the New York Academy of Sciences*, vol. 954, no. 1, pp. 245–267, 2001.

[154] R. Alcaraz, D. Abásolo, R. Hornero, and J. J. Rieta, "Optimal parameters study for sample entropy-based atrial fibrillation organization analysis," *Comput Methods Programs Biomed*, vol. 99, pp. 124–32, Jul 2010.

[155] W. Chen, Z. Wang, H. Xie, and W. Yu, "Characterization of surface EMG signal based on fuzzy entropy," *Neural Systems and Rehabilitation Engineering, IEEE Transactions on*, vol. 15, no. 2, pp. 266–272, 2007.

[156] L. A. Zadeh, "Fuzzy sets," *Information and control*, vol. 8, no. 3, pp. 338–353, 1965.

[157] J. Shi, Y. Cai, J. Zhu, J. Zhong, and F. Wang, "SEMG-based hand motion recognition using cumulative residual entropy and extreme learning machine," *Medical & Biological Engineering & Computing*, vol. 51, no. 4, pp. 417–427, 2013.

[158] D. Gasecki, M. Kwarciany, A. Rojek, K. Kowalczyk, P. Boutouyrie, W. Nyka, S. Laurent, and K. Narkiewicz, "Subacute blood pressure variability and heart rate predict functional outcome after ischemic stroke: 5b. 06," *Journal of Hypertension*, vol. 29, p. e70, 2011.

[159] A. Avolio, "Heart rate variability and stroke: strange attractors with loss of complexity," *Journal of hypertension*, vol. 31, no. 8, pp. 1529–1531, 2013.

[160] J. Gomez-Garcia, J. Martinez-Vargas, and G. Castellanos-Dominguez, "Complexity-based analysis for the detection of heart murmurs," in *Engineering in Medicine and Biology Society, EMBC, 2011 Annual International Conference of the IEEE*, pp. 2728–2731, IEEE, 2011.

[161] M. Julián, R. Alcaraz, and J. Rieta, "Comparative study of nonlinear metrics to discriminate atrial fibrillation events from the surface ECG," in *Computing in Cardiology (CinC), 2012*, pp. 197–200, 2012.

[162] I. Rezek and S. J. Roberts, "Stochastic complexity measures for physiological signal analysis," *Biomedical Engineering, IEEE Transactions on*, vol. 45, no. 9, pp. 1186–1191, 1998.

[163] T. Inouye, K. Shinosaki, H. Sakamoto, S. Toi, S. Ukai, A. Iyama, Y. Katsuda, and M. Hirano, "Quantification of EEG irregularity by use of the entropy of the power spectrum," *Electroencephalogr Clin Neurophysiol*, vol. 79, pp. 204–10, Sep 1991.

[164] J. W. Sleigh, D. A. Steyn-Ross, M. L. Steyn-Ross, C. Grant, and G. Ludbrook, "Cortical entropy changes with general anaesthesia: theory and experiment," *Physiol Meas*, vol. 25, pp. 921–34, Aug 2004.

[165] R. K. Ellerkmann, V.-M. Liermann, T. M. Alves, I. Wenningmann, S. Kreuer, W. Wilhelm, H. Roepcke, A. Hoeft, and J. Bruhn, "Spectral entropy and bispectral index as measures of the electroencephalographic effects of sevoflurane," *Anesthesiology*, vol. 101, no. 6, pp. 1275–1282, 2004.

[166] N. Kannathal, M. L. Choo, U. R. Acharya, and P. Sadasivan, "Entropies for detection of epilepsy in {EEG}," *Computer Methods and Programs in Biomedicine*, vol. 80, no. 3, pp. 187 – 194, 2005.

[167] R. Acharya, A. Kumar, P. Bhat, C. Lim, S. lyengar, N. Kannathal, and S. Krishnan, "Classification of cardiac abnormalities using heart rate signals," *Medical and Biological Engineering and Computing*, vol. 42, no. 3, pp. 288–293, 2004.

[168] A. Lempel and J. Ziv, "On the complexity of finite sequences," *Information Theory, IEEE Transactions on*, vol. 22, no. 1, pp. 75–81, 1976.

[169] M. Aboy, R. Hornero, D. Abásolo, and D. Alvarez, "Interpretation of the lempel-ziv complexity measure in the context of biomedical signal analysis," *IEEE Trans Biomed Eng*, vol. 53, pp. 2282–8, Nov 2006.

[170] N. Radhakrishnan and B. N. Gangadhar, "Estimating regularity in epileptic seizure time-series data. a complexity-measure approach," *IEEE Eng Med Biol Mag*, vol. 17, no. 3, pp. 89–94, 1998.

[171] X. S. Zhang, R. J. Roy, and E. W. Jensen, "EEG complexity as a measure of depth of anesthesia for patients," *IEEE Trans Biomed Eng*, vol. 48, pp. 1424–33, Dec 2001.

[172] D. Abásolo, R. Hornero, C. Gómez, M. García, and M. López, "Analysis of EEG background activity in alzheimer's disease patients with Lempel–Ziv complexity and central tendency measure," *Medical engineering & physics*, vol. 28, no. 4, pp. 315–322, 2006.

[173] R. Hornero, M. Aboy, and D. Abásolo, "Analysis of intracranial pressure during acute intracranial hypertension using Lempel–Ziv complexity: further evidence," *Medical & biological engineering & computing*, vol. 45, no. 6, pp. 617–620, 2007.

[174] T. A. Kuusela, T. T. Jartti, K. U. O. Tahvanainen, and T. J. Kaila, "Nonlinear methods of biosignal analysis in assessing terbutaline-induced heart rate and blood pressure changes," *American Journal of Physiology - Heart and Circulatory Physiology*, vol. 282, no. 2, pp. H773–H781, 2002.

[175] M. Ferrario, M. G. Signorini, and G. Magenes, "Complexity analysis of the fetal heart rate variability: early identification of severe intrauterine growth-restricted fetuses," *Medical & Biological Engineering & Computing*, vol. 47, no. 9, pp. 911–919, 2009.

[176] X. S. Zhang, Y. S. Zhu, N. V. Thakor, and Z. Z. Wang, "Detecting ventricular tachycardia and fibrillation by complexity measure," *IEEE Trans Biomed Eng*, vol. 46, pp. 548–55, May 1999.

[177] R. Nagarajan, "Quantifying physiological data with Lempel-Ziv complexity–certain issues," *IEEE Trans Biomed Eng*, vol. 49, pp. 1371–3, Nov 2002.

[178] H. E. Hurst, "Long-term storage capacity of reservoirs," *Trans. Amer. Soc. Civil Eng.*, vol. 116, pp. 770–808, 1951.

[179] B. B. Mandelbrot and J. W. Van Ness, "Fractional brownian motions, fractional noises and applications," *SIAM review*, vol. 10, no. 4, pp. 422–437, 1968.

[180] M. Akay, *Nonlinear Biomedical Signal Processing Volumen II*. IEEE Press, 2001.

[181] S. Havlin, L. Amaral, Y. Ashkenazy, A. Goldberger, P. Ivanov, C.-K. Peng, and H. Stanley, "Application of statistical physics to heartbeat diagnosis," *Physica A: Statistical Mechanics and its Applications*, vol. 274, no. 1, pp. 99 – 110, 1999.

[182] P. C. Ivanov, L. A. Amaral, A. L. Goldberger, S. Havlin, M. G. Rosenblum, Z. R. Struzik, and H. E. Stanley, "Multifractality in human heartbeat dynamics," *Nature*, vol. 399, pp. 461–5, Jun 1999.

[183] B. J. West, M. Latka, M. Glaubic-Latka, and D. Latka, "Multifractality of cerebral blood flow," *Physica A: Statistical Mechanics and its Applications*, vol. 318, no. 3, pp. 453–460, 2003.

[184] I.-H. Song, S.-M. Lee, I.-Y. Kim, D.-S. Lee, and S. Kim, "Mutifractal analysis of electroencephalogram time series in humans," in *Computational Intelligence and Bioinspired Systems* (J. Cabestany, A. Prieto, and F. Sandoval, eds.), vol. 3512 of *Lecture Notes in Computer Science*, pp. 921–926, Springer Berlin Heidelberg, 2005.

[185] L. D. Sherman, C. W. Callaway, and J. J. Menegazzi, "Ventricular fibrillation exhibits dynamical properties and self-similarity," *Resuscitation*, vol. 47, no. 2, pp. 163–173, 2000.

[186] L. Mainardi and R. Sassi, "Analysis of scaling behaviour of ECG signal during atrial fibrillation," in *Computers in Cardiology*, pp. 627–630, IEEE (Institute of Electrical and Electronics Engineers), 2005.

[187] A.-L. Barabási and T. Vicsek, "Multifractality of self-affine fractals," *Physical Review A*, vol. 44, no. 4, p. 2730, 1991.

[188] T. Di Matteo, T. Aste, and M. Dacorogna, "Scaling behaviors in differently developed markets," *Physica A: Statistical Mechanics and its Applications*, vol. 324, no. 1, pp. 183–188, 2003.

[189] T. Di Matteo, "Multi-scaling in finance," *Quantitative Finance*, vol. 7, no. 1, pp. 21–36, 2007.

[190] D. Grech and Z. Mazur, "Can one make any crash prediction in finance using the local Hurst exponent idea?," *Physica A: Statistical Mechanics and its Applications*, vol. 336, pp. 133–145, 2004.

[191] M. Porter, W. Spear, J. G. Akar, R. Helms, N. Brysiewicz, P. Santucci, and D. J. Wilber, "Prospective study of atrial fibrillation termination during ablation guided by automated detection of fractionated electrograms," *Journal of Cardiovascular Electrophysiology*, vol. 19, no. 6, pp. 613–620, 2008.

[192] E. J. Ciaccio, A. B. Biviano, and H. Garan, "The dominant morphology of fractionated atrial electrograms has greater temporal stability in persistent as compared with paroxysmal atrial fibrillation," *Computers in Biology and Medicine*, vol. 43, no. 12, pp. 2127 – 2135, 2013.

[193] J. S. Bendat and A. G. Piersol, *Random Data: Analysis and Measurement Procedures*. Wiley-Interscience, New York, 2nd ed., 1986.

[194] J. Theiler, S. Eubank, A. Longtin, B. Galdrikian, and J. Doyne Farmer, "Testing for nonlinearity in time series: the method of surrogate data," *Physica D: Nonlinear Phenomena*, vol. 58, no. 1, pp. 77–94, 1992.

[195] T. Nakamura, M. Small, and Y. Hirata, "Testing for nonlinearity in irregular fluctuations with long-term trends," *Physical Review E*, vol. 74, no. 2, p. 026205, 2006.

[196] T. Schreiber and A. Schmitz, "Surrogate time series," *Physica D: Nonlinear Phenomena*, vol. 142, no. 3, pp. 346–382, 2000.

[197] S. Petrutiu, A. Sahakian, J. Ng, and S. Swiryn, "Analysis of the surface electrocardiogram to predict termination of atrial fibrillation: The 2004 Computers in Cardiology/Physionet Challenge," *Computers in Cardiology*, vol. 31, pp. 105–108, 2004.

[198] R. R. Sun and Y. Y. Wang, "Predicting spontaneous termination of atrial fibrillation based on the RR interval," *Proc Inst Mech Eng H*, vol. 223, pp. 713–26, Aug 2009.

[199] M. Mohebbi and H. Ghassemian, "Predicting termination of paroxysmal atrial fibrillation using empirical mode decomposition of the atrial activity and statistical features of the heart rate variability," *Medical & biological engineering & computing*, vol. 52, no. 5, pp. 415–427, 2014.

[200] W. Chen, J. Zhuang, W. Yu, and Z. Wang, "Measuring complexity using fuzzyen, apen, and sampen," *Medical Engineering & Physics*, vol. 31, no. 1, pp. 61–68, 2009.

[201] S. Petrutiu, A. V. Sahakian, and S. Swiryn, "Abrupt changes in fibrillatory wave characteristics at the termination of paroxysmal atrial fibrillation in humans," *Europace*, vol. 9, no. 7, pp. 466–470, 2007.

[202] K. M. Ropella, A. V. Sahakian, J. M. Baerman, and S. Swiryn, "Effects of procainamide on intra-atrial electrograms during atrial fibrillation: implications for detection algorithms," *Circulation*, vol. 77, pp. 1047–54, May 1988.

[203] U. Richter, A. Bollmann, D. Husser, and M. Stridh, "Right atrial organization and wavefront analysis in atrial fibrillation," *Med Biol Eng Comput*, vol. 47, pp. 1237–46, Dec 2009.

[204] L. Uldry, V. Jacquemet, N. Virag, L. Kappenberger, and J.-M. Vesin, "Estimating the time scale and anatomical location of atrial fibrillation spontaneous termination in a biophysical model," *Medical & biological engineering & computing*, vol. 50, no. 2, pp. 155–163, 2012.

[205] D. Husser, D. S. Cannom, A. K. Bhandari, M. Stridh, L. Sörnmo, S. B. Olsson, and A. Bollmann, "Electrocardiographic characteristics of fibrillatory waves in new-onset atrial fibrillation," *Europace*, vol. 9, pp. 638–42, Aug 2007.

[206] P. Manimaran, P. K. Panigrahi, and J. C. Parikh, "Wavelet analysis and scaling properties of time series," *Phys. Rev. E*, vol. 72, p. 046120, Oct 2005.

[207] G. Calcagnini, F. Censi, A. Michelucci, and P. Bartolini, "Descriptors of wavefront propagation. Endocardial mapping of atrial fibrillation with basket catheter," *IEEE Eng Med Biol Mag*, vol. 25, no. 6, pp. 71–8, 2006.

[208] K. Yoshida, A. Chugh, E. Good, T. Crawford, J. Myles, S. Veerareddy, S. Billakanty, W. S. Wong, M. Ebinger, F. Pelosi, K. Jongnarangsin, F. Bogun, F. Morady, and H. Oral, "A critical decrease in dominant frequency and clinical outcome after catheter ablation of persistent atrial fibrillation," *Heart Rhythm*, vol. 7, pp. 295–302, Mar 2010.

[209] N. Ortigosa, Ó. Cano, G. Ayala, A. Galbis, and C. Fernández, "Atrial fibrillation subtypes classification using the general fourier-family transform," *Medical Engineering & Physics*, vol. 36, no. 4, pp. 554 – 560, 2014.

List of Figures

List of Tables

Lisf of Acronyms

AA	Atrial activity
ABS	Averaged beat subtraction
Acc	Accuracy
AF	Atrial fibrillation
AROC	Area under the ROC curve
AV	Atrioventricular
ASVC	Adaptive Single Value Cancelation
DACL	Dominant atrial cycle length
DAF	Dominant atrial frequency
ECG	Electrocardiogram
ECV	Electrical cardioversion
EEG	Electroencephalogram
EGM	Electrogram
f waves	Fibrillatory waves
FFT	Fast Fourier Transform
FIR	Finite impulse response
FuzzEn	Fuzzy entropy
H	Hurst exponent
$H(q)$	q-order generalized Hurst exponent
ICV	Inferior vena cava
IIR	Infinite impulse response
LA	Left atrium
LZC	Lempel-Ziv complexity
MAW	Main atrial wave
NSR	Normal sinus rhythm
PAF	Paroxysmal atrial fibrillation
PCA	Principal component analysis
PSD	Power spectral density
PV	Pulmonary vein

QRST	QRS complex and T wave
RA	Right atrium
ROC	Receiver operating characteristic
SA	Sinoatrial
SampEn	Sample entropy
SCV	Superior vena cava
Se	Sensitivity
Sp	Specificity
SpecEn	Spectral entropy
WCT	Wilson central terminal